UNIVERSIDADE FEDERAL DE VIÇOSA

ON THE USE OF GENETIC PARAMETERS AND STOMATAL DISTRIBUTION TO IMPROVE DROUGHT TOLERANCE IN EUCALYPTUS

Leonardo Araujo Oliveira
Doctor Scientiae

VIÇOSA - MINAS GERAIS
2024

LEONARDO ARAUJO OLIVEIRA

ON THE USE OF GENETIC PARAMETERS AND STOMATAL DISTRIBUTION TO IMPROVE DROUGHT TOLERANCE IN EUCALYPTUS

Thesis submitted to the Plant Physiology Graduate Program of the Universidade Federal de Viçosa in partial fulfillment of the requirements for the degree of *Doctor Scientiae*.

Adviser: Samuel C Vitor Martins

Co-advisers: Amanda Ávila Cardoso
Genaina A de Souza
Fabio Murilo da Matta

VIÇOSA - MINAS GERAIS
2024

Ficha catalográfica elaborada pela Biblioteca Central da Universidade Federal de Viçosa - Campus Viçosa

T

O48o
2024

Oliveira, Leonardo Araujo, 1994-

On the use of genetic parameters and stomatal distribution to improve drought tolerance in eucalyptus / Leonardo Araujo Oliveira. – Viçosa, MG, 2024.

1 tese eletrônica (96 f.): il. (algumas color.).

Texto em inglês.

Orientador: Samuel Cordeiro Vitor Martins.

Tese (doutorado) - Universidade Federal de Viçosa, Departamento de Biologia Vegetal, 2024.

Inclui bibliografia.

DOI: https://doi.org/10.47328/ufvbbt.2024.790

Modo de acesso: World Wide Web.

1. Eucalipto - Resistência à seca. 2. Eucalipto - Melhoramento genético. 3. Padrões de herança. 4. Estômatos. I. Martins, Samuel Cordeiro Vitor, 1986-. II. Universidade Federal de Viçosa. Departamento de Biologia Vegetal. Programa de Pós-Graduação em Fisiologia Vegetal. III. Título.

CDD 22. ed. 634.973766

Bibliotecário(a) responsável: Bruna Silva CRB-6/2552

LEONARDO ARAUJO OLIVEIRA

ON THE USE OF GENETIC PARAMETERS AND STOMATAL DISTRIBUTION TO IMPROVE DROUGHT TOLERANCE IN EUCALYPTUS

Thesis submitted to the Plant Physiology Graduate Program of the Universidade Federal de Viçosa in partial fulfillment of the requirements for the degree of *Doctor Scientiae*.

APPROVED: February 23, 2024.

Assent:

Leonardo Araujo Oliveira
Author

Samuel Cordeiro Vitor Martins
Adviser

ACKNOWLEDGMENTS

My deepest gratitude goes to my entire family, especially my mother, Marilza. Regardless of the goals I set for myself and the sacrifices I had to make to achieve them, she was always by my side, supporting me and loving me unconditionally. Thank you for understanding my absence and for making the most of the short time we have together.

To my advisor, Samuel Martins, I express my sincere gratitude for all the teachings and exchanges over the last six years. His kindness and support in carrying out my various projects, as well as his light-hearted way of dealing with work and students, have been valuable sources of learning.

To my friend and co-supervisor, Amanda Cardoso, whose enthusiasm, support, and companionship were fundamental to the success of my thesis. Thank you for believing in me, many times before I even believed in myself, and for allowing me to have an international experience in your laboratory. Living together and learning over the years has been crucial to the professional development I have achieved.

I would like to thank my co-supervisor, Genaina de Souza, for her support and unwavering presence throughout practically my entire academic life, from the second year of my undergraduate degree to the end of my doctorate. Your support guided my choice of postgraduate course and helped me overcome the challenges of this journey. What's more, I would like to thank you and your husband Alex for becoming part of my family and for giving me the honor of being Laurinha's godfather.

I would also like to express my gratitude to the friends that Viçosa has given me. To Alexandre, Ana Clara, Lucas, Maria Luiza, Matheus, Thaline, and Toninho who have been there since I graduated and are still there today.

To the friends that post-graduation has given me, Guilherme, Pablo, Eduardo, Bruno Luan, Daniel, Antônio, and Bruno Nerso, thank you for starting as work colleagues and subject colleagues, and becoming more and more essential as time went by. And especially Moab, thank you very much for your partnership and the lessons learned during long hours of conversations on the most varied topics.

Special thanks to Talitha for her constant presence and support throughout this period, both in the lab and in my personal life. The lessons learned during our relationship were many and contributed significantly to my evolution as a professional and, above all, as a person.

To my colleagues in the United States, Rafaella, Cris, Ana Paula, Tiago, Matt, Day, and Amauri, who made my homesickness easier and my life in the US funnier. I would like to thank Eduardo for arriving earlier in Raleigh, meeting most of this group, and introducing them to me as soon as I arrived.

Many thanks to all the professors in the Plant Physiology program for their teachings. And especially to Professor Fábio DaMatta, for his friendship, trust, and the many opportunities to collaborate.

To the Universidade Federal de Viçosa (UFV), I express my gratitude for the opportunity to complete all my academic training, from my undergraduate degree in Agronomy to my master's and doctorate in Plant Physiology. I would also like to thank the funding institutions and North Carolina State University (NCSU) for the opportunity to be a visiting scholar in the Pack. To the staff of the different laboratories where I carried out my research, especially Guilherme, Rosana, and Aurora.

I would like to thank the Coordenação de Aperfeiçoamento de Pessoal de Nível Superior (CAPES) for granting me the scholarship and the assistance provided by USDA Hatch 7003279 through the Cardoso Laboratory at NCSU, I express my sincere gratitude.

My deepest thanks go to everyone who contributed in any way to this work. I do not mention them individually to avoid injustice, but each contribution is valued and remembered with gratitude.

Thank you for the assistance provided by USDA Hatch 7003279 through the Cardoso Lab at NCSU.

This study was financed in part by the Coordenação de Aperfeiçoamento de Pessoal de Nível Superior – Brasil (CAPES) – Finance Code 001.

ABSTRACT

OLIVEIRA, Leonardo Araujo, D.Sc., Universidade Federal de Viçosa, February, 2024. **On the use of genetic parameters and stomatal distribution to improve drought tolerance in Eucalyptus**. Adviser: Samuel Cordeiro Vitor Martins. Co-advisers: Amanda Ávila Cardoso, Genaina Aparecida de Souza and Fabio Murilo da Matta.

By having stomata on both leaf surfaces, amphistomatic species increase stomatal conductance to CO2 to achieve higher photosynthetic rates; however, the potential for greater water loss from the leaves also increases. In Eucalyptus, this is particularly interesting because amphistomatic Eucalyptus are common in more arid environments. Therefore, in this study, we investigated whether amphistomatic Eucalyptus species exhibit greater water supply and/or greater leaf resistance to drought than hypostomatic species to compensate for their "leaky" leaves. The only leaf-level drought resistance mechanisms observed in amphistomatous species were a higher modulus of elasticity, greater capacitance, and almost erect leaves. The higher rates of residual water loss, not accompanied by an increase in water distribution efficiency or leaf desiccation protection mechanisms, associated with the drier environments where amphistomatic eucalypts are common, suggest that these species may be more vulnerable to drought compared to hypostomatic species. In addition, we used the database generated during the characterization of seven of the eight species used in the previous study, applying the REML (Restricted Maximum Likelihood) / BLUP (Best Linear Unbiased Prediction), which makes it possible to estimate the variance components and predict the genetic values of individuals, as well as estimating genetic parameters such as heritability, accuracy and coefficient of genotypic variation. We carried out this analysis on anatomical variables, gas exchange, water relations, allometry, and growth, as well as the content of compounds from the metabolism. This information, which is scarce in the literature, indicates interesting characteristics for inclusion in breeding programs, speeding up the development of genotypes adapted to different environmental conditions from the juvenile stage. Reducing the time needed to develop new genotypes and increasing the efficiency of breeding programs.

Keywords: amphistomatic; hypostomatic; eucalyptus; leaf residual water loss; heritability; accuracy; plant breeding.

RESUMO

OLIVEIRA, Leonardo Araujo, D.Sc., Universidade Federal de Viçosa, fevereiro de 2024. **Sobre a utilização de parâmetros genéticos e da distribuição estomática para melhorar a tolerância à seca em eucalipto**. Orientador: Samuel Cordeiro Vitor Martins. Coorientadores: Amanda Ávila Cardoso, Genaina Aparecida de Souza e Fabio Murilo da Matta.

Devido à presença de estômatos em ambas as superfícies foliares, as espécies anfistomáticas possuem maior condutância estomática (gs) ao CO2 para atingir taxas fotossintéticas mais elevadas; no entanto, o potencial para uma maior perda de água nas folhas também aumenta. Em Eucalyptus, isto é particularmente interessante porque os Eucalyptus anfistomáticos são comuns em ambientes mais áridos. Assim, neste estudo, investigámos se as espécies anfistomáticas de Eucalyptus apresentam um maior fornecimento de água e/ou uma maior resistência das folhas à seca do que as espécies hipostomáticas para compensar as suas folhas "com vazamentos". E os únicos mecanismos de resistência à seca ao nível da folha observados nas espécies anfistomáticas foram um maior módulo de elasticidade, uma maior capacitância e folhas quase erectas. As maiores taxas de perdas residuais de água, não acompanhadas por aumento da eficiência na distribuição de água nem por mecanismos de proteção contra a dessecação das folhas, associadas aos ambientes mais secos onde os eucaliptos anfistomáticos são comuns, sugerem que essas espécies podem ser mais vulneráveis à seca em comparação com as espécies hipostomáticas. Além disso, usamos o banco de dados gerado durante a caracterização de sete das oito espécies utilizadas no estudo anterior, aplicando a metodologia REML (Máxima Verosimilhança Restrita) / BLUP (Melhor Previsão Linear Não Enviesada), que permite estimar os componentes de variância e prever os valores genéticos dos indivíduos, além de estimar de parâmetros genéticos como herdabilidade, acurácia e coeficiente de variação genotípica. Fizemos esta análise em variáveis anatômicas, de trocas gasosa, de relações hídricas, de alometria e crescimento, além de teores de compostos do metabolismo primário foliar. Essas informações, escassas na literatura, indicam características interessantes para inclusão em programas de melhoramento genético, acelerando o desenvolvimento de genótipos adaptados a diferentes condições ambientais desde a fase juvenil. Reduzindo o tempo necessário para desenvolver novos genótipos e aumentando a eficiência dos programas de melhoramento.

Palavras-chave: anfiestomatia; hipoestomatia; eucalipto; perda residual de agua da folha; herdabilidade; acurácia; melhoramento vegetal.

LIST OF ACRONYMS AND ABBREVIATIONS

A	Net assimilation rate
Acc	Accuracy
Amin	Amino acid content
$\mathrm{A}_{\mathrm{sapwood}}$	Sapwood cross-sectional area
b	Lumen breadth
BLUP	Best linear unbiased prediction
Carot	Carotenoid content
C_{i}	Intercellular CO_2 concentration
C_{FT}	Leaf capacitance at full turgor
Chlor *a*	Chlorophyll *a* content
Chlor *b*	Chlorophyll *b* content
C_{TLP}	Leaf capacitance after turgor loss point
CVg	Genotypic coefficient of variation
D	Stem diameter
$\mathrm{D}_{\mathrm{hSperry}}$	Sperry hydraulic vessel diameter
DM	Dry mass
D_{s}	Stomatal density
E	Transpiration rates
ETR	Electron transport rate
FOV	Field of view
Fruct	Fructose content
Gluc	Glucose content
$g_{\mathrm{leaf\text{-}res}}$	Leaf residual conductance
g_{s}	Stomatal conductance to H_2O
g_{wmax}	Maximum theoretical stomatal conductance to water vapor
H	Plant height
h^2	Heritability
H_{V}	Huber value
IS	Intercellular space
K_{leaf}	Leaf hydraulic conductance
K_{plant}	Whole-plant hydraulic conductance
K_{t}	Theoretical hydraulic conductance

LBT	Leaf blade thickness
LMA	Leaf mass per area
LRT	Likelihood ratio test
n	Sample size
N_{XV}	Number of xylem vessels
Prol	Proline content
Prot	Protein content
P_{50}	Water potential at 50% cumulative embolism
P_{88}	Water potential at 88% cumulative embolism
PLRC	Percentage loss of leaf rehydration capacity
$PLRC_{50}$	Leaf water potential at 50% decline in PLRC
PPFD	Photosynthetic photon flux density
R_d	Dark respiration
REML	Restricted maximum likelihood
RWC	Relative water content
RWC_{TLP}	Relative water content at the turgor loss point
SD	Stomatal density
SD_{Aba}	Abaxial stomatal density
SD_{Ada}	Adaxial stomatal density
S_{Den}	Specific density of the stem
SD_{Total}	Total stomatal density
SE	Standard error
SLA	Specific leaf area
$SMRI_{50}$	Stomatal margin retention index
SSM_{50}	Stomatal safety margin
Starch	Starch content
Suc	Sucrose content
S_{Vol}	Stem volume
SWC	Saturated water content
t	Cell wall thickness
TDM	Total dry mass
T_{LA}	Total leaf area
TLE	Thickness of the lower epidermis
TLP	Thickness of lacunose parenchyma

TPP	Thickness of palisade parenchyma
TUE	Thickness of the upper epidermis
$(t/b)^2$	Cell wall thickness to lumen breadth ratio
t_{leaf_crit}	Critical time for leaf death
Ve	Environmental variance
Vp	Phenotypic variance
Vg	Genetic variance
V_D	Vein density
VPD	Vapor pressure deficit
WUE_i	Intrinsic water use efficiency
XA	Xylem area
XLA	Xylem area to leaf area ratio

LIST OF SYMBOLS

ε	Bulk modulus of elasticity
Ψ_{100}	Osmotic potential at full turgor
Ψ_{Midday}	Midday leaf water potential
$\Psi_{Predawn}$	Predawn leaf water potential
Ψ_{TLP}	Water potential at turgor loss point
Ψ_{w}	Leaf water potential

SUMMARY

GENERAL INTRODUCTION

Eucalyptus is the most widely planted species worldwide, especially in tropical and subtropical regions (Myburg et al. 2014, Messier et al. 2022), probably covering more than 20 million hectares worldwide (Rejmánek and Richardson 2011). However, climate change has led to rising temperatures and changing rainfall patterns, which are two of the conditions that most affect plant growth (Trenberth et al. 2014). This can even lead to the mortality of these forests, which was evident in 2015 in the state of Minas Gerais, in southeastern Brazil, where drought events caused the mortality of approximately 2,000 km^2 of eucalyptus plantations (Gonçalves et al. 2017), highlighting the vulnerability of these systems to environmental changes. In addition, Barros Filho (2014) reported that, after the drought event, it was possible to observe the differential mortality of eucalyptus clones. This highlights the imminent threat of mortality in the face of drought and the existence of genetic variability in drought tolerance in eucalyptus. Therefore, identifying the traits that lead to differential responses to water deficit conditions among eucalyptus is paramount. This knowledge is crucial not only for properly allocating species according to their suitability but also for aiding in the development of more productive and tolerant plants through genetic improvement (Marcatti et al. 2017, Binkley et al. 2018). This has led to the emergence of new approaches to selecting promising materials for regions where the risk of periods of drought may increase in the future.

Stomatal distribution plays a crucial role in regulating CO_2 balance and water loss in plant leaves, influencing their photosynthetic efficiency and response to drought (Hetherington and Woodward 2003). In the context of eucalyptus species, anatomical, physiological, and hydraulic characteristics are intrinsically related to their ability to adapt to variable environmental conditions, including drought tolerance (Oliveira et al. 2022), as well as directly influencing their productivity in conditions of both drought and optimal water availability. Although amphistomaty (the presence of stomata on both leaf faces) is found in around 130 eudicot families (Metcalfe et al. 1951), it is relatively rare, being more common in fast-growing herbaceous species (Metcalfe et al. 1951, Parkhurst 1978), plants from desert environments in western North America (Mott et al. 1982, Gibson 1996) and in eucalyptus trees in arid zones (Wood 1934, de Boer et al. 2016). According to de Boer et al. (2016), of the 73 species and subspecies of eucalyptus studied in an aridity gradient in southwestern Australia, 67 are amphistomatic. This finding raises questions about what characteristics enable these plants to better adapt to such environments compared to hypoestomatic ones, as well as the costs and benefits associated with amphistomaty.

Amphistomaty increases the number of stomata per epidermal area and can result in increases of up to 20% in photosynthetic rates (A) (Parkhurst and Mott 1990, Beerling and Kelly 1996, Franks et al. 2009); however, increasing the stomatal conductance (g_s) comes at the cost of increased water loss through transpiration as well. If this water loss is not promptly compensated for by the plant's internal water supply system, the stomata will close to decrease g_s (Andrade et al. 2022). Although the higher number of stomata increases the maximum theoretical stomatal conductance to water vapor (g_{wmax}), actual g_s is ultimately limited by the hydraulic efficiency and/or water storage capacity of the plant (Brodribb and Holbrook 2006, Brodribb et al. 2007, Caringella et al. 2015, Scoffoni et al. 2016, Machado et al. 2021). When soil water supply decreases, stomata gradually close to regulate water loss and prevent leaf dehydration (Drake et al. 2013, Martin-StPaul et al. 2017a, Buckley 2019, Márquez et al. 2022, Blackman et al. 2023). However, even with the transpiration process minimized, leaves still lose water through leakage at two main sites: cuticle and stomata (Kerstiens, 1996b, Richardson et al. 2007, Bueno et al. 2019). This inevitable water leakage has a major impact on water use and conservation strategies among species (Kerstiens, 1996a, Martin-StPaul et al. 2017, Duursma et al. 2019, Machado et al. 2021). It can lead plant tissues to hydraulic failure and, consequently, to their death (Martin-StPaul et al. 2017, Machado et al. 2021). As amphistomatic leaves exhibit greater stomatal densities, they also tend to have higher $g_{leaf\text{-}res}$ (Muchow & Sinclair, 1989, Machado et al. 2021). Therefore, it is expected that these leaves possess compensatory mechanisms to mitigate the increased potential water loss. However, studies addressing this issue are still scarce.

Understanding the different physiological processes and the interrelationship among the structures and functions of plant tissues is of paramount importance to identify which characteristics can confer greater tolerance to adverse conditions. This information can be used through genetic improvement to develop ideotypes for multiple purposes (Scolforo et al. 2017, Marcatti et al. 2017, Binkley et al. 2018), often during their juvenile stages. This can contribute to reducing the time needed to develop new genotypes, given that the forest genetic improvement process is known to be time-consuming, and characterized by long reproductive cycles (Castro et al. 2021).

In addition to identifying the traits of interest, it is crucial to determine whether these traits are heritable and whether there is genotypic variability among the studied genotypes for that specific trait. The information available is scarce, and the limited data available comes from plants grown in different locations, at different ages, and using a variety of measurement methods for the same trait (Pita-Barbosa et al. 2023). To get around this limitation, we used the REML (Restricted Maximum Likelihood) / BLUP (Best Linear Unbiased Prediction) methodology, which makes it possible to estimate variance components and predict genetic values for individuals (Resende 2009, 2015). Using this approach, we estimated genetic parameters for traits such as leaf anatomy, gas exchange, water relations, growth, and basic metabolism in seven eucalyptus species, including six of the nine most cultivated species in the world (*E. camaldulensis*, *E. tereticornis*, *E. pellita*, *E. grandis*, *E. urophylla* and *E. dunnii*) (Stanturf et al. 2013, Seng Hua et al. 2022). We aimed to select the most relevant traits to be used in phenotyping promising genotypes, to facilitate decision-making and enhance the efficiency of eucalyptus breeding programs.

REFERENCES

Andrade MT, Oliveira LA, Pereira TS, Cardoso AA, Batista-Silva W, Damatta FM, Zsögön A, Martins SCV (2022) Impaired auxin signaling increases vein and stomatal density but reduces hydraulic efficiency and ultimately net photosynthesis. J Exp Bot 73:4147–4156.

Barros Filho NF (2014) Discriminação isotópica do 13C e nutrição com cálcio e boro em clones de eucalipto submetidos ao défice hídrico. Federal University of Viçosa, Viçosa

Beerling DJ, Kelly CK (1996) Evolutionary comparative analyses of the relationship between leaf structure and function. New Phytologist 134:35–51.

Binkley D, Campoe OC, Alvares C, Carneiro RL, Cegatta Í, Stape JL (2018) The interactions of climate, spacing and genetics on clonal *Eucalyptus* plantations across Brazil and Uruguay. For Ecol Manage 405:271–283.

Blackman CJ, Halliwell B, Hartill GE, Brodribb TJ (2023) Petiole XLA (xylem to leaf area ratio) integrates hydraulic safety and efficiency across a diverse group of eucalypt leaves. Plant Cell Environ 47:49–58.

de Boer HJ, Price CA, Wagner-Cremer F, Dekker SC, Franks PJ, Veneklaas EJ (2016) Optimal allocation of leaf epidermal area for gas exchange. New Phytologist 210:1219–1228.

Brodribb TJ, Feild TS, Jordan GJ (2007) Leaf maximum photosynthetic rate and venation are linked by hydraulics. Plant Physiol 144:1890–1898.

Brodribb TJ, Holbrook NM (2006) Declining hydraulic efficiency as transpiring leaves desiccate: Two types of response. Plant Cell Environ 29:2205–2215.

Buckley TN (2019) How do stomata respond to water status? New Phytologist 224:21–36.

Bueno A, Alfarhan A, Arand K, Burghardt M, Deininger AC, Hedrich R, Leide J, Seufert P, Staiger S, Riederer M. 2019. Effects of temperature on the cuticular transpiration barrier of two desert plants with water-spender and water-saver strategies. Journal of Experimental Botany 70: 1613–1625.

Caringella MA, Bongers FJ, Sack L (2015) Leaf hydraulic conductance varies with vein anatomy across *Arabidopsis thaliana* wild-type and leaf vein mutants. Plant Cell Environ 38:2735–2746.

Castro CAO, dos Santos GA, Takahashi EK, Nunes ACP, Souza GA, Resende MDV (2021) Accelerating *Eucalyptus* breeding strategies through top grafting applied to young seedlings. Ind Crops Prod 171

Drake PL, Froend RH, Franks PJ (2013) Smaller, faster stomata: Scaling of stomatal size, rate of response, and stomatal conductance. J Exp Bot 64:495–505.

Duursma RA, Blackman CJ, Lopéz R, Martin-StPaul NK, Cochard H, Medlyn BE (2019) On the minimum leaf conductance: its role in models of plant water use, and ecological and environmental controls. New Phytologist 221:693–705.

Franks PJ, Drake PL, Beerling DJ (2009) Plasticity in maximum stomatal conductance constrained by negative correlation between stomatal size and density: An analysis using *Eucalyptus* globulus. Plant Cell Environ 32:1737–1748.

Gibson AC (1996) Structure-Function Relations of Warm Desert Plants. Springer Berlin Heidelberg, Berlin, Heidelberg.

Global Forest Resources Assessment 2020 (2020) FAO.

Gonçalves JLM, Alvares CA, Rocha JHT, Brandani CB, Hakamada R (2017) Eucalypt plantation management in regions with water stress. South For 79:169–183.

Hetherington AM, Woodward & FI (2003) The role of stomata in sensing and driving environmental change. Nature 424:901–908.

Kerstiens G. 1996a. Cuticular water permeability and its physiological significance. Journal of Experimental Botany 47: 1813–1832.

Kerstiens G. 1996b. Signalling across the divide: a wider perspective of cuticular structure-function relationships. Trends in Plant Science 1: 125–129.

Machado R, Loram-Lourenço L, Farnese FS, Alves RD, de Sousa LF, Silva FG, Filho SC, Torres-Ruiz JM, Cochard H, Menezes-Silva PE. Where do leaf water leaks come from? Trade-offs underlying the variability in minimum conductance across tropical savanna species with contrasting growth strategies. New Phytologist. 2021 Feb;229(3):1415-30.

Marcatti GE, Resende RT, Resende MD V., Ribeiro CAAS, dos Santos AR, da Cruz JP, Leite HG (2017) GIS-based approach applied to optimizing recommendations of *Eucalyptus* genotypes. For Ecol Manage 392:144–153.

Márquez DA, Stuart-Williams H, Farquhar GD, Busch FA (2022) Cuticular conductance of adaxial and abaxial leaf surfaces and its relation to minimum leaf surface conductance. New Phytologist 233:156–168.

Martin-StPaul N, Delzon S, Cochard H (2017) Plant resistance to drought depends on timely stomatal closure. Ecol Lett 20:1437–1447.

Messier C, Bauhus J, Sousa-Silva R, Auge H, Baeten L, Barsoum N, Bruelheide H, Caldwell B, Cavender-Bares J, Dhiedt E, Eisenhauer N, Ganade G, Gravel D, Guillemot J, Hall JS, Hector A, Hérault B, Jactel H, Koricheva J, Kreft H, Mereu S, Muys B, Nock CA, Paquette A, Parker JD, Perring MP, Ponette Q, Potvin C, Reich PB, Scherer-Lorenzen M, Schnabel F, Verheyen K, Weih M, Wollni M, Zemp DC (2022) For the sake of resilience and multifunctionality, let's diversify planted forests! Conserv Lett 15

Metcalfe C R., Chalf L., Chattaway M M., Hare C L., Richardson R F., Slatter E M. (1951) Anatomy of the dicotyledons. leaves, stem, and wood in relation to taxonomy, with notes on economic uses.

Mott KA, Gibson AC, O'Leary JW (1982) The adaptive significance of amphistomatic leaves. Plant Cell Environ 5:455–460.

Muchow RC, Sinclair TR. 1989. Epidermal conductance, stomatal density and stomatal size among genotypes of Sorghum bicolor (L.) Moench. Plant, Cell & Environment 12: 425–431.

Myburg AA, Grattapaglia D, Tuskan GA, Hellsten U, Hayes RD, Grimwood J, Jenkins J, Lindquist E, Tice H, Bauer D, Goodstein DM, Dubchak I, Poliakov A, Mizrachi E, Kullan ARK, Hussey SG, Pinard D, Van Der Merwe K, Singh P, Van Jaarsveld I, Silva-Junior OB, Togawa RC, Pappas MR, Faria DA, Sansaloni CP, Petroli CD, Yang X, Ranjan P, Tschaplinski TJ, Ye CY, Li T, Sterck L, Vanneste K, Murat F, Soler M, Clemente HS, Saidi N, Cassan-Wang H, Dunand C, Hefer CA, Bornberg-Bauer E, Kersting AR, Vining K, Amarasinghe V, Ranik M, Naithani S, Elser J, Boyd AE, Liston A, Spatafora JW, Dharmwardhana P, Raja R, Sullivan C, Romanel E, Alves-Ferreira M, Külheim C, Foley W, Carocha V, Paiva J, Kudrna D, Brommonschenkel SH, Pasquali G, Byrne M, Rigault P, Tibbits J, Spokevicius A, Jones RC, Steane DA, Vaillancourt RE, Potts BM, Joubert F, Barry K, Pappas GJ, Strauss SH, Jaiswal P, Grima-Pettenati J, Salse J, Van De Peer Y, Rokhsar DS, Schmutz J (2014) The genome of *Eucalyptus grandis*. Nature 510:356–362.

Oliveira LA, Cardoso AA, Andrade MT, Pereira TS, Araújo WL, Santos GA, Damatta FM, Martins SCV (2022) Exploring leaf hydraulic traits to predict drought tolerance of *Eucalyptus* clones. Tree Physiol 42:1750–1761.

Parkhurst DF (1978) The adaptive significance of stomatal occurrence on one or both surfaces of leaves. Journal of Ecology 66:367–383.

Parkhurst DF, Mott KA (1990) Intercellular diffusion limits to CO_2 uptake in leaves. Plant Physiol 94:1024–1032.

Pita-Barbosa A, Oliveira LA, de Barros NF, Hodecker BER, Oliveira FS, Araújo WL, Martins SCV (2023) Developing a roadmap to define a potential ideotype for drought tolerance in *Eucalyptus*. Forest Science 69:101–114.

Rejmánek M, Richardson DM (2011) The eucalypts. In: Rejmánek M, Richardson DM (eds) Encyclopedia of biological invasions. University of California Press, Berkeley and Los Angeles, pp 203–209.

Resende MDV (2009) Genética biométrica e estatística no melhoramento de plantas perenes, First. Embrapa.

Resende MDV (2015) Genética quantitativa e de populações, 1st edn. Editora UFV, Viçosa.

Richardson A, Wojciechowski T, Franke R, Schreiber L, Kerstiens G, Jarvis M, Fricke W. 2007. Cuticular permeance in relation to wax and cutin development along the growing barley (Hordeum vulgare) leaf. Planta 225: 1471–1481.

Scoffoni C, Chatelet DS, Pasquet-Kok J, Rawls M, Donoghue MJ, Edwards EJ, Sack L (2016) Hydraulic basis for the evolution of photosynthetic productivity. Nat Plants 2

Scolforo HF, Scolforo JRS, Stape JL, McTague JP, Burkhart H, McCarter J, de Castro Neto F, Loos RA, Sartorio RC (2017) Incorporating rainfall data to better plan eucalyptus clones deployment in eastern Brazil. For Ecol Manage 391:145–153.

Seng Hua L, Wei Chen L, Antov P, Kristak L, Md Tahir P (2022) Engineering wood products from *Eucalyptus* spp. Advances in Materials Science and Engineering 2022

Stanturf JA, Vance ED, Fox TR, Kirst M (2013) *Eucalyptus* beyond Its Native Range: Environmental Issues in Exotic Bioenergy Plantations. International Journal of Forestry Research 2013:1–5.

Trenberth KE, Dai A, Van Der Schrier G, Jones PD, Barichivich J, Briffa KR, Sheffield J (2014) Global warming and changes in drought. Nat Clim Chang 4:17–22.

Wood JG (1934) The physiology of xerophytism in Australian plants: the stomatal frequencies, transpiration and osmotic pressures of sclerophyll and tomentose-succulent leaved plants. Journal of Ecology 22:69–87.

CHAPTER 1: Amphistomaty in Eucalyptus is decoupled from greater water supply and leaf resistance to drought

Leonardo A. Oliveira, Talitha S. Pereira, Eduardo J. Haverroth, Moab T. Andrade, Pablo H. N. Carvalho, Genaina A. Souza, Amanda A. Cardoso, Samuel C. V. Martins

ABSTRACT

By having stomata on both leaf surfaces, amphistomatic species increase the stomatal conductance (g_s) to CO_2 to achieve higher photosynthetic rates; however, the potential for higher leaf water loss is also increased. In *Eucalyptus* this is particularly interesting because amphistomatic *Eucalyptus* are common in more arid environments. Therefore, in this study, we investigated whether amphistomatic eucalyptus species have a greater water supply and/or higher leaf resistance to drought compared to hypostomatic species. We aimed to determine if these traits compensate for the higher stomatal density and consequent increased water loss. Amphistomatic species displayed both higher g_s and leaf residual conductance than hypostomatic ones; however, the higher g_s were not sustained by a greater water supply at the leaf or branch level when compared with hypostomatic leaves. Amphistomatic leaves also did not exhibit higher embolism resistance, nor were they able to sustain rehydration capacity at lower water potentials. The only drought resistance mechanisms at the leaf level in amphistomatic species were higher modulus of elasticity, higher capacitance, and nearly erect leaves. These findings are surprising, especially considering the prevalence of amphistomatic *Eucalyptus* in drier environments. They suggest that these leaves may be more vulnerable to drought compared to hypostomatic species. Amphistomatous species may possess tolerance or avoidance mechanisms at the stem or root level, such as a deeper root system, which could mitigate the xylem vulnerability observed in their leaves.

INTRODUCTION

Stomata are tiny pores on the leaf epidermis that regulate CO_2 uptake and water loss (Hetherington & Woodward 2003). Depending on where stomata can be found (lower, upper, or both leaf surfaces) species are classified into hypostomatic, epistomatic, or amphistomatic (Parkhurst 1978). Although amphistomaty is found in 130 Eudicot families (Metcalfe et al. 1951), species with amphistomatic leaves are relatively rare compared to those with hypostomatic leaves. Overall, amphistomaty is mainly associated with fast-growing annual herbs, a small number of shrubs, and evergreen trees (Salisbury 1927, Wood 1934, Metcalfe et al. 1951, Parkhurst 1978, de Boer et al. 2016). Interestingly, amphistomaty is also found in some water-limited environments such as desert plants in western North America (Mott, Gibson & O'Leary 1982; Gibson 1996) and eucalyptus trees in arid zones (Wood 1934; de Boer et al. 2016). According to de Boer et al. (2016), of the 73 species and subspecies of eucalyptus studied in an aridity gradient in southwestern Australia, 67 are amphistomatic.

The distribution of stomata in both leaf surfaces makes it possible to increase the number of stomata per area of the epidermis. It is believed that amphistomaty may be responsible for increasing maximum photosynthetic rates by up to 20% (Parkhurst & Mott 1990; Beerling & Kelly 1996; Franks, Drake & Beerling 2009). In addition, it has been suggested that amphistomaty may reduce the resistance of the leaf boundary layer (Foster & Smith 1986; Baresch et al. 2019; Xiong & Flexas 2020) and increase mesophyll conductance, an important factor limiting photosynthesis (Parkhurst 1978, Flexas et al. 2008, de Boer et al. 2012, Drake et al. 2019). The greater presence of stomata and increased conductance to CO_2 would be an advantageous evolutionary adaptation in open environments with excess light, where CO_2 concentration can be a limiting factor for photosynthetic rates (A) (Parkhurst 1978, Mott et al. 1982, Carpenter 1994, Brodribb et al. 2013, Jordan et al. 2014, Muir 2018).

Increasing the stomatal conductance (g_s) might allow higher A, however, it comes at the cost of increasing water loss through transpiration as well. If this water loss is not promptly compensated for by the plant's internal water supply system, the stomata will close to decrease g_s (Andrade et al. 2022). Therefore, maximum g_s is limited by the availability of water in leaf tissues, which is influenced primarily by leaf hydraulic conductance (K_{leaf}) (Brodribb and Holbrook 2006, Brodribb et al. 2007, Caringella et al. 2015, Scoffoni et al. 2016). It has been shown that higher K_{leaf} sustains higher rates of g_s and, therefore, A (Brodribb et al. 2007, Scoffoni et al. 2016, McAdam et al. 2017). Even when not limited by K_{leaf}, if the soil water supply decreases, stomata will gradually close to regulate water loss and prevent leaf dehydration (Drake et al. 2013, Martin-StPaul et al. 2017, Buckley 2019, Márquez et al. 2022, Blackman et al. 2023). However, even with the transpiration process minimized, leaves still lose water through leakage at two main sites: cuticle and stomata (Kerstiens, 1996b, Richardson et al. 2007, Bueno et al. 2019).

The residual water loss is called leaf residual conductance ($g_{leaf\text{-}res}$) and is particularly important for water use and conservation strategies among species (Kerstiens, 1996, Martin-StPaul et al. 2017, Duursma et al. 2019, Machado et al. 2021). Once $g_{leaf\text{-}res}$ is responsible for the water losses and slowly depletes internal water stores (thus decreasing water potentials), it dictates the time it takes to reach hydraulic failure (Muchow and Sinclair 1989, Martin-StPaul et al. 2017, Mantova et al. 2022). Hydraulic failure occurs when the plant's water transport system suffers an extensive embolism, measured in leaves and stems as the water potential associated with a 50% loss of hydraulic function (P_{50}), and has been extensively used as a proxy for drought tolerance (Brodribb et al. 2014, Blackman et al. 2016, Griffin-Nolan et al. 2019, Ocheltree et al. 2020, Oliveira et al. 2022, Huang et al. 2024). As amphistomatic leaves exhibit greater stomatal densities, they also tend to have higher $g_{leaf\text{-}res}$ (Muchow & Sinclair, 1989, Machado et al. 2021), since the stomata are the main entry and exit points through which gas exchange occurs, although they represent a small percentage of the leaf area (Lange et al. 1971). Therefore, it is expected that these leaves possess compensatory mechanisms to mitigate the increased potential water loss. However, studies addressing this issue are still scarce.

Comprehending the impact of stomatal distribution on other functional traits is crucial for understanding the advantages and limitations of amphistomatic leaves. The main objectives of this study were (i) to investigate whether amphistomatic leaves possess a more efficient hydraulic system, enabling them to maintain an adequate water supply to sustain higher g_s, and (ii) to determine if amphistomatic leaves exhibit tolerance mechanisms at the leaf level to compensate for their greater water loss. To achieve these goals, we conducted experiments using *Eucalyptus* species with hypostomatic and amphistomatic leaves grown in a common garden. This approach allowed us to account for genetic variation between amphistomatic and hypostomatic groups while minimizing the phenotypic variation across species (de Villemereuil et al. 2016, Li et al. 2018). Four amphistomatic and four hypostomatic species were selected (Table 1) and six of them rank globally among the nine most widely planted *Eucalyptus* (Seng Hua et al. 2022).

MATERIAL AND METHODS

Plant material and growing conditions

In this study, *Eucalyptus* species with amphistomatic and hypostomatic leaves were compared (Table 1). Species with amphistomatic leaves included *E. camaldulensis*, *E. tereticornis*, *E. pellita*, *E. cinerea*. Species with hypostomatic leaves were *E. grandis*, *E. urophylla*, *E. dunnii* and *E. pilularis*. Noteworthy, six of these species - *E. camaldulensis*, *E. tereticornis*, E. *pellita*, *E. grandis*, *E. urophylla*, and *E. dunnii*) - are among the most widely planted Eucalyptus species worldwide (Seng Hua et al. 2022).

Saplings with 120-day-old were obtained from the Sociedade de Investigações Florestais/Universidade Federal de Viçosa (UFV) nursery and grown in the gardens of the UFV, located in Viçosa (20°45'S, 42°54'W, 650 m altitude), southeast Brazil between June and December of 2021. The saplings were transplanted into 20 L pots (one plant per pot) containing soil, washed sand, and commercial substrate Tropstrato HT® (3:2:1, v:v:v). Plants were irrigated daily to field capacity and fertilized according to the recommendations for the crop. They were maintained under natural light conditions with a photosynthetic photon flux density (PPFD) ranging from 1,000 to 1,500 μmol m^{-2} s^{-1}), temperatures ranging from 22 to 26°C maximum and 13 to 19°C minimum, and air humidity ranging from 90 to 98% maximum and 40 to 55% minimum. Light intensity was measured between 11:00 and 13:00 h (solar time) using a quantum sensor (LI-191R; LI-COR, Lincoln, NE, USA). Temperature and relative humidity data were obtained from the automatic meteorological station in Viçosa. Data are available on the National Meteorological Institute of Brazil website (https://portal.inmet.gov.br/dadoshistoricos). Measurements and samplings were performed when plants were at the age of seven months. Six individual plants (n = 6) per species were utilized. Fully expanded leaves were sampled from lateral branches located in the middle third of the canopy, and branches were sampled from the same region.

Characterization of the climate of origin

To characterize the climatic conditions of the species center of diversity, geographic points were extracted throughout the distribution area of each species from records available in the Atlas of Living Australia (https://www.ala.org.au/). To avoid oversampling effects, latitude and longitude were rounded to the nearest 0.25 degrees, and duplicate species-location combinations were removed. Subsequently, average annual precipitation was extracted from WorldClim (https://www.worldclim.org/), which represents average annual and seasonal trends and extremes between the years 1970 and 2000 (Fick and Hijmans 2017), using QGIS 3.0 (QGIS Development Team, 2018) for each coordinate. The aridity index was calculated as the annual potential evapotranspiration divided by the average annual precipitation. Annual potential evapotranspiration was taken from the CGIAR Consortium for Spatial Information (Zomer et al. 2008) and was the 1950-2000 annual average modeled from WorldClim for a 30″ grid containing genotype provenance locations (https://cgiarcsi.community/data/global-aridity-and-pet-database).

Anatomy of leaves and petioles

Completely expanded leaves were fixed in FAA_{50} (Johansen 1940) for 48 h and stored in 70% ethanol (v:v). Subsamples of leaves and petioles (or leaf midrib close to the branch insertion for *E. cinerea*) were embedded in methacrylate according to the manufacturer's recommendations (Leica Microsystems Nussloch, Heidelberg, Germany), cross-sectioned into 5 µm thick sections using an automatic advance rotary microtome (Leica RM2155, Leica Microsystems Inc., Derfild, USA), stained with toluidine blue (O'brien et al. 1964), and mounted in synthetic resin (Permount®). In addition, leaf samples of approximately 200 mm^2 were collected from the middle portion of each leaf, avoiding the central vein, clarified by the method of de Strittmatter (1973), and mounted in glycerinated gelatin to obtain images for quantifying vein density and stomatal characteristics.

The images were taken using a light microscope (AX70 TRF, Olympus Optical, Tokyo, Japan) coupled with a digital camera (Zeiss AxioCam HRc, Göttingen, Germany). Five fields of view (FOV) were obtained from each diaphanization sample at 4x magnification to measure vein density. Vein density was calculated as the total length of second, third, fourth, fifth, and sixth-order veins divided by the FOV area. Additionally, five FOV at 20x magnification were captured to measure stomatal size (on both surfaces), and stomatal densities, including abaxial stomatal density ($SD_{Abaxial}$), adaxial stomatal density ($SD_{Adaxial}$), and total stomatal density (SD_{Total}), which is the sum of $SD_{Abaxial}$ and $SD_{Adaxial}$. The length of the guard cells was measured to calculate the maximum theoretical stomatal conductance to water vapor (g_{wmax}) according to Franks et al. (2009):

$$g_{wmax} = SD_{Total}\, d_w\, a \,/\, [v(l+\pi/2\sqrt{(a/\pi)})]$$

where d_W if the diffusivity of water vapor in air, a is the maximum area of the open stomatal pore, v is the molar volume of air, and l is the stomatal pore depth for fully open stomata. The standard constants d_W and v were determined for 25°C and are $24.9\times10^{-6}\ m^2\ s^{-1}$ and $24.4\times10^{-3}\ m^3\ mol^{-1}$, respectively. The maximum area of the open stomatal pore (a) was calculated as $\pi(p/2)^2$, where p is the stomatal pore length, approximated as guard cell length (L)/2 based on Franks and Farquhar (2001) method. The value of l for fully open stomata was assumed to be L/4, assuming guard cells inflate to a circular cross-section, as suggested by Franks et al. (2009).

From the leaf cross-section, three FOVs with 10x magnification were captured. The thickness of the abaxial and adaxial epidermis, the leaf blade thickness, and the thickness of the palisade and spongy parenchyma were measured in five parts of the lamina in each FOV. The percentage of intercellular space was determined by calculating the proportion of intercellular spaces to the entire internal area of the leaf blade.

From the cross-sections of the petiole, one FOV was obtained with a 10x magnification. The number of xylem vessels and long and short internal vessel diameters were measured. Based on the diameters of the vessel elements, Sperry hydraulic diameter (Dh_{Sperry}) was calculated using the following equations (Lewis and Boose 1995):

$$D_h=\sqrt{\frac{2a^2b^2}{a^2+b^2}}$$

where a and b represent the long and short internal vessel diameters, respectively, and n is the viscosity of water at 25°C. Dh_{Sperry} was calculated using the following equation (Sperry and Ikeda 1997):

$$\mathrm{Dh}_{\mathrm{Sperry}}=\frac{1}{n}\Sigma_{1}^{n}\left(\frac{Dh^{5}}{Dh^{4}}\right)_{i}$$

where n represents the number of xylem vessels in the sample, 1 represents the first xylem vessel of the sample, and *i* represents all xylem vessels of the sample.

The total xylem area (XA) of the petiole was measured in one FOV was obtained with a 4x magnification. Each leaf used for anatomical analysis was scanned with a desk scanner and the leaf area was measured using Image J. And the xylem area to leaf area ratio (XLA) was estimated for each leaf as the total XA in cross-section dived by projected leaf area (Blackman et al. 2023).

For an estimation of cell wall thickness to lumen breadth ratio $(t/b)^2$ two FOVs were obtained with a 20x magnification. The wall thickness (t) and corresponding vessel lumen diameter (b) were determined in 20 vessels for each petiole. The cell wall thickness was the medium of four meditations for each xylem vessel and the lumen diameter (b) was a medium from two measurements for each vessel.

Leaf gas exchange

Leaf gas exchange was assessed using a gas exchange system (LI-6400XT, Li-COR, Nebraska, US). The net assimilation rate (A), the stomatal conductance to water vapor (g_s), the transpiration rate (E), and the intercellular CO_2 concentration (C_i) were measured under artificial PPFD of 1000 µmol m^{-2} s^{-1} at the leaf level. All measurements were performed under ambient conditions of relative VPD and CO_2. Intrinsic water use efficiency (WUE_i) was calculated as A over g_s. Dark respiration (R_d) was measured at 08:00 PM using the same gas exchange system, with the chamber temperature set to 25°C.

Leaf residual conductance

The leaf residual conductance ($g_{\text{leaf-res}}$) was measured for intact leaves using the weight loss method for detached leaves (Slavic., 1974, Machado et al., 2021. Sack et al., 2003). Leaves were collected in the late afternoon, placed in ziplock bags, transported to the laboratory, and had their petioles maintained under water for at least 12 h. After this, the petioles were sealed with parafilm tape, and the leaves were weighed on an analytical balance every 15 min for 3 h. Temperature and humidity were monitored for later calculation of the vapor pressure deficit (VPD). Initial and final leaf areas were obtained by scanning and measuring them using Image-Pro Plus 4.5. The $g_{\text{leaf-res}}$ was calculated from the slope of the linear relationship of leaf mass versus time and normalized by leaf area (sum of the adaxial and abaxial projected areas), atmospheric pressure, and VPD. For the slope estimation, only the linear part of the regression was used ($R^2 > 0.99$), suggesting maximal stomatal closure (Billon et al., 2020).

Leaf hydraulic conductance

Leaf hydraulic conductance (K_{leaf}) was measured using the evaporative flow method (Sack et al. 2002, Brodribb and Holbrook 2006). Leaf petioles were cut underwater, connected to a flow meter system (equipped with a 30 PSI pressure transducer, Honeywell International Inc, North Carolina, US), and placed under a light source of c. 1,000 µmol m^{-2} s^{-1} PPFD and fan-induced turbulent air to increase leaf transpiration. Pressure variation, water temperature, and leaf temperature were recorded with a datalogger (Campbell Scientific, Shepshed, LE129GX, UK). E was derived from the tension created within the leaf-driven system through a known and recorded resistance following maximum stability (after c. 30 min). The leaves were then removed from the system, bagged for 10 min (to allow them to equilibrate), and their leaf water potential (Ψ_w) was measured with a pressure chamber (model 1000, PMS Instruments, New York, US). After that, the leaves were scanned, and their area was measured using Image-Pro Plus 4.5. Finally, E was normalized by leaf area, and K_{leaf} was calculated as $K_{\text{Leaf}} = -E / \Psi_w$. Due to the lack of petiole in *E. cinerea*, we could not measure the K_{leaf} of this species.

Pressure-volume curves

Leaves were collected, packed in zip-lock bags containing damp paper towels, and transported to the laboratory. They were cut under water and the petiole remained immersed for approximately 12 h to allow complete rehydration ($\Psi_w < 0.1$ MPa). Leaf mass and Ψ_w measurements were repeated during slow bench dehydration at c. 25°C and c. 60% relative humidity. In the end, leaves were then scanned, and their area was obtained using Image-Pro Plus 4.5. Next, leaves were placed in an oven at c. 70ºC until constant weight (equal to dry weight). Leaf dry weight was used to calculate RWC, and PV curves were constructed by plotting the inverse of Ψ_w against RWC (Tyree & Hammel 1972). The following parameters were estimated from each curve: osmotic potential at full turgor (Ψ_{100}), water potential at turgor loss point (Ψ_{TLP}), relative water content at the point of turgor loss (RWC_{TLP}), leaf capacitance at full turgor (C_{FT}) and after turgor loss point (C_{TLP}) and bulk modulus of elasticity (ε). Additionally, leaf mass per area (LMA) was estimated. Due to the lack of petiole in *E. cinerea*, we couldn't perform pressure-volume curves for this species.

Branch hydraulic conductivity

The native branch hydraulic conductivity (K_{branch}) was measured following the method described by (Sperry et al. 1988). Briefly, branches were cut using pruning shears underwater in a bucket, where they were kept for c. 12 h, covered with black plastic bags. Next, branches were recut underwater on both sides so that a segment of straight and unbranched branches of c. 15 cm was obtained. The segment was connected on one end with a silicone hose coupled to a Milli-Q water reservoir at the height of 1.2 m, providing a hydraulic charge of 0.0118 MPa, and on the other end, connected to a 0.2 mL glass volumetric pipette. After releasing the pressure on the branch, the water flowed through the branch segment, and the flow rate (mL s^{-1}) was calculated from the time required for the water column to advance in the pipette graduation, generating a linear relationship between volume and time, as a function of branch conductivity. For K_{branch} estimation, flow rates were normalized by branch length and sapwood area. The branch base was perfused with 1% Safranin after the measurement. A cross-section was obtained using a razor blade and photographed with a camera (Omax A3550S) attached to a stereomicroscope (LabMotic-EM250, San Antonio, TX, USA). The sapwood cross-sectional area ($A_{sapwood}$) was later determined using the ImageJ software, and K_{branch} was calculated as:

$$K_{branch} = (F/(dP/dx))/A_{sapwood}$$

where F is the flow rate (mol s^{-1}), dP/dx is the pressure gradient, and the $A_{sapwood}$ (m^2) is the average sapwood cross-sectional area at the base of the branch (Tyree and Ewers 1991). The K_{branch} values were corrected for a temperature of c. 25ºC due to changes in the viscosity of the water that occur according to temperature variations of the water, which was measured with a type K temperature sensor.

Huber value

The same branches used to measure K_{branch} were used to determine the Huber value. A small sample from the branch's base was stained with 1% Safranin and photographed using a camera attached to a stereomicroscope, and the images were used to measure the sapwood area using Image Pro Plus 4.5. The total leaf area per branch was measured by scanning the leaves and the Huber value was calculated as the ratio between the sapwood area and the total leaf area of the branch (Huber 1928).

Leaf vulnerability to embolism and hydraulic safety margin

Leaf vulnerability to embolism was determined by the optical vulnerability method (Brodribb et al. 2016). Plants were harvested early in the morning, and their roots were washed until the soil was entirely removed. They were then placed in a bucket filled with water and transferred to the laboratory. The abaxial face of an intact mature leaf still attached to the plant was placed on a scanner (Epson Perfection V800; Epson, California, USA) using clear glass and adhesive tape. Plants were next removed from the bucket and allowed to slowly dehydrate under laboratory conditions (c. 25°C and 60% relative humidity). Images were taken every 3 min, and leaf Ψ_w was measured using a pressure chamber every c. 4 h. Images were obtained up to 5 h after the last embolic event was observed. The image area captured included the midrib and at least eight major (second-order) veins. The stack of images was analyzed using ImageJ, following instructions from http://www.opensourceov.org and Brodribb et al. (2016). The degree of embolism was calculated as the cumulative area of the embolized xylem normalized by the total area of embolism. A linear regression was fitted between drying time and Ψ_w to determine the Ψ_w at the time that each image was captured. Finally, the declines in Ψ_w were plotted against the percentage of the cumulative embolized area (%) for each leaf. For each vulnerability curve, were obtained the Ψ_w at 50% cumulative xylem embolized area (P_{50}). The stomatal safety margin (SSM_{50}) was calculated for each genotype as the difference between Ψ_{TLP} and P_{50}. Given the difficulties in measuring Ψ_w in *E. cinerea*, we didn’t construct optical vulnerability curves for this species.

We then estimated the rate at which the stomatal safety margin was crossed, by considering the rate of water loss after stomatal closure ($g_{leaf\text{-}res}$), denominated stomatal margin retention index ($SMRI_{50}$) was calculated as follows as described in (Petek-Petrik et al. 2023).

Critical time for leaf death index

Using only leaf traits, we modified the index of desiccation time to tree mortality under drought developed by Blackman et al. (2016) to estimate an index representing the critical time for leaf death ($t_{\text{leaf\_crit}}$) after plants reached the turgor loss point, expressed by VPD multiplied by one hour.

$$t_{\text{leaf\_crit}} = \frac{C_{TLP}\ x\ (P_{88} - \Psi_{TLP})}{g_{min}\ x\ VPD}$$

where C_{TLP} is the capacitance after the turgor loss point (mol m^{2} MPa^{-1}), P_{88} is the water potential at 88% cumulative xylem embolized (MPa), Ψ_{TLP} is the water potential at turgor loss point (Ψ_{TLP}), $g_{\text{leaf-res}}$ is the leaf residual conductance (mol m^{2} s^{-1}), and VPD is the vapor pressure deficit of the atmosphere (mol mol^{-1}).

Loss of leaf rehydration capacity

Ten fully expanded leaves were collected from each plant, stored in zip lock bags, transported to the laboratory, and placed inside desiccators with their petioles immersed in water for at least 12 h. Leaves were then placed on a bench and allowed to slowly dehydrate under ambient conditions while being regularly weighed. At every 10% variation in their initial weight, and then placed again in the desiccator with their petioles immersed in water for another 12 h. After this, we assessed leaf turgid and dry weights (after being completely dried for 72 h at 70 °C). The percentage loss of leaf rehydration capacity (PLRC) and RWC (%) was calculated as described (Trueba et al. 2019). For each plant, a linear equation between Ψ_w and RWC was obtained through the RWC, and Ψ_w measured on leaves from OV curves and was adjusted, allowing the RWC values of the PLRC curve to be converted into Ψ_w as described by (Oliveira et al. 2022). From these curves, the Ψ_w at 50% decline in PLRC (PLRC_{50}) wewasre obtained.

Statistical analysis

All analyses were performed using R statistical software version 4.2.2. The data were submitted to an analysis of variance and the significant differences between the means of the amphistomatic and hypostomatic plants were performed using an unpaired Student's t-test ($\alpha<0.05$).

RESULTS

Stomatal structure and function on leaf gas exchange

Despite having 26% less $SD_{Abaxial}$, amphistomatic species exhibited, on average, 32% greater SD_{Total} than hypostomatic species (Figure 1). For simplicity, all comparisons presented in the Results refer to amphistomatic species being compared with hypostomatic species. Amphistomatic species also exhibited, on average, 128% higher $g_{leaf\text{-}res}$ and 126% higher g_{wmax}. Although the amphistomatic species exhibited 55% higher g_s, this increase did not result in higher A or transpiration for the environmental conditions evaluated in this study (Figure 2). The higher g_s, decoupled from increases in A, resulted in 28% less WUE_i in amphistomatic species. Additionally, a 43% higher R_d was found in amphistomatic species.

Leaf and stem hydraulics

Amphistomatic and hypostomatic species exhibited similar leaf vein densities (Figure 3). Amphistomatic species, however, exhibited 28% fewer xylem vessels per petiole as well as less XLA. Similar petiole vessel diameter ($D_{hSperry}$) was observed independently from stomatal distribution, but the leaf xylem from amphistomatic species exhibited 15% lower cell wall reinforcement $(t/b)^2$. Despite having fewer xylem vessels per petiole and lower XLA, amphistomatic species had on average similar K_{leaf}, K_{branch}, and Huber values compared to hypostomatic ones (Figure 4).

Among the plant water relations variables, Ψ_{100}, RWC_{TLP}, and Ψ_{TLP} were similar among the species (Figure 5). Amphistomatic species, however, exhibited 40% higher ε, 29% higher C_{FT}, and 68% higher C_{TLP}.

Leaf resistance to embolism and desiccation

Among the amphistomatic species, the average P_{50} ranged from -3.12 to -3.8 MPa, while for the hypostomatic species, P_{50} varied between -3.15 to -4.02 MPa (Figure 6). Given the similar Ψ_{TLP} and P_{50} among the species, they also exhibited a similar SSM_{50}. The $PLRC_{50}$ was also significantly less negative for amphistomatic species. The $SMRI_{50}$ and t_{leaf_crit} values were around 55% of those observed in hypostomatic plants (Figure 6 and Table 2).

DISCUSSION

Amphistomatic species have a higher potential for water loss and lower water-use efficiency

Maximum theoretical stomatal conductance (g_{wmax}) depends mainly on stomatal density (SD) and aperture. Here, as stomata length was used to estimate the stomatal pore area, and the eucalyptus species used in this study did not differ in stomata length (Figure S3), the g_{wmax} values were defined mainly by the contribution of SD. Notably, g_{wmax} and g_s were 130% and 150% higher, respectively, in amphistomatic species compared to hypostomatic species (Figure 1). The greater observed differences in g_s compared to those predicted by g_{wmax} suggest that variations in stomatal apertures also significantly contributed to these results. As the increases in g_s were not accompanied by proportional increases in photosynthesis, this resulted in lower WUE_i. This reduction in WUE_i could represent a potential disadvantage for amphistomatic species (Figure 2). In addition, this disadvantage can be even amplified when considering the higher $g_{leaf\text{-}res}$ presented by the amphistomatic species because of their higher stomatal density (Muchow and Sinclair 1989, Machado et al. 2021), which aligns with our findings (Figure 1).

Amphistomatic leaves are often associated with greater photosynthetic potential under high light due to their g_s and shorter pathways between the stomata and the chloroplasts (Mott et al. 1982); however, our study did not reveal any differences in photosynthesis between amphistomatic and hypostomatic species (Figure 2). Noteworthy, our gas exchange measurements were carried out by illuminating only the adaxial leaf surface, similar to what occurs in situ for horizontally oriented leaves. Given that the amphistomatic *Eucalyptus* species assessed in this study had leaves nearly vertically oriented (Figure S4), we speculate that if these leaves had received light at both surfaces, they might have demonstrated higher photosynthetic rates for a given g_s (Richardson et al. 2017).

Higher water loss decoupled from greater embolism resistance might result in higher drought sensitivity in amphistomatic species

Given the higher potential for water loss during well-watered (higher g_s) or drought conditions (higher $g_{leaf\text{-}res}$), we would expect amphistomatic species to exhibit higher drought resistance (e.g. higher embolism resistance and/or maintenance of rehydration capacity at lower water levels). However, amphistomatic species exhibited similar P_{50} and higher $PLRC_{50}$ than hypostomatic species (Figure 6). The P_{50} for all *Eucalyptus* species ranged from -3.12 to -4.02 MPa, which aligns with recent reports for this species (Li et al. 2018; Creek et al. 2018; Oliveira et al. 2022).

Exhibiting more negative P_{50} represents an advantage for drought resistance, however, having stomatal closure at higher water potentials is also critical for plants to prevent drought-induced damage (Choat et al. 2012b; Petek-Petrik et al. 2023). Nevertheless, as inferred by their similar Ψ_{TLP}, the eucalyptus species here studied closed stomata at similar water potentials. A higher $g_{leaf\text{-}res}$ means that plants will lose water faster during drought (Blackman et al. 2016; Oliveira et al. 2022; Petek-Petrik et al. 2023; Haverroth et al. 2023; Pereira et al. 2024), potentially reaching severe dehydration levels in shorter periods. A few indexes have been proposed to predict the onset of hydraulic dysfunction in plants (Blackman et al. 2016, 2019; Petek-Petrik et al. 2023). These indexes, which utilize both leaf and whole-plant parameters, have shown strong predictive power for *Eucalyptus* species (Blackman et al. 2016, 2019). However, some of the whole-plant traits used in these indexes can be difficult to measure. Here, to demonstrate how $g_{leaf\text{-}res}$ would impact the drought susceptibility of amphistomatic species, we developed an adapted index (t_{leaf_crit}) to identify the critical period for leaf mortality, using exclusively leaf characteristics. On average, the t_{leaf_crit} of amphistomatic was considerably lower than that of hypostomatic species (Student's t-test, $P = 0.1$) (Table 2). This result suggests that amphistomatic leaves would likely reach embolism and damage sooner compared to the hypostomatic ones (Figure 6).

Higher modulus of elasticity, leaf capacitance, and nearly vertical foliage might slow down dehydration in amphistomatic species

Critical traits potentially improving the drought resistance of amphistomatic leaves include high ε, high capacitance before and after the Ψ_{TLP} (C_{FT} and C_{TLP}) (Figure 5), and nearly vertically oriented leaves (Figure S4). High leaf capacitance indicates a greater buffering in water potential variations for similar changes in water content (Bartlett et al. 2012, Bartlett et al. 2016, Pereira et al. 2024). The high capacitance of amphistomatic species probably resulted from their greater leaf thickness and lower quantity of intercellular spaces in the leaf mesophyll (Figure S2). Having a high capacitance, especially after turgor loss, might represent an interesting mechanism of amphistomatic leaves to slower declines in Ψ_w during drought by their leaky leaves, and increase the time required to lead to hydraulic failure (Table 2). Indeed, we showed in Table 2 that $t_{\mathrm{leaf\_crit}}$ changes from 19 to 15 hours if the index is calculated using the average capacitance from both groups.

The surface angle of a leaf directly determines the flux of solar radiation per unit leaf area (Ehleringer et al. 1991; Ezcurra et al. 1991). High leaf angle increases light capture when the sun is at low angles (morning/afternoon and winter) and decreases light interception when the sun is at higher angles (noon and summer) (Falster & Westoby 2003). This trait is often observed in species adapted to arid conditions (King 1997; Drake et al. 2019) as it reduces the light interception at midday, minimizing adverse environmental effects (Mediavilla and Escudero 2023), thus reducing the risk of overheating (King 1997) and decreasing susceptibility to photoinhibition (Ryel et al. 1993; Valladares & Pugnaire 1999; Werner et al. 2001). In amphistomatic *Eucalyptus*, having high leaf angles might also lower the stomatal aperture at midday, thus reducing water loss when VPD is at its highest. In this case, the actual g_s of amphistomatic species at midday might be lower *in situ* than the values assessed in our study using the Li-COR, in which leaves were directly hit with an artificial PPFD of 1000 μmol m^{-2} s^{-1}, since the inclination of the leaf may affect the distribution of light between the adaxial and abaxial surface (Mediavilla and Escudero 2023).

Together, the high ε, high capacitance, and high leaf angle likely delay the time for amphistomatic *Eucalyptus* to reach critical dehydration levels and irreversible damage. A dry-down experiment, however, is necessary to confirm whether these traits are sufficient to counteract the high potential for water loss observed in these species.

Deeper roots and resprout capacity might result in drought resistance in amphistomatic species

The physiological connection between water uptake and the preservation of water content is of utmost importance for the proper functioning of plants in dry environments. Therefore, given that amphistomatic *Eucalyptus* inhabit drier environments than their hypostomatic counterparts, amphistomatic species may possess drought resistance mechanisms beyond their leaves. One potential mechanism is exhibiting deep roots to maximize water uptake (Schenk & Jackson 2005; Pivovaroff et al. 2016; Fan et al. 2017). Deep rooting can afford species to have lower embolism resistance due to their access to deeper water sources (McCulloh et al. 2019). The depth of water absorption by the root determines how quickly different species approach hydraulic vulnerability thresholds during a drought event and can explain the differential vulnerability of adult species at the field level (Kahmen et al. 2022).

Studies with hypostomatic *Eucalyptus* (*E. grandis* and *E. urophylla*) revealed the presence of fine roots at depths of 17 and 16 m, respectively, in young plants (6- and 7-year-old) (Germon et al. 2019; Silva et al. 2020). Amphistomatic species may have even deeper roots, similar to other tree species from arid environments, which access groundwater at depths of nearly 30 m (Zencichis et al. 2002). Three amphistomatic species of *Eucalyptus* (*E. camaldulensis*, *E. tereticornis*, and *E. victrix*) have already been demonstrated to rely on water tables (Pfautsch et al. 2015; Franklin et al. 2020), which might support amphistomatic species having deeper roots than hypostomatic ones. Studies using hydrogen isotopic discrimination or trenching to measure the depth of the root system of a wide range of amphistomatic and hypostomatic species of *Eucalyptus* would represent a large step towards a better understanding of the drought resistance within these groups.

Additionally, three out of four amphistomatic species of *Eucalyptus* selected for this study exhibit lignotuber (Table 1). This structure allows plants to resprout after disturbances such as fire (Enright et al. 2014; Clarke et al. 2015) and drought (Matusick et al. 2016). Resprout from lignotuber buds constitutes a predominant resilience mechanism in *Eucalyptus* species and might benefit amphistomatic species threatened by drought.

CONCLUSION

Amphistomatic species exhibit higher stomatal density and thus higher stomatal conductance than hypostomatic ones. The “leaky” leaves of amphistomatic species, however, were decoupled from a greater water supply from leaves and branches, earlier stomatal closure, or higher leaf resistance to embolism and loss in the rehydration capacity when compared to hypostomatic species. Potential drought resistance mechanisms observed in amphistomatic species at the leaf level were the presence of a high modulus of elasticity, high capacitance pre- and post-turgor, and high leaf angle. Based on our findings, amphistomatic leaves of *Eucalyptus* are likely more susceptible to drought than hypostomatic ones. One might consider amphistomatic *Eucalyptus* especially endangered by drought events when accounting for their broad occurrence in dry biomes.

Studies including dry-down experiments as well as assessments of minimum soil water potentials experienced by plants *in situ* during natural droughts are needed to confirm whether amphistomatic species are indeed susceptible to drought risks. Additional studies assessing the presence of additional drought resistance mechanisms at the root or stem levels in amphistomatic *Eucalyptus* are also critical.

Acknowledgments

LAO acknowledges the financial support received from the Brazilian Federal Agency for the Support and Evaluation of Graduate Education (CAPES) and the use of the plant anatomy laboratory at Universidade Federal de Viçosa. During the final stages, this study was supported by the USDA National Institute of Food and Agriculture, Hatch Project 7003279 (AAC). SCVM acknowledges the research fellowship granted by the Conselho Nacional de Desenvolvimento Científico e Tecnológico (CNPq grant number 308280/2020-2).

Conflicts of Interest

The authors declare no conflicts of interest associated with this work.

REFERENCES

Andrade MT, Oliveira LA, Pereira TS, Cardoso AA, Batista-Silva W, Damatta FM, Zsögön A, Martins SCV (2022) Impaired auxin signaling increases vein and stomatal density but reduces hydraulic efficiency and ultimately net photosynthesis. J Exp Bot 73:4147–4156.

Baresch A, Crifò C, Boyce CK (2019) Competition for epidermal space in the evolution of leaves with high physiological rates. New Phytologist 221:628–639.

Bartlett MK, Klein T, Jansen S, Choat B, Sack L (2016) The correlations and sequence of plant stomatal, hydraulic, and wilting responses to drought. Proc Natl Acad Sci U S A 113:13098–13103.

Bartlett MK, Scoffoni C, Sack L (2012) The determinants of leaf turgor loss point and prediction of drought tolerance of species and biomes: A global meta-analysis. Ecol Lett 15:393–405.

Beerling DJ, Kelly CK (1996) Evolutionary comparative analyses of the relationship between leaf structure and function. New Phytologist 134:35–51.

Billon LM, Blackman CJ, Cochard H, Badel E, Hitmi A, Cartailler J, Souchal R. 2020. The DroughtBox: a new tool for phenotyping residual branch conductance and its temperature dependence during drought. Plant, Cell & Environment 43: 1584-1594.

Blackman CJ, Halliwell B, Hartill GE, Brodribb TJ (2023) Petiole XLA (xylem to leaf area ratio) integrates hydraulic safety and efficiency across a diverse group of eucalypt leaves. Plant Cell Environ 47:49–58.

Blackman CJ, Li X, Choat B, Rymer PD, De Kauwe MG, Duursma RA, Tissue DT, Medlyn BE (2019) Desiccation time during drought is highly predictable across species of *Eucalyptus* from contrasting climates. New Phytologist 224:632–643.

Blackman CJ, Pfautsch S, Choat B, Delzon S, Gleason SM, Duursma RA (2016) Toward an index of desiccation time to tree mortality under drought. Plant Cell Environ 39:2342–2345.

de Boer HJ, Drake PL, Wendt E, Price CA, Schulze ED, Turner NC, Nicolle D, Veneklaas EJ (2016) Apparent overinvestment in leaf venation relaxes leaf morphological constraints on photosynthesis in arid habitats. Plant Physiol 172:2286–2299.

de Boer HJ, Eppinga MB, Wassen MJ, Dekker SC (2012) A critical transition in leaf evolution facilitated the Cretaceous angiosperm revolution. Nat Commun 3

Brodribb TJ, Feild TS, Jordan GJ (2007) Leaf maximum photosynthetic rate and venation are linked by hydraulics. Plant Physiol 144:1890–1898.

Brodribb TJ, Holbrook NM (2006) Declining hydraulic efficiency as transpiring leaves desiccate: Two types of response. Plant Cell Environ 29:2205–2215.

Brodribb TJ, Jordan GJ, Carpenter RJ (2013) Unified changes in cell size permit coordinated leaf evolution. New Phytologist 199:559–570.

Brodribb TJ, McAdam SAM, Jordan GJ, Martins SCV (2014) Conifer species adapt to low-rainfall climates by following one of two divergent pathways. Proc Natl Acad Sci U S A 111:14489–14493.

Brodribb TJ, Skelton RP, Mcadam SAM, Bienaimé D, Lucani CJ, Marmottant P (2016) Visual quantification of embolism reveals leaf vulnerability to hydraulic failure. New Phytologist 209:1403–1409.

Buckley TN (2019) How do stomata respond to water status? New Phytologist 224:21–36.

Bueno A, Alfarhan A, Arand K, Burghardt M, Deininger AC, Hedrich R, Leide J, Seufert P, Staiger S, Riederer M. 2019. Effects of temperature on the cuticular transpiration barrier of two desert plants with water-spender and water-saver strategies. Journal of Experimental Botany 70: 1613–1625.

Caringella MA, Bongers FJ, Sack L (2015) Leaf hydraulic conductance varies with vein anatomy across Arabidopsis thaliana wild-type and leaf vein mutants. Plant Cell Environ 38:2735–2746.

Carpenter RJ (1994) Cuticular morphology and aspects of the ecology and fossil history of North Queensland-rainforest Proteaceae. Botanical Journal of the Linnean Society 116:249–303.

Choat B, Jansen S, Brodribb TJ, Cochard H, Delzon S, Bhaskar R, Bucci SJ, Feild TS, Gleason SM, Hacke UG, Jacobsen AL, Lens F, Maherali H, Martínez-Vilalta J, Mayr S, Mencuccini M, Mitchell PJ, Nardini A, Pittermann J, Pratt RB, Sperry JS, Westoby M, Wright IJ, Zanne AE (2012) Global convergence in the vulnerability of forests to drought. Nature 491:752–755.

Clarke PJ, Lawes MJ, Murphy BP, Russell-Smith J, Nano CEM, Bradstock R, Enright NJ, Fontaine JB, Gosper CR, Radford I, Midgley JJ, Gunton RM (2015) A synthesis of postfire recovery traits of woody plants in Australian ecosystems. Science of the Total Environment 534:31–42.

Cowan IR, Farquhar GD (1977) Stomatal function in relation to leaf metabolism and environment. In: Symposia of the Society for Experimental Biology.

Creek D, Blackman CJ, Brodribb TJ, Choat B, Tissue DT (2018) Coordination between leaf, stem, and root hydraulics and gas exchange in three arid-zone angiosperms during severe drought and recovery. Plant Cell Environ 41:2869–2881.

Drake PL, de Boer HJ, Schymanski SJ, Veneklaas EJ (2019) Two sides to every leaf: water and CO 2 transport in hypostomatous and amphistomatous leaves. New Phytologist 222:1179–1187.

Drake PL, Froend RH, Franks PJ (2013) Smaller, faster stomata: Scaling of stomatal size, rate of response, and stomatal conductance. J Exp Bot 64:495–505.

Duursma RA, Blackman CJ, Lopéz R, Martin-StPaul NK, Cochard H, Medlyn BE (2019) On the minimum leaf conductance: its role in models of plant water use, and ecological and environmental controls. New Phytologist 221:693–705.

Ehleringer JR, Phillips SL, Schuster WSF, Sandquist DR (1991) Differential utilization of summer rains by desert plants. Oecologia 88:430–434.

Enright NJ, Fontaine JB, Lamont BB, Miller BP, Westcott VC (2014) Resistance and resilience to changing climate and fire regime depend on plant functional traits. Journal of Ecology 102:1572–1581.

Ezcurra E, Montaña C, Arizaga S, Montana C (1991) Architecture, light Interception, and distribution of Larrea species in the monte desert, Argentina. Ecology 72:23–34.

Falster DS, Westoby M (2003) Leaf size and angle vary widely across species: What consequences for light interception? New Phytologist 158:509–525.

Fan Y, Miguez-Macho G, Jobbágy EG, Jackson RB, Otero-Casal C (2017) Hydrologic regulation of plant rooting depth. Proc Natl Acad Sci U S A 114:10572–10577.

Fick SE, Hijmans RJ (2017) WorldClim 2: new 1-km spatial resolution climate surfaces for global land areas. International Journal of Climatology 37:4302–4315.

Flexas J, Ribas-Carbó M, Diaz-Espejo A, Galmés J, Medrano H (2008) Mesophyll conductance to CO2: Current knowledge and future prospects. Plant Cell Environ 31:602–621.

Foster JR, Smith WK (1986) Influence of stomatal distribution on transpiration in low-wind environments. Plant Cell Environ 9:751–759.

Franklin HM, Chen C, Carroll AR, Saeck E, Fisher P, Burford MA (2020) Leaf litter of two riparian tree species has contrasting effects on nutrients leaching from soil during large rainfall events. Plant Soil 457:389–406.

Franks PJ, Drake PL, Beerling DJ (2009) Plasticity in maximum stomatal conductance constrained by negative correlation between stomatal size and density: An analysis using *Eucalyptus globulus*. Plant Cell Environ 32:1737–1748.

Franks PJ, Farquhar GD (2001) The effect of exogenous abscisic acid on stomatal development, stomatal mechanics, and leaf gas exchange in Tradescantia virginiana. Plant Physiol 125:935–942.

Germon A, Jourdan C, Bordron B, Robin A, Nouvellon Y, Chapuis-Lardy L, de Moraes Gonçalves JL, Pradier C, Guerrini IA, Laclau JP (2019) Consequences of clear-cutting and drought on fine root dynamics down to 17 m in coppice-managed eucalypt plantations. For Ecol Manage 445:48–59.

Gibson AC (1996) Structure-Function Relations of Warm Desert Plants. Springer Berlin Heidelberg, Berlin, Heidelberg.

Griffin-Nolan RJ, Ocheltree TW, Mueller KE, Blumenthal DM, Kray JA, Knapp AK (2019) Extending the osmometer method for assessing drought tolerance in herbaceous species. Oecologia 189:353–363.

Haverroth EJ, Oliveira LA, Andrade MT, Taggart M, McAdam SAM, Zsögön A, Thompson AJ, Martins SCV, Cardoso AA (2023) Abscisic acid acts essentially on stomata, not on the xylem, to improve drought resistance in tomato. Plant Cell Environ 46:3229–3241.

Hetherington AM, Woodward & FI (2003) The role of stomata in sensing and driving environmental change. Nature 424:901–908.

Huang R, Di N, Xi B, Yang J, Duan J, Li X, Feng J, Choat B, Tissue D (2024) Herb hydraulics: Variation and correlation for traits governing drought tolerance and efficiency of water transport. Science of the Total Environment 907

Huber B. (1928) Weitere quantitative Untersuchungen über das Wasserleitungssystem der Pflanzen.

Johansen DA (1940) Plant Microtechnique. McGraw-Hill, , New York.

Jordan GJ, Carpenter RJ, Brodribb TJ (2014) Using fossil leaves as evidence for open vegetation. Palaeogeogr Palaeoclimatol Palaeoecol 395:168–175.

Kahmen A, Basler D, Hoch G, Link RM, Schuldt B, Zahnd C, Arend M (2022) Root water uptake depth determines the hydraulic vulnerability of temperate European tree species during the extreme 2018 drought. Plant Biol 24:1224–1239.

Kerstiens G. 1996a. Cuticular water permeability and its physiological significance. Journal of Experimental Botany 47: 1813–1832.

Kerstiens G. 1996b. Signalling across the divide: a wider perspective of cuticular structure-function relationships. Trends in Plant Science 1: 125–129.

King DA (1997) The functional significance of leaf angle in *Eucalyptus*. Aust J Bot 45:619–639.

Lange, O. L., Lösch, R., Schulze, E. D., & Kappen, L. (1971). Responses of stomata to changes in humidity. Planta, 100, 76-86.

Lewis AM, Boose ER (1995) Estimating Volume Flow Rates Through Xylem Conduits. Am J Bot 82:1112–1116.

Li X, Blackman CJ, Choat B, Duursma RA, Rymer PD, Medlyn BE, Tissue DT (2018) Tree hydraulic traits are coordinated and strongly linked to climate-of-origin across a rainfall gradient. Plant Cell Environ 41:646–660.

Lucani CJ, Brodribb TJ, Jordan G, Mitchell PJ (2019) Intraspecific variation in drought susceptibility in *Eucalyptus globulus* is linked to differences in leaf vulnerability. Functional Plant Biology 46:286–293.

Machado R, Loram-Lourenço L, Farnese FS, Alves RD, de Sousa LF, Silva FG, Filho SC, Torres-Ruiz JM, Cochard H, Menezes-Silva PE. Where do leaf water leaks come from? Trade-offs underlying the variability in minimum conductance across tropical savanna species with contrasting growth strategies. New Phytologist. 2021 Feb;229(3):1415-30.

Mantova M, Herbette S, Cochard H, Torres-Ruiz JM (2022) Hydraulic failure and tree mortality: from correlation to causation. Trends Plant Sci 27:335–345.

Márquez DA, Stuart-Williams H, Farquhar GD, Busch FA (2022) Cuticular conductance of adaxial and abaxial leaf surfaces and its relation to minimum leaf surface conductance. New Phytologist 233:156–168.

Martin-StPaul N, Delzon S, Cochard H (2017) Plant resistance to drought depends on timely stomatal closure. Ecol Lett 20:1437–1447.

Matusick G, Ruthrof KX, Fontaine JB, Hardy GESJ (2016) *Eucalyptus* forest shows low structural resistance and resilience to climate change-type drought. Journal of Vegetation Science 27:493–503.

McAdam SAM, Eléouët MP, Best M, Brodribb TJ, Carins Murphy M, Cook SD, Dalmais M, Dimitriou T, Gélinas-Marion A, Gill WM, Hegarty M, Hofer JMI, Maconochie M, McAdam EL, McGuiness P, Nichols DS, Ross JJ, Sussmilch FC, Urquhart S (2017) Linking auxin with photosynthetic rate via leaf venation. Plant Physiol 175:351–360.

McCulloh KA, Domec JC, Johnson DM, Smith DD, Meinzer FC (2019) A dynamic yet vulnerable pipeline: Integration and coordination of hydraulic traits across whole plants. Plant Cell Environ 42:2789–2807.

Mediavilla, S., & Escudero, A. (2023). Photosynthetic performance under adaxial and abaxial illumination in three Mediterranean Quercus species differing in branch architecture and individual leaf area. Photosynthesis Research, 158(3), 181-194.

Metcalfe C R., Chalf L., Chattaway M M., Hare C L., Richardson R F., Slatter E M. (1951) Anatomy of the dicotyledons. leaves, stem, and wood in relation to taxonomy, with notes on economic uses.

Mott KA, Gibson AC, O'Leary JW (1982) The adaptive significance of amphistomatic leaves. Plant Cell Environ 5:455–460.

Muchow R. C., Sinclair T. R. (1989) Epidermal conductance, stomatal density and stomatal size among genotypes of Sorghum. Plant Cell Environ 12:425–431.

Muir CD (2018) Light and growth form interact to shape stomatal ratio among British angiosperms. New Phytologist 218:242–252.

O'brien TP, Feder N, Mccully ME (1964) Polyehromatic staining of plant cell walls by Toluidine Blue O. Protoplasma 63:368–373.

Ocheltree TW, Mueller KM, Chesus K, LeCain DR, Kray JA, Blumenthal DM (2020) Identification of suites of traits that explains drought resistance and phenological patterns of plants in a semi-arid grassland community. Oecologia 192:55–66.

Oliveira LA, Cardoso AA, Andrade MT, Pereira TS, Araújo WL, Santos GA, Damatta FM, Martins SCV (2022) Exploring leaf hydraulic traits to predict drought tolerance of *Eucalyptus* clones. Tree Physiol 42:1750–1761.

Parkhurst DF (1978) The adaptive significance of stomatal occurrence on one or both surfaces of leaves. Journal of Ecology 66:367–383.

Parkhurst DF, Mott KA (1990) Intercellular diffusion limits to CO2 uptake in leaves. Plant Physiol 94:1024–1032.

Pereira TS, Oliveira LA, Andrade MT, Haverroth EJ, Cardoso AA, Martins SCV (2024) Linking water-use strategies with drought resistance across herbaceous crops. Physiol Plant 176:e14114.

Petek-Petrik A, Petrík P, Lamarque LJ, Cochard H, Burlett R, Delzon S (2023) Drought survival in conifer species is related to the time required to cross the stomatal safety margin. J Exp Bot 74:6847–6859.

Pfautsch S, Dodson W, Madden S, Adams MA (2015) Assessing the impact of large-scale water table modifications on riparian trees: A case study from Australia. Ecohydrology 8:642–651.

Pivovaroff AL, Pasquini SC, De Guzman ME, Alstad KP, Stemke JS, Santiago LS (2016) Multiple strategies for drought survival among woody plant species. Funct Ecol 30:517–526.

Richardson A, Wojciechowski T, Franke R, Schreiber L, Kerstiens G, Jarvis M, Fricke W. 2007. Cuticular permeance in relation to wax and cutin development along the growing barley (Hordeum vulgare) leaf. Planta 225: 1471–1481.

Richardson F, Brodribb TJ, Jordan GJ (2017) Amphistomatic leaf surfaces independently regulate gas exchange in response to variations in evaporative demand. Tree Physiol 37:869–878.

Ryel RJ, Beyschlag W, Caldwell MM, Caldwellt MM (1993) Foliage orientation and carbon gain in two tussock grasses as assessed with a new whole-plant gas-exchanage model foliage orientation and carbon gain in two tussock grasses as assessed with a new whole-plant gas-exchange model. Funct Ecol 7:115–124.

Sack L, Melcher PJ, Zwieniecki MA, Holbrook NM (2002) The hydraulic conductance of the angiosperm leaf lamina: A comparison of three measurement methods. J Exp Bot 53:2177–2184.

Sack L, Cowan PD, Jaikumar N, Holbrook NM. 2003. The ‘hydrology’ of leaves: co-ordination of structure and function in temperate woody species. Plant, Cell & Environment 26: 1343–1356.

Salisbury EJ (1927) On the causes and ecological significance of stomatal frequency, with special reference to the woodland flora. Philosophical Transactions of the Roval Society of London 216:1–65.

Schenk HJ, Jackson RB (2005) Mapping the global distribution of deep roots in relation to climate and soil characteristics. Geoderma 126:129–140.

Scoffoni C, Chatelet DS, Pasquet-Kok J, Rawls M, Donoghue MJ, Edwards EJ, Sack L (2016) Hydraulic basis for the evolution of photosynthetic productivity. Nat Plants 2

Seng Hua L, Wei Chen L, Antov P, Kristak L, Md Tahir P (2022) Engineering wood products from *Eucalyptus spp*. Advances in Materials Science and Engineering 2022:1–14.

Silva VE, Nogueira TAR, Abreu-Junior CH, He Z, Buzetti S, Laclau JP, Teixeira Filho MCM, Grilli E, Murgia I, Capra GF (2020) Influences of edaphoclimatic conditions on deep rooting and soil water availability in Brazilian *Eucalyptus* plantations. For Ecol Manage 455:117673.

Slavic B. 1974. Methods of studying plant water relations. Berlin, Germany: Springer.

Sperry JS, Donnelly JR, Tyree MT (1988) A method for measuring hydraulic conductivity and embolism in xylem. Plant Cell Environ 11:35–40.

Sperry J S., Ikeda T (1997) Xylem cavitation in roots and stems of Douglas-fir and white fir. Tree Physiol 17:275–280.

de Strittmatter C (1973) Nueva tecnica de diafanizacion. Boletin de la sociedad Argentina de Botanica 15:126–129.

Trueba S, Pan R, Scoffoni C, John GP, Davis SD, Sack L (2019) Thresholds for leaf damage due to dehydration: declines of hydraulic function, stomatal conductance and cellular integrity precede those for photochemistry. New Phytologist 223:134–149.

Tyree MT, Hammel HT (1972) The measurement of the turgor pressure and the water relations of plants by the pressure-bomb technique. J Exp Bot 23:267–282.

Tyree M T., Ewers F W. (1991) The hydraulic architecture of trees and other woody plants. New Phytologist 119:345–360.

Valladares F, Pugnaire FI (1999) Tradeoffs between irradiance capture and avoidance in semi-arid environments assessed with a crown architecture model. Ann Bot 83:459–469.

De Villemereuil P, Gaggiotti OE, Mouterde M, Till-Bottraud I (2016) Common garden experiments in the genomic era: New perspectives and opportunities. Heredity (Edinb) 116:249–254.

Werner C, Ryel RJ, Correia O, Beyschlag W (2001) Effects of photoinhibition on whole-plant carbon gain assessed with a photosynthesis model. Plant Cell Environ 24:27–40.

Wood JG (1934) The physiology of xerophytism in Australian plants: the stomatal frequencies, transpiration and osmotic pressures of sclerophyll and tomentose-succulent leaved plants. Journal of Ecology 22:69–87.

Xiong D, Flexas J (2020) From one side to two sides: the effects of stomatal distribution on photosynthesis. New Phytologist 228:1754–1766.

Zencich SJ, Froend RH, Turner J V., Gailitis V (2002) Influence of groundwater depth on the seasonal sources of water accessed by Banksia tree species on a shallow, sandy coastal aquifer. Oecologia 131:8–19.

Zomer RJ, Trabucco A, Bossio DA, Verchot L V. (2008) Climate change mitigation: A spatial analysis of global land suitability for clean development mechanism afforestation and reforestation. Agric Ecosyst Environ 126:67–80.

TABLES

Table 1. Summary table of the eight *Eucalyptus* species used in this study. Data include stomatal distribution (amphistomatic – amph or hypostomatic – hypo), presence or absence of lignotuber, mean annual precipitation, mean annual potential evapotranspiration, and aridity index (mean native ratio of precipitation to potential evapotranspiration). The presence of lignotuber for these species is described according to EUCLID Eucalypts of Australia Edition (https://apps.lucidcentral.org/euclid/text/intro/index.html). Annual precipitation, evapotranspiration, and aridity index represent averages of their native distributions.

Species	Stomatal distribution	Lignotuber	Precipitation (mm/year)	Evapotranspiration (mm/year)	Aridity index (P/E_p)
E. camaldulensis	Amph	Absent	524 ± 174	1781 ±274	0.31 ± 0.1
E. tereticornis	Amph	Present	1102 ± 355	1805 ± 187	0.62 ± 0.2
E. pellita	Amph	Present	2315 ± 842	1835 ± 116	1.26 ± 0.5
E. cinerea	Amph	Present	787 ± 134	1490 ± 100	0.53 ± 0.1
E. grandis	Hypo	Absent	1479 ± 238	1622 ± 78	0.91 ± 0.2
E. urophylla	Hypo	Absent	1646 ± 440	1663 ± 139	1.01 ± 0.3
E. dunnii	Hypo	Present	1471 ± 259	1497 ± 62	0.99 ± 0.2
E. pilularis	Hypo	Absent	1310 ± 223	1564 ± 83	0.84 ± 0.1

Table 2. Critical time for leaf death index in seven *Eucalyptus spp*. Data include stomatal distribution (amphistomatic – amph or hypostomatic – hypo), t_{leaf_crit} (VPD-h), the critical time for leaf dieback; t_{leaf_crit} $g_{leaf\text{-}res}$ (VPD-h), the critical time for leaf dieback using the average of $g_{leaf\text{-}res}$ from both groups of leaves; t_{leaf_crit} C_{TLP} (VPD-h) the critical time for leaf dieback using average of C_{TLP} from both groups of leaves.

Species	**Stomatal distribution**	t_{leaf_crit}	t_{leaf_crit} $g_{leaf\text{-}res}$	t_{leaf_crit} C_{TLP}
E. camaldulensis	Amph	27.8 ± 6.0	31.1 ± 5.7	28.7 ± 3.7
E. tereticornis	Amph	13.8 ± 2.0	20.8 ± 3.5	12.0 ± 1.7
E. pellita	Amph	14.4 ± 2.3	29.8 ± 5.8	11.5 ± 1.0
Average	**Amph**	**19.2 ± 2.9 b**	**27.4 ± 3.1 a**	**15 ± 1.8 b**
E. grandis	Hypo	26.7 ± 4.8	16.3 ± 2.9	34.5 ± 6.7
E. urophylla	Hypo	42.0 ± 4.7	36.0 ± 4.2	40.1 ± 4.6
E. dunnii	Hypo	43.4 ± 6.6	18.5 ± 3.1	60.2 ± 11.0
E. pilularis	Hypo	15.3 ± 2.0	10.5 ± 1.2	40.1 ± 4.6
Average	**Hypo**	**31.8 ± 3.3 a**	**20.3 ± 2.4 a**	**42.2 ± 4.0 a**

Data are means ± standard error ($n = 6$). Letters denote differences between amphistomatic and hypostomatic species according to Student's t-test ($P < 0.05$).

FIGURES

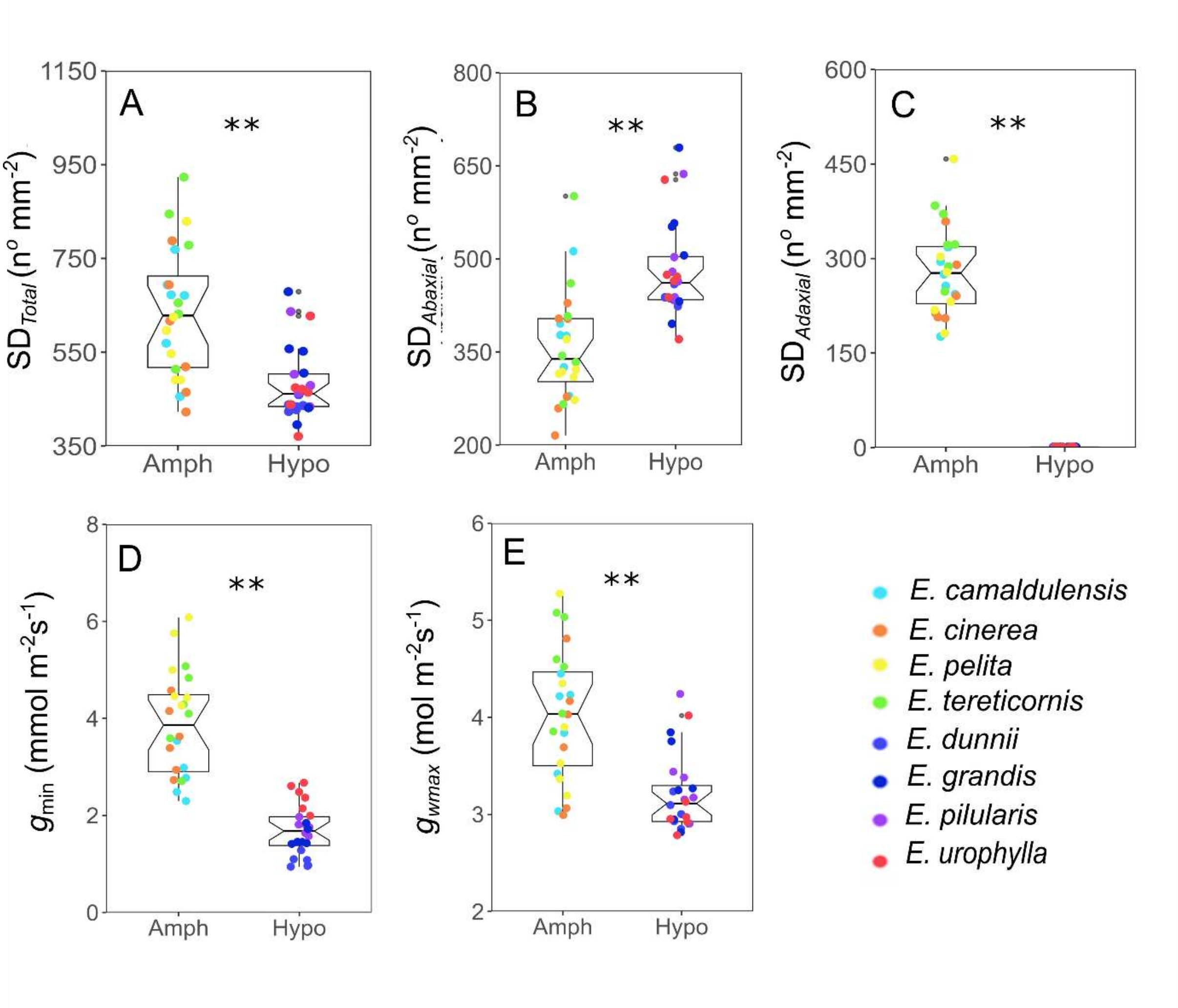

Figure 1. Stomatal dimensions (A, B, C), minimum leaf conductance (D), and maximum theoretical stomatal conductance to water vapor (E) of amphistomatic (Amph) and hypostomatic (Hypo) species of *Eucalyptus*. Species are represented by different colors as per the legend. For the box plot, the lower and upper hinges correspond to the first and third quartiles (interquartile range, IQR), the horizontal lines inside the boxes are the medians, the upper/lower whisker extends from the hinge to the largest/smallest value no further than 1.5 × IQR from the hinges, and data beyond the end of the whiskers are plotted individually (small grey circles). SD$_{Total}$, total stomatal density; SD$_{Abaxial}$, stomatal density on the abaxial epidermis; SD$_{Adaxial}$, stomatal density on the adaxial epidermis; $g_{leaf-res}$, leaf residual conductance; g_{wmax}, maximum theoretical stomatal conductance to water vapor. Asterisks indicate significant differences between amphistomatic and hypostomatic groups according to Student's t-test: $^{**}P < 0.01$.

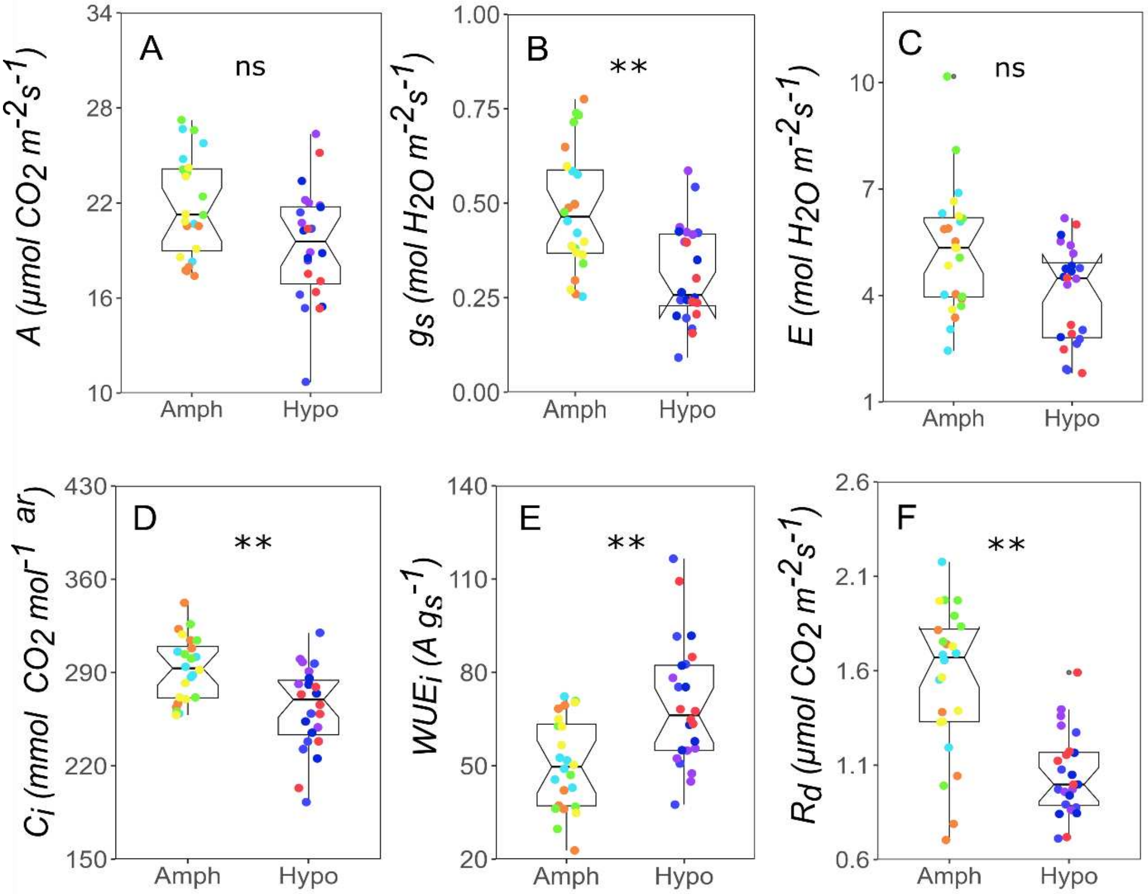

Figure 2. Leaf gas exchange of amphistomatic (Amph) and hypostomatic (Hypo) species of *Eucalyptus*. Species are represented by different colors as per legend included in Figure 1. For the box plot, the lower and upper hinges correspond to the first and third quartiles (interquartile range, IQR), the horizontal lines inside the boxes are the medians, the upper/lower whisker extends from the hinge to the largest/smallest value no further than 1.5 × IQR from the hinges, and data beyond the end of the whiskers are plotted individually (small grey circles). *A*, net assimilation rate; g_s, stomatal conductance to water vapor; *E*, transpiration rate; C_i, intercellular CO_2 concentration; WUE_i, intrinsic water use efficiency; R_d, dark respiration. Asterisks indicate significant differences between amphistomatic and hypostomatic groups according to Student’s t-test: $^{**}P < 0.01$; ns, not significant.

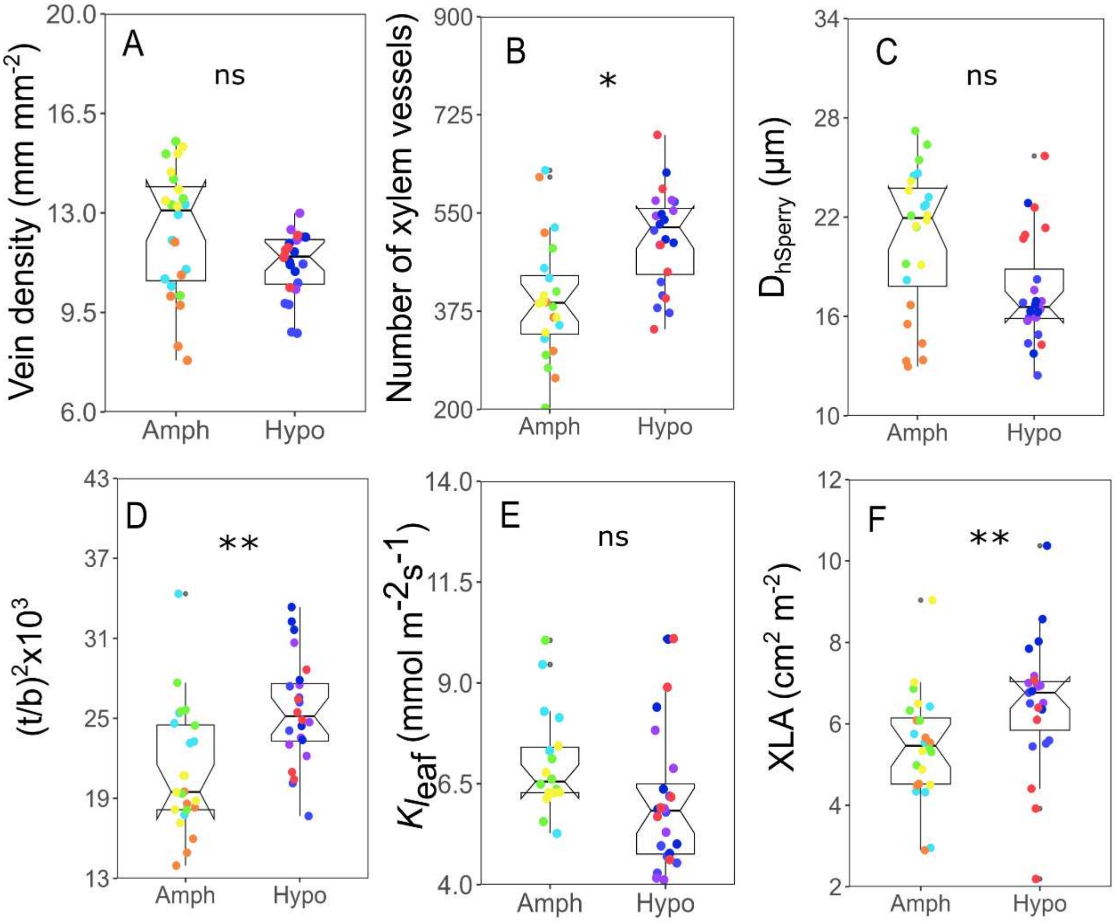

Figure 3. Leaf xylem dimensions and hydraulic traits of amphistomatic (Amph) and hypostomatic (Hypo) species of *Eucalyptus*. Species are represented by different colors as per the legend included in Figure 1. For the box plot, the lower and upper hinges correspond to the first and third quartiles (interquartile range, IQR), the horizontal lines inside the boxes are the medians, the upper/lower whisker extends from the hinge to the largest/smallest value no further than 1.5 × IQR from the hinges, and data beyond the end of the whiskers are plotted individually (small grey circles). Dh_{Sperry}, Sperry hydraulic diameter of the xylem conduits of the petiole; $(t/b)^2$, ratio between xylem wall thickness (t) and xylem lumen diameter (b) of the petiole; K_{leaf}, leaf hydraulic conductance; XLA, xylem area to leaf area ratio. Asterisks indicate significant differences between amphistomatic and hypostomatic groups according to Student's t-test: *$P < 0.05$, ** $P < 0.01$; ns, not significant.

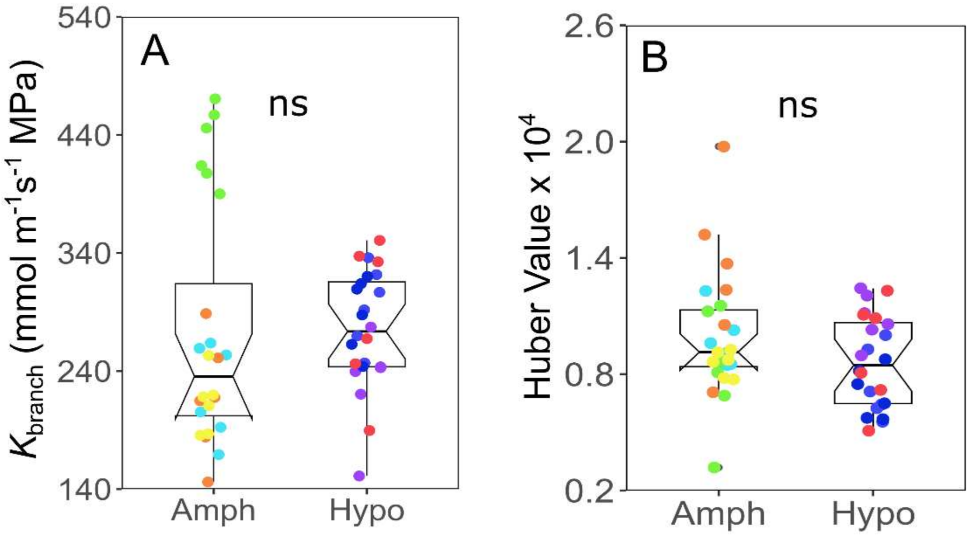

Figure 4. Branch hydraulic traits of amphistomatic (Amph) and hypostomatic (Hypo) species of *Eucalyptus*. Species are represented by different colors as per the legend included in Figure 1. For the box plot, the lower and upper hinges correspond to the first and third quartiles (interquartile range, IQR), the horizontal lines inside the boxes are the medians, the upper/lower whisker extends from the hinge to the largest/smallest value no further than 1.5 × IQR from the hinges, and data beyond the end of the whiskers are plotted individually (small grey circles). K_{branch}, branch hydraulic conductivity. Asterisks indicate significant differences between amphistomatic and hypostomatic groups according to Student's t-test: $*P < 0.05$, $**P < 0.01$; ns, not significant.

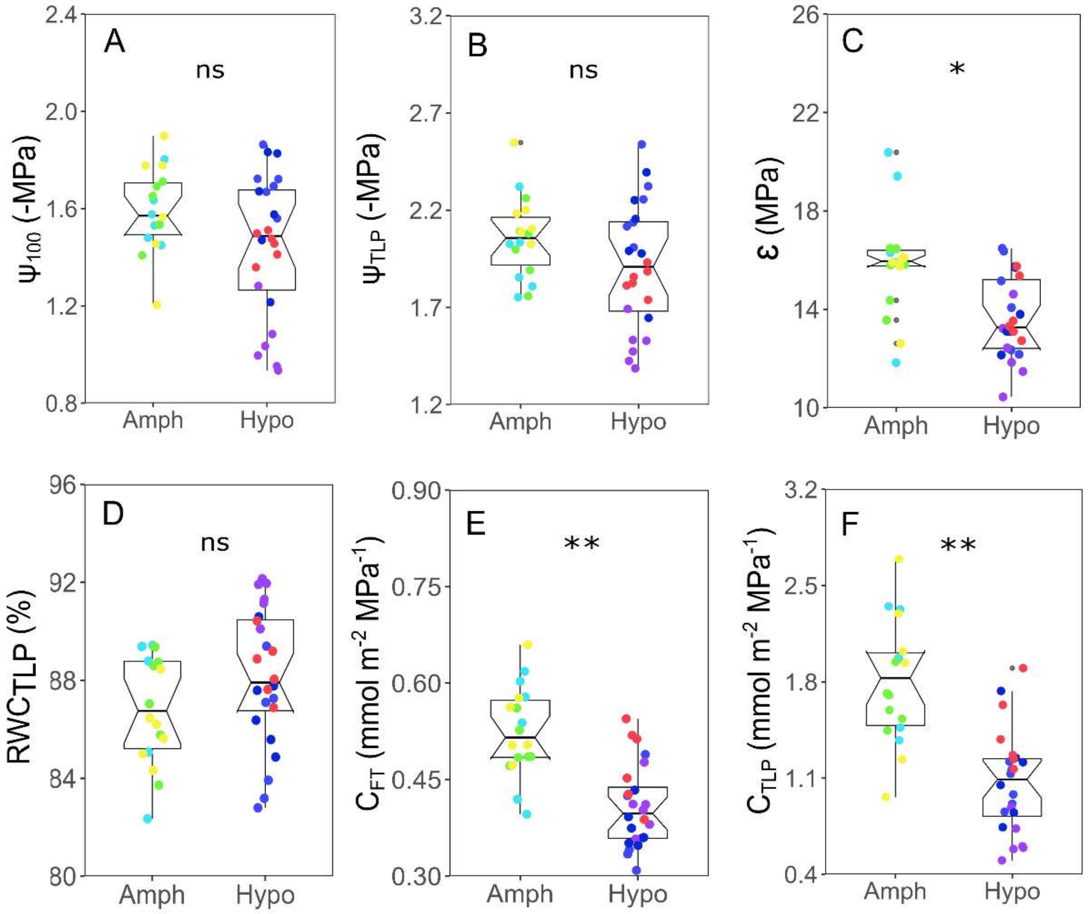

Figure 5. Plant-water relations traits obtained from pressure–volume curves of amphistomatic (Amph) and hypostomatic (Hypo) species of *Eucalyptus*. Species are represented by different colors as per the legend included in Figure 1. For the box plot, the lower and upper hinges correspond to the first and third quartiles (interquartile range, IQR), the horizontal lines inside the boxes are the medians, the upper/lower whisker extends from the hinge to the largest/smallest value no further than 1.5 × IQR from the hinges, and data beyond the end of the whiskers are plotted individually (small grey circles). Ψ_{100}, mean osmotic potential at full turgor; Ψ_{TLP}, water potential at the turgor loss point; ε, bulk elastic modulus; RWC_{TLP}, relative water content at the turgor loss point; C_{FT}, capacitance at full turgor; C_{TLP}, capacitance at the turgor loss point. Asterisks indicate significant differences between amphistomatic and hypostomatic groups according to Student's t-test: *P <0 .05, **P < 0.01; ns, not significant.

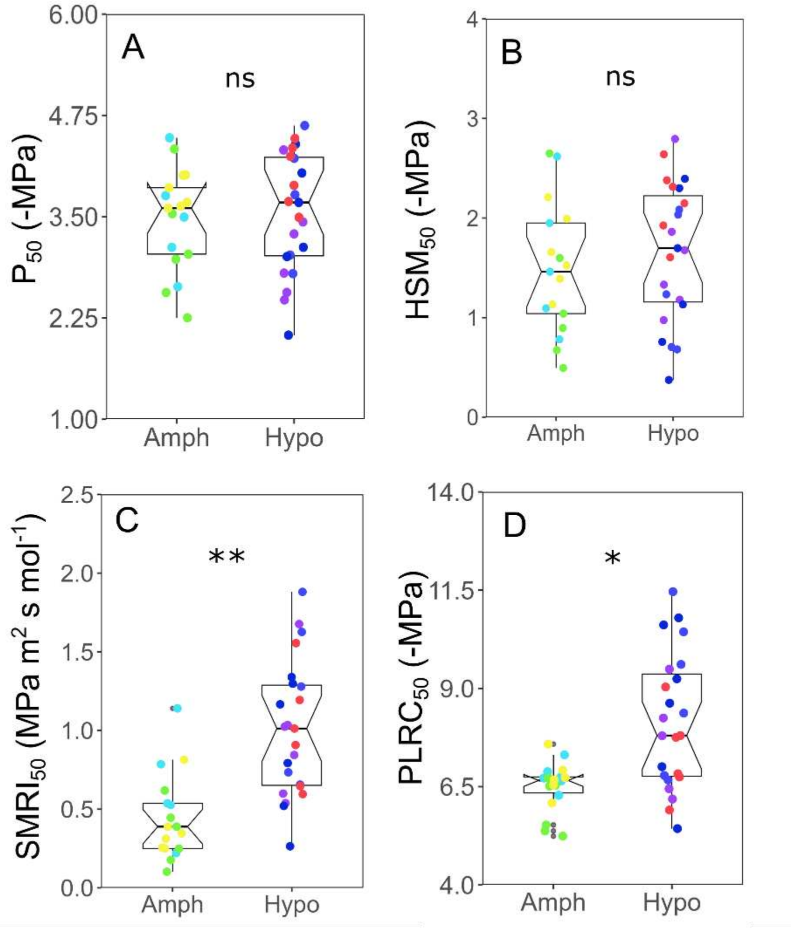

Figure 6. Plant-water relations traits obtained from optical vulnerability curves and curves of loss of leaf rehydration capacity of amphistomatic (Amph) and hypostomatic (Hypo) species of *Eucalyptus*. Species are represented by different colors as per the legend included in Figure 1. For the box plot, the lower and upper hinges correspond to the first and third quartiles (interquartile range, IQR), the horizontal lines inside the boxes are the medians, the upper/lower whisker extends from the hinge to the largest/smallest value no further than 1.5 × IQR from the hinges, and data beyond the end of the whiskers are plotted individually (small grey circles). P_{50}, water potential at 50% cumulative xylem embolized area; SSM_{50}, stomatal safety margin; $PLRC_{50}$, water potentials at 50% loss in the percentage of rehydration capacity: $SMRI_{50}$, stomatal margin retention index. Asterisks indicate significant differences between amphistomatic and hypostomatic groups according to Student's t-test: *$P < 0.05$, ns, not significant.

SUPPLEMENTARY DATA

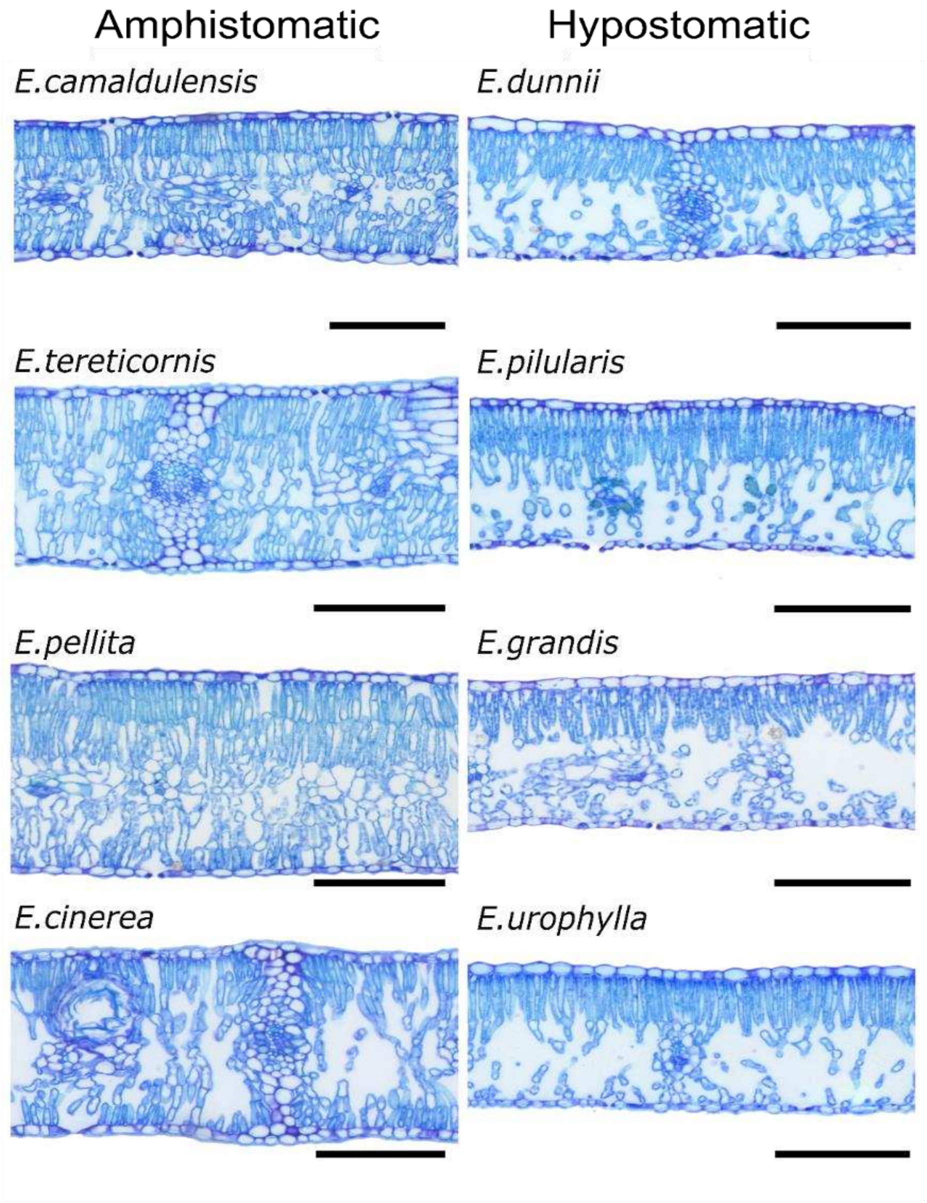

Supplementary Figure S1. Leaf cross-sections of the *Eucalyptus* species were assessed in this study. Bars = 250 µm.

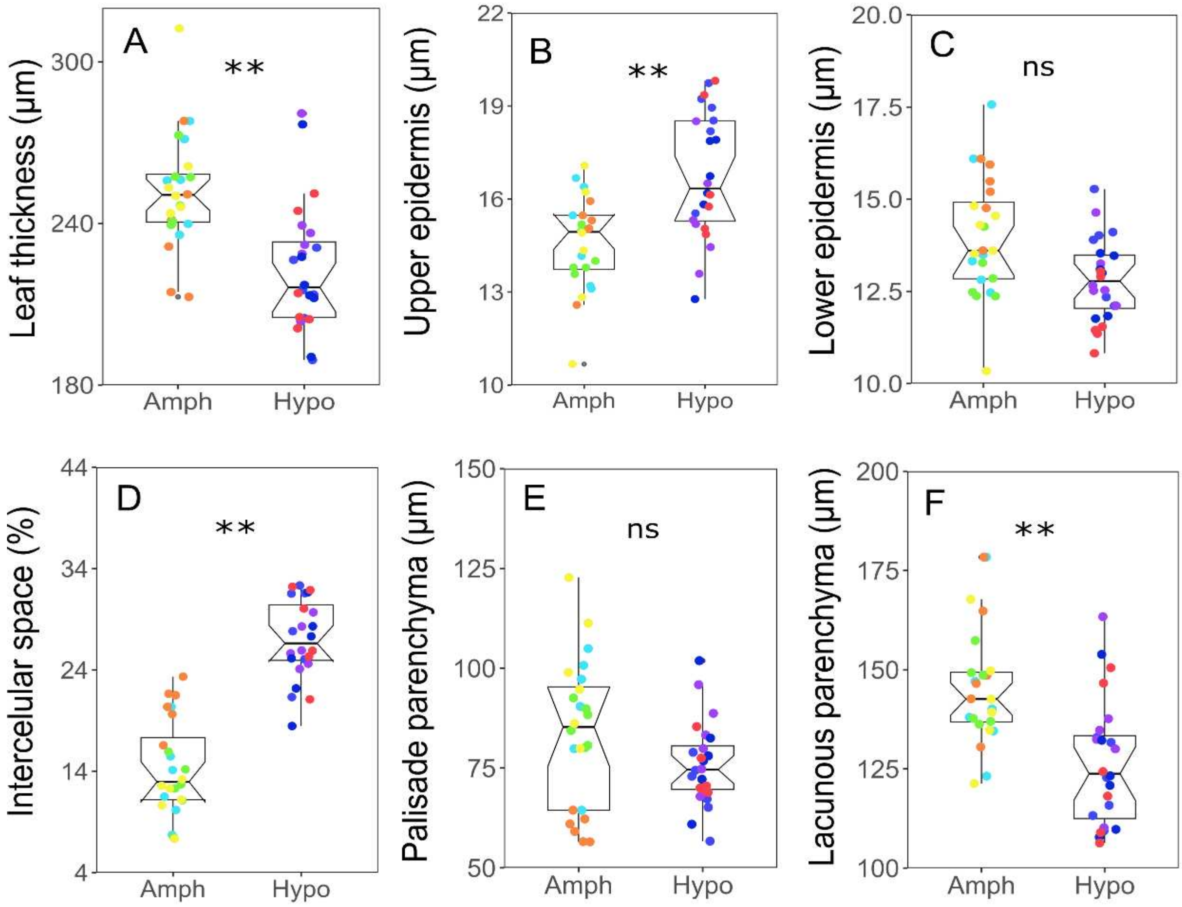

Supplementary Figure S2. Internal leaf structure of amphistomatic (Amph) and hypostomatic (Hypo) species of *Eucalyptus*. Species are represented by different colors as per legend included in Figure 1. For the box plot, the lower and upper hinges correspond to the first and third quartiles (interquartile range, IQR), the horizontal lines inside the boxes are the medians, the upper/lower whisker extends from the hinge to the largest/smallest value no further than 1.5 × IQR from the hinges, and data beyond the end of the whiskers are plotted individually (small grey circles). Asterisks indicate significant differences between amphistomatic and hypostomatic groups according to Student's t-test: *$P < 0.05$, **$P < 0.01$; ns, not significant.

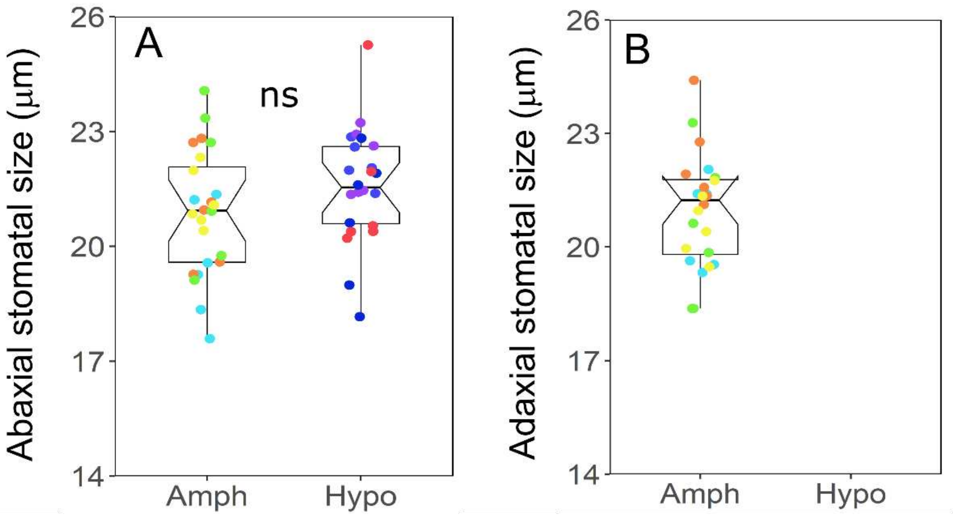

Supplementary Figure S3. Stomatal size of amphistomatic (Amph) and hypostomatic (Hypo) species of *Eucalyptus*. Species are represented by different colors as per legend included in Figure 1. For the box plot, the lower and upper hinges correspond to the first and third quartiles (interquartile range, IQR), the horizontal lines inside the boxes are the medians, the upper/lower whisker extends from the hinge to the largest/smallest value no further than 1.5 × IQR from the hinges, and data beyond the end of the whiskers are plotted individually (small grey circles). Asterisks indicate significant differences between amphistomatic and hypostomatic groups according to Student's t-test: ns, not significant.

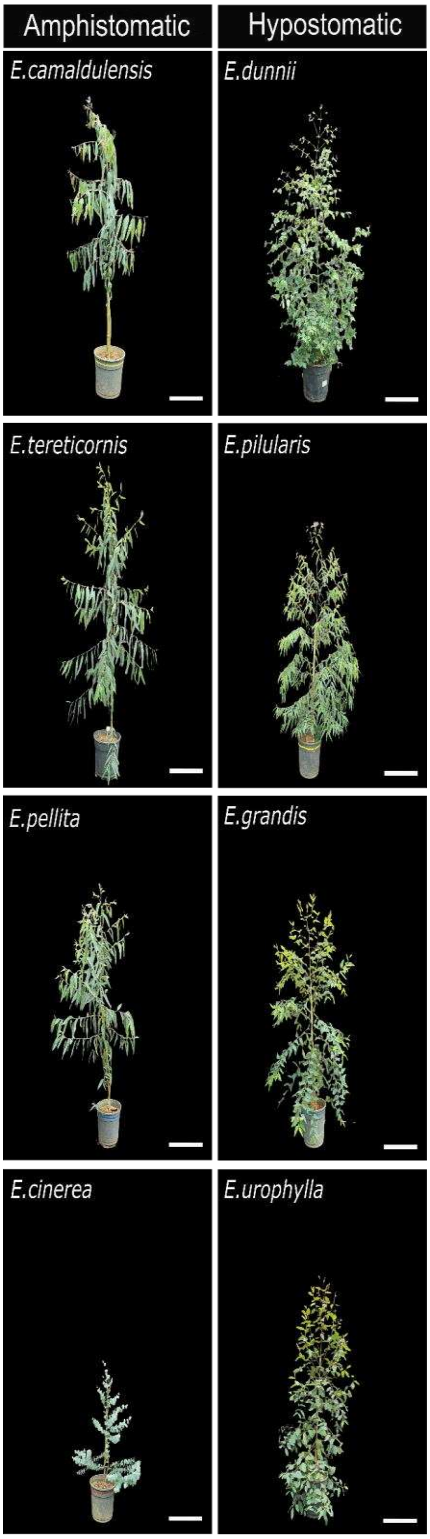

Supplementary Figure S4. Representative images of the *Eucalyptus* species were assessed in this study. Plants were seven months old when images were taken. Bars = 30 cm.

CHAPTER 2: **Selection for drought tolerance in eucalyptus: genetic control and the importance of physiological biomarkers**

Leonardo A. Oliveira, Talitha S. Pereira, Moab T. Andrade, Marcos D.V. Resende, Ulisses Figueiredo, Amanda A. Cardoso, Genaina A. Souza, Samuel C. V. Martins

ABSTRACT

The cultivation of eucalyptus is rapidly expanding due to its many features of interest. However, due to global climate change, many regions where it is grown will become unsuitable in the future. To accelerate genetic improvement and develop eucalyptus genotypes more adapted to future edaphoclimatic conditions, an ecophysiological approach is of utmost importance. Thus, in this study, genetic parameters such as heritability and accuracy for growth traits, hydraulic parameters, water relations, gas exchange, basic metabolism, and leaf anatomy were estimated in seven eucalyptus species (six of them among the nine most cultivated in the world). The methodology used mixed model methodology, REML (Restricted Maximum Likelihood)/BLUP (Best Linear Unbiased Prediction) procedure. Based on criteria such as the variability of these traits within the studied species, high heritability, and precision in evaluation, thirty-two variables were identified as potential biomarkers for genotyping in eucalyptus genetic improvement programs for various purposes.

INTRODUCTION

Planted forest area is growing significantly worldwide (FAO, 2020), with *Eucalyptus* L'Hér (Myrtaceae) plantations playing a significant role in this expansion. Currently, species of *Eucalyptus* are the most widely planted globally, especially in tropical and subtropical regions (Myburg et al. 2014, Messier et al. 2022), covering more than 20 million hectares around the world (Rejmánek and Richardson 2011). According to the 2021 Annual Report of the Brazilian Tree Industry (IBÁ 2021), the total area of planted forests in Brazil reached 9.55 million hectares, of which 7.47 million (78%) consisted of eucalyptus forests. The cultivation of eucalyptus has been rapidly expanding due to its accelerated growth, high yield, trunk ideal for wood production, high genetic variability, resistance to pests and diseases, and high tolerance to acidic soils with low fertility and high aluminum content (Eldridge et al. 1994, Chen 2005, Estopa et al. 2023). Additionally, eucalyptus is adaptable to a wide climatic range (Maydel Von, et al. 2018, Zhou et al. 2018, Ramantswana et al. 2020, Zhang and Wang 2021).

Due to the remarkable adaptability of eucalyptus species, their cultivation has expanded into more marginal areas, where they are exposed to edaphoclimatic conditions that would be prohibitive for the development of many other crops. However, with the ongoing global climate changes, these regions are increasingly experiencing rises in temperature and vapor pressure deficit (VPD), along with changes in precipitation patterns (IPCC 2019). These changes may be responsible for a drastic reduction in the productivity of these forests and could even lead to their demise. This was evident in 2015 in the state of Minas Gerais, in the southeastern region of Brazil, where drought events caused the mortality of approximately 2,000 km^2 of eucalyptus plantations (Gonçalves et al. 2017), highlighting the vulnerability of these systems to environmental alterations.

To sustain its rapid expansion and high productivity in the face of climate change scenarios, it becomes increasingly necessary to develop eucalyptus genotypes that are better adapted to edaphoclimatic conditions that may limit their optimal growth. Studies related to genetic improvement for drought tolerance are of great importance in the global context. The genetic improvement with an ecophysiological focus aims to identify characteristics that are related to the growth and survival of a large and diverse group of genotypes (which can be pure species or hybrids resulting from the crossbreeding of different species) to develop ideotypes for various purposes (Scolforo et al. 2017, Marcatti et al. 2017, Binkley et al. 2018). This approach can assist breeders in identifying traits that can be used to select plants at early stages, as forest genetic improvement is still a time-consuming process with long reproductive cycles, making the development of new genotypes challenging (Castro et al. 2021). Early selection is based on the use of stable key attributes that correlate with the necessary characteristics for plants to be highly productive in their selected locations and exhibit high heritability. In this process, traits of younger plants are employed as predictors of characteristics that manifest in the productive stage, thus anticipating genetic gains (Moraes et al. 2014, Corrêa et al. 2017).

The anatomical, physiological, and hydraulic parameters operate in an integrated manner, playing a crucial role in the growth, development, and drought tolerance of eucalyptus plants (Oliveira et al. 2022, Pita-Barbosa et al. 2023). Understanding how plant functional traits can affect fitness is a key focus of studies aimed at unraveling the role of natural selection in the evolution of population and species differences (Geber and Griffen, 2003, Kingsolver and Huey, 2003), as well as making it possible for plant breeders to use these traits. A notable example is the distribution of stomatal and their density, which is responsible for the trade-off between CO_2 absorption and water loss through the leaves (Hetherington and Woodward 2003). As drought progresses, most stomata close to minimize water loss rates, thereby protecting the hydraulic transport system and preventing collapses, ensuring the continuity of this transport (Martin-StPaul et al. 2017). However, a portion of the stomata remains partially open, or some structures associated with the stomata are leaky, contributing, along with water loss through leaf cuticles, to a considerable water loss (Duursma et al. 2019, Machado et al. 2021). Over time, this loss can deplete water stocks, leading to the collapse of the plant's hydraulic system and death (Martin-StPaul et al. 2017). This example illustrates how a seemingly simple and isolated characteristic, when contextualized, can have a significant impact. The importance of an eco-physiological approach is highlighted, assisting breeders in identifying promising markers for the selection of genotypes more adapted to low water availability. Nevertheless, attaining this objective necessitates crucial information on the heritability of eco-physiological characteristics. Presently, such information is in short supply, and the limited data we possess are derived from plants situated in diverse locations, spanning various ages, and employing different measurement methods for the same characteristic (Pita-Barbosa et al. 2023).

The recommended methodology for estimating genetic parameters such as heritability for forest species like eucalyptus is REML (Restricted Maximum Likelihood) / BLUP (Best Linear Unbiased Prediction). This method allows for the estimation of variance components and the prediction of genetic values for individuals (Resende 2009, 2015). In addition, to enable the ranking of genotypes based on their estimated genotypic values, it maximizes the precision of selection, reduces the gap between predicted and true genetic values, and enhances the probability of selecting the most promising individuals (Resende 2009, Corrêa et al. 2017).

The objective of this study was to estimate genetic parameters such as heritability and accuracy for growth traits, hydraulic parameters, water relations, gas exchange, basic metabolism, and leaf anatomy in seven eucalyptus species (six of them among the nine most cultivated globally - *E. camaldulensis*, *E. tereticornis*, *E. pellita*, *E. grandis*, *E. urophylla*, and *E. dunnii*) (Stanturf et al. 2013, Seng Hua et al. 2022). The aim was to identify desirable traits in genotypes adapted to water-restricted conditions, with coefficients of genetic variation indicating their maintenance in subsequent generations. This assists in selecting attributes of greater interest for use in phenotyping promising genotypes, facilitates decision-making, enhances the efficiency of eucalyptus breeding programs, and enables an increase in genetic gain over time.

MATERIAL AND METHODS

Plant material and growing conditions

Saplings with 120-day-old of seven *Eucalyptus* species (*E. camaldulensis*, *E. tereticornis*, *E. pellita*, *E. grandis*, *E. urophylla*, *E. dunnii* and *E. pilularis*) were obtained from the Sociedade de Investigações Florestais/Universidade Federal de Viçosa (UFV) nursery and cultivated in the gardens of the UFV, both in Viçosa (20°45’S, 42°54’W, 650 m altitude), southeast Brazil between June and December of 2021. The seedlings were transplanted into 20 L pots (one plant per pot) containing soil, washed sand, and commercial substrate Tropstrato HT® (3:2:1, v:v:v). Plants were irrigated daily to field capacity and fertilized according to the recommendations for the crop. They were maintained under natural conditions of light [photosynthetic photon flux density (PPFD) ranging from 1,000 to 1,500 µmol m^{-2} s^{-1}), temperature (max temperature ranging from 22 to 26°C and min temperature ranging from 13 to 19°C) and air humidity (max relative humidity ranging from 90 to 98% and min relative humidity ranging from 40 to 55%). Light intensity was measured between 11:00 and 13:00 h (solar time) using a quantum sensor (LI-191R; LI-COR, Lincoln, NE, USA). Temperature and relative humidity data were obtained from the automatic meteorological station in Viçosa. Data are available on the National Meteorological Institute of Brazil website (https://portal.inmet.gov.br/dadoshistoricos). Measurements and samplings were performed when plants were at the age of seven months. The experiment was set up in a completely randomized design with seven treatments (species) and six replications, where an experimental unit consisted of a 20 L pot containing one plant. Fully expanded leaves were sampled from lateral branches located in the middle third, and branches were sampled from this same region.

Leaf residual conductance

The leaf residual conductance ($g_{\text{leaf-res}}$) was measured for intact leaves using the weight loss method for detached leaves (Slavic, 1974, Sack et al., 2003, Machado et al., 2021). Leaves were collected in the late afternoon, placed in ziplock bags, transported to the laboratory, and had their petioles maintained under water for at least 12 h. After this, the petioles were sealed with parafilm tape, and the leaves were weighed on an analytical balance every 15 min for 3 h. Temperature and humidity were monitored for later calculation of the vapor pressure deficit (VPD). Initial and final leaf areas were obtained by scanning and measuring them using Image-Pro Plus 4.5. The $g_{\text{leaf-res}}$ was calculated from the slope of the linear relationship of leaf mass versus time and normalized by leaf area (sum of the adaxial and abaxial projected areas), atmospheric pressure, and VPD. For the slope estimation, only the linear part of the regression was used ($R^2 > 0.99$), suggesting maximal stomatal closure (Billon et al., 2020).

Leaf hydraulic conductance

Leaf hydraulic conductance (K_{leaf}) was measured using the evaporative flow method (Sack et al. 2002, Brodribb and Holbrook 2006). Leaf petioles were cut underwater, connected to a flow meter system (equipped with a 30 PSI pressure transducer, Honeywell International Inc, North Carolina, US), and placed under a light source of c. 1,000 µmol m^{-2} s^{-1} PPFD and fan-induced turbulent air to increase leaf transpiration. Pressure variation, water temperature, and leaf temperature were recorded with a datalogger (CampberRL Scientific, Shepshed, LE129GX, UK). E was derived from the tension created within the leaf-driven system through a known and recorded resistance following maximum stability (after c. 30 min). The leaves were then removed from the system, bagged for 10 min (to allow them to equilibrate), and their leaf water potential (Ψ_w) was measured with a pressure chamber (model 1000, PMS Instruments, New York, US). After that, the leaves were scanned, and their area was measured using Image-Pro Plus 4.5. Finally, E was normalized by leaf area, and K_{leaf} was calculated as $K_{Leaf} = -E / \Psi_w$. Due to the lack of petiole in *E. cinerea*, we could not measure the K_{leaf} of this species.

Pressure-volume curves

Leaves were collected, packed in zip-lock bags containing damp paper towels, and transported to the laboratory. They were cut under water and the petiole remained immersed for approximately 12 h to allow complete rehydration ($\Psi_w < 0.1$ MPa). Leaf mass and Ψ_w measurements were repeated during slow bench dehydration at c. 25°C and c. 60% relative humidity. In the end, leaves were then scanned, and their area was obtained using Image-Pro Plus 4.5. Next, leaves were placed in an oven at c. 70ºC until constant weight (equal to dry weight). Leaf dry weight was used to calculate RWC, and PV curves were constructed by plotting the inverse of Ψ_w against RWC (Tyree and Hammel 1972). The following parameters were estimated from each curve: osmotic potential at full turgor (Ψ_{100}), water potential at turgor loss point (Ψ_{TLP}), relative water content at the point of turgor loss (RWC_{TLP}), leaf capacitance at full turgor (C_{FT}) and after turgor loss point (C_{TLP}) and bulk modulus of elasticity (ε). Additionally, specific leaf area (SLA) was estimated as the ratio of leaf area to leaf dry mass and saturated water content (SWC) as the ratio of leaf water content to leaf fresh weight.

Anatomy of leaves and petioles

Completely expanded leaves were fixed in FAA_{50} (Johansen 1940) for 48 h and stored in 70% ethanol (v:v). Subsamples of leaves and petioles (or leaf midrib close to the branch insertion for *E. cinerea*) were embedded in methacrylate according to the manufacturer's recommendations (Leica Microsystems Nussloch, Heidelberg, Germany), cross-sectioned into 5 µm thick sections using an automatic advance rotary microtome (Leica RM2155, Leica Microsystems Inc., Derfild, USA), stained with toluidine blue (O'brien et al. 1964), and mounted in synthetic resin (Permount®). In addition, leaf samples of approximately 200 mm^2 were collected from the middle portion of each leaf, avoiding the central vein, clarified by the method of de Strittmatter (1973), and mounted in glycerinated gelatin to obtain images for quantifying vein density and stomatal characteristics.

The images were taken using a light microscope (AX70 TRF, Olympus Optical, Tokyo, Japan) coupled with a digital camera (Zeiss AxioCam HRc, Göttingen, Germany). Five fields of view (FOV) were obtained from each diaphanization sample at 4x magnification to measure vein density (V_D). V_D was calculated as the total length of second, third, fourth, fifth, and sixth-order veins divided by the FOV area. Additionally, five FOV at 20x magnification were captured to measure stomatal densities, including abaxial stomatal density (SD_{Aba}), adaxial stomatal density (SD_{Ada}), and total stomatal density (SD_{Total}), which is the sum of SD_{Aba} and SD_{Adal}.

From the leaf cross-section, three FOVs with 10x magnification were captured. The thickness of the abaxial and adaxial epidermis, the leaf blade thickness, and the thickness of the palisade and spongy parenchyma were measured in five parts of the lamina in each FOV. The percentage of intercellular space was determined by calculating the proportion of intercellular spaces to the entire internal area of the leaf blade.

From the cross-sections of the petiole, one FOV was obtained with a 10x magnification. The number of xylem vessels and long and short internal vessel diameters were measured. Based on the diameters of the vessel elements, Sperry hydraulic diameter (Dh_{Sperry}) was calculated using the following equations (Lewis and Boose 1995):

$$D_h = \sqrt{\frac{2a^2b^2}{a^2+b^2}}$$

where a and b represent the long and short internal vessel diameters, respectively, and n is the viscosity of water at 25°C. Dh_{Sperry} was calculated using the following equation (Sperry and Ikeda 1997):

$$\mathrm{Dh_{Sperry}} = \frac{1}{n} \Sigma_1^n \left(\frac{Dh^5}{Dh^4}\right)_i$$

where n represents the number of xylem vessels in the sample, 1 represents the first xylem vessel of the sample, and *i* represents all xylem vessels of the sample.

For an estimation of cell wall thickness to lumen breadth ratio $(t/b)^3$ two FOVs were obtained with a 20x magnification. The wall thickness (t) and corresponding vessel lumen diameter (b) were determined in 20 vessels for each petiole. The cell wall thickness was the medium of four meditations for each xylem vessel and the lumen diameter (b) was a medium from two measurements for each vessel.

Huber value

Branches were cut using pruning shears underwater in a bucket, where they were kept for c. 12 h, covered with black plastic bags. A small sample from the branch's base was stained with 1% Safranin and photographed using a camera attached to a stereomicroscope, and the images were used to measure the sapwood area using Image Pro Plus 4.5. The total leaf area per branch was measured by scanning the leaves and the Huber value was calculated as the ratio between the sapwood area and the total leaf area of the branch (Huber 1928).

Gas exchange, chlorophyll fluorescence, and light curves

Gas exchange parameters and chlorophyll fluorescence were determined under ambient temperature and vapor pressure conditions using a gas exchange system (LI-6400XT) equipped with an integrated fluorescence chamber (LI-6400-40, LI-COR Inc.). Net CO_2 assimilation rate (*A*), transpiration rate (*E*), and stomatal conductance to water vapor (g_s) were measured on attached leaves under artificial photosynthetically active radiation (RFA), i.e. 1000 µmol photons m^{-2} s^{-1} at the leaf level, and 400 µmol CO_2 mol^{-1} air.

In light-adapted leaves, the actual quantum yield of photosystem II (ΦPSII) was determined according to the procedure described by Genty et al. (1989), and the electron transport rate (ETR) was then calculated as:

$$\mathrm{ETR} = \alpha\ \beta \times \mathrm{PPFD} \times \Phi\mathrm{PSII}$$

where PPFD is the photosynthetically active photon flux density, α is the leaf absorptance and β is the optical cross-section of photosystem II. Intrinsic water use efficiency (WUE_i) was estimated as A/g_s.

Quantification of metabolites

One fully expanded leaf per plant was collected between 12 and 13h on a sunny day and immediately frozen in liquid nitrogen and stored at -80ºC. The samples were then freeze-dried at -48ºC and macerated in a cell disruptor (mini-Bead beater-96, Bio Spec Products, Bartlesville, OK, USA) using 3.2 mm metal spheres. To quantify the metabolites, 10 mg of dry mass (DM) of leaf samples were used, which were subjected to hot methanolic extraction (Lisec et al. 2006). Chlorophyll levels were determined as previously described by Wellburn (1994). Starch, sucrose, fructose, and glucose were measured according to the methodology described by (Fernie et al. 2001) and proline was quantified according to Carillo and Gibon (2011). Total amino acids (Yemm et al. 1955), starch (Fernie et al. 2001), and total protein (Bradford 1976) were quantified in the methanolic insoluble fraction. The content of all compounds was normalized to dry mass.

Plant hydraulic conductance

On the evening preceding the initiation of the plant hydraulic conductance (K_{plant}) analysis, thorough irrigation was administered to ensure complete rehydration of the plants. Subsequently, the pots were shielded with plastic film. To assess Ψ_w and pot weight, measurements were taken at both predawn and midday utilizing a Scholander pressure chamber and a precision balance with a sensitivity of 0.1 g, respectively. Whole-plant transpiration per unit leaf area was determined by calculating the difference in pot weight between predawn and midday. Total leaf area (TLA) was estimated by multiplying the LMA average of all the leaves on one branch per plant by the total dry mass of the leaves. This leaf area estimation was then employed to normalize transpiration. The calculation of K_{plant} was calculated using the following equation (Kramer and Boyer 1995):

$$K_{plant} = \text{whole-plant transpiration} / [(\Psi_{Predawn} - \Psi_{Midday}).$$

Leaf vulnerability to embolism and hydraulic safety margin

Leaf vulnerability to embolism was determined by the optical vulnerability method (Brodribb et al. 2016). Plants were harvested early in the morning, and their roots were washed until the soil was entirely removed. They were then placed in a bucket filled with water and transferred to the laboratory. The abaxial face of an intact mature leaf still attached to the plant was placed on a scanner (Epson Perfection V800; Epson, California, USA) using clear glass and adhesive tape. Plants were next removed from the bucket and allowed to slowly dehydrate under laboratory conditions (c. 25°C and 60% relative humidity). Images were taken every 3 min, and leaf Ψ_w was measured using a pressure chamber every c. 4 h. Images were obtained up to 5 h after the last embolic event was observed. The image area captured included the midrib and at least eight majors (second-order) veins. The stack of images was analyzed using ImageJ, following instructions from http://www.opensourceov.org and Brodribb et al. (2016). The degree of embolism was calculated as the cumulative area of the embolized xylem normalized by the total area of embolism. A linear regression was fitted between drying time and Ψ_w to determine the Ψ_w at the time that each image was captured. Finally, the declines in Ψ_w were plotted against the percentage of the cumulative embolized area (%) for each leaf. For each vulnerability curve, were obtained the Ψ_w at 50% cumulative xylem embolized area (P_{50}). The stomatal safety margin (sSM_{50}) was calculated for each genotype as the difference between Ψ_{TLP} and P_{50}.

Growth parameters and stem density

Plant height (H) was measured using a millimeter ruler (from ground level to the highest pair of leaves) and the average stem diameter (D) was measured using a digital caliper (calculated from two perpendicular diameter measurements 2 cm above the soil surface), and the stem volume (S_{vol}) was estimated according to the following equation:

$$\text{Stem volume} = \pi\ a\ b\frac{h}{3}$$

where 'a' and 'b' are the perpendicular radii of the stem and h is the height.

After the optical vulnerability curves, destructive analyses were carried out. Three-centimeter-long samples near the base of the stem were collected, their bark removed, and their volume measured using the water displacement method with the aid of a beaker. The samples were then dried in an oven at 70°C for 72 hours to determine their dry mass and the specific density of the stem was calculated as the dry mass of the stem section divided by the volume of the same section when still fresh.

The leaves, stem and roots were cut and kept in an oven at 70 °C for 72 hours and then weighed to determine the dry mass, and the total dry mass (TDM) was determined as the sum of the biomass of leaves, stem, and roots.

Statistical analysis

The analyses were carried out for all the traits, estimating the variance components and predicting the genotypic effects (random) using the mixed model approach, using the restricted maximum likelihood/best linear unbiased prediction (REML/BLUP) method (Resende, 2007a). To do this, the following statistical model was used:

$$y = \mathrm{Xu} + \mathrm{Zg} + \mathrm{e}$$

where y is the vector of data, u is the scalar referring to the general average (fixed effect), g is the vector of genotypic effects of species (assumed to be random) and e is the vector of errors or residues (random). X and Z represent the incidence matrices for u and g, respectively.

Equations of the mixed model:

$$\begin{bmatrix} X'X & X'Z \\ Z'X & Z'Z + A^{-1}\left(\left(1-h^2\right)/h^2\right) \end{bmatrix} \begin{bmatrix} \hat{b} \\ \hat{g} \end{bmatrix} = \begin{bmatrix} X'y \\ Z'y \end{bmatrix}$$

Heritability at the mean of cultivars (h^2) and accuracy were estimated, and the significant effects such as the genotypic variance between species (Vg) was tested using the Likelihood Ratio Tests (LRT) where deviance analyses were obtained for each character evaluated (Resende, 2007a).

The predicted genotypic values for twelve traits of interest were used to calculate the selection index, based on the average of the ranks (Mulamba and Mock

1978). The genetic analyses were carried out using the SELEGENREML/BLUP software (Resende 2007, 2015, 2016).

Selection index

The predicted genotypic values were used to calculate the selection index, based on the average of the ranks (Mulamba and Mock 1978), and the correlations of the characteristics (possible selected phenotypic markers) with the tolerant and susceptible phenotypes. The lowest rank value indicates plants that are more tolerant of water deficit.

The traits selected to make up the proposed ideotype aim to identify plants with greater resistance to embolism (P_{50}), greater control of their water status ($<g_{\text{leaf-res}}$, $>C_{\text{FT}}$ and C_{TLP}), greater water distribution capacity within the leaves (V_D), greater intrinsic water use efficiency (WUE_i), greater capacity of the stems to supply the water demand of the leaves (H_v), greater photosynthetic rates (*A*) (Oliveira et al. 2022, Pita-Barbosa et al. 2023). He used the characteristics referring to higher net yields (TDM, H, D, and S_{Vol}), which have been commonly used as fitness indicators in selection studies where it is not possible to obtain fitness assessments of genotypes at the field level (Franklin and Morrissey, 2017).

RESULTS

The fifty-four parameters analyzed were categorized into two main groups based on their genotypic differences. The first group, made up of thirty-eight variables (Tables 1 to 6), showed statistically significant differences ($P<0.01$ or $P<0.05$) in the means of the characteristics between the species studied, as indicated by the likelihood ratio test. In contrast, the second group, made up of sixteen traits (Tables S1 and S2), showed no significant variability in the means between the species, despite many of them exhibiting high heritability and accuracy, leading to the suppression of these results (Tables S1 and S2).

The genotypic coefficient of variation (CVg) values for 59% of the parameters are considered high (Tables 1 to 6). The CVg for the leaf anatomical characteristics ranged from 5.26 for TLL to 124.7 for SD_{Ada} (Tables 1 and 2). Within the gas exchange parameters, the range of CVg was smaller, varying from 5.12 for WUE to 27.24 for g_s (Table 3). As for the water relations parameters, they ranged from 2.04 for RWC_{TLP} to

45.13 for $g_{\text{leaf-res}}$ (Table 4). Allometric and growth parameters ranged from 9.82 for D to 28.73 for LA_{uni} (Table 5). For the content of primary metabolism compounds, CVg variations ranged from 2.49 to 31.55 for Suc and Chlo a, respectively (Table 6).

The accuracy (Acc) of the estimation of the characteristics ranged from 0.87 for TUE to 0.99 for SD_{Ada} for the leaf anatomical characteristics (Tables 1 and 2). For the gas exchange characteristics, the Acc ranged from 0.85 for WUE_i and *E* to 0.92 for g_s (Table 3). For the water relations characteristics, Acc ranged from 0.65 for P_{50} to 0.98 for SWC (Table 4). About allometric and growth characteristics, Acc ranged from 0.86 for H_V to 0.98 for H (Table 5). The contents of the basic metabolism compounds in the leaves (Table 6) ranged from 0.89 for Gluc to 0.99 for Suc. This shows that most of the variables are highly accurate.

The evaluation of leaf anatomical characteristics (Table 1, 2) revealed different heritability (h^2), ranging from 0.75 for the TUE to 0.99 for SD_{Ada}. In terms of gas exchange parameters (Table 3), h^2 ranged from 0.72 for *E* to 0.85 for g_s. For the water relations parameters (Table 4), the h^2 ranged from 0.42 for the P_{50} to 0.96 for the SWC, highlighting a significant range in h^2 within this group. In the context of allometric and growth parameters (Table 5), the h^2 of the characteristics ranged from 0.74 for the H_V to 0.96 for H. As for the contents of the basic metabolism compounds in the leaves (Table 6), the h^2 ranged from 0.79 for the Gluc content to 0.96 for the Suc content. These results indicate consistently high h^2 values for most of the attributes studied.

By analyzing the results of h^2, Acc, CVg, and the LRT test together, it was possible to select 32 variables that could potentially be used in breeding programs for a wide variety of purposes: V_D, SD_{Aba}, SD_{Ada}, SD_{Total}, g_{wmax}, Dh_{Sperry}, K_t, Nxv, IS, TPP, *A*, g_s, *E*, WUE_i, Ψ_{100}, Ψ_{TLP}, C_{FT}, C_{TLP}, SWC, $g_{\text{leaf-res}}$, LA_{uni}, SLA, H, D, H_v, S_{Vol}, TDM, Chlo *a*, Carot, Starch, Gluc, and Fruc. These variables showed good heritability and variability within the species studied, and the genetic parameters were estimated with good precision. And although P_{50} has only average heritability and accuracy and a low CVg, we used it in the index because of its importance for drought tolerance in plants (Choat et al. 2012, Martin-StPaul et al. 2017).

Based on the Mulamba and Mock index, we were able to classify the seven species studied based on characteristics that can give them advantages under conditions of water deficit, as well as another group of variables related to their productivity. According to these criteria, the species were classified in the following order: *E. urophylla*, *E. dunnii*, *E. camaldulensis*, *E. pilularis*, *E. pellita*, *E. tereticornis*, *E. grandis* (Table 7). The species in the top positions are the ones that most closely match the characteristics of good productivity and potentially greater drought tolerance.

DISCUSSION

The integrated analysis of structural and functional characteristics is emerging as an essential approach in studies dedicated to plant adaptation responses and strategies, covering a variety of purposes. This approach makes it possible to gain an in-depth understanding of the mechanisms underlying these adaptive processes, which can be delineated by various collaborative strategies, contributing synergistically to confer greater resilience to adverse conditions and promoting significant productivity increases. Once the key traits responsible for this improved resilience have been identified, the presence of intra genotypic variability, high heritability, and accuracy make these traits suitable for application in the early phenotyping of superior genotypes, highlighting their potential contribution to genetic improvement programs.

The availability of genetic parameters such as heritability and accuracy for numerous structural and physiological characteristics can be very useful when planning breeding programs (Moraes et al. 2014). According to the classification proposed by Resende (2009), heritability values between 0.15 and 0.50 are considered moderate and those above this are considered high for perennial species (Resende and Alves 2020, 2022). High heritability values show that traits have adequate genetic control and are easily transferable to future generations, and the higher the heritability value, the greater the gains obtained from selection for that particular trait (Majidi et al. 2009, Coser et al. 2022). Meanwhile, high accuracy values (above 70%) show that the traits studied have a significant correlation between true and predicted genetic values, leading to great confidence in the evaluation of individuals (Resende and Duarte 2007, Resende and Alves 2020, 2022). As for the coefficient of genotypic variation, values above 10-15% are considered moderate to high, indicating that genotypic variability is significant to the mean of the trait under study, suggesting that there is potential for selecting superior genotypes (Kushwah et al. 2021). Therefore, considering the association of estimated heritability values, accuracy, and coefficient of genotypic variation found in this study, 50% of the variables analyzed are candidates to be inserted as biomarkers in eucalyptus breeding programs for the most diverse purposes, revealing excellent possibilities for selecting eucalyptus genotypes based on the characteristics identified here.

To optimize the effectiveness of breeding programs, it is imperative to consider the simultaneous selection of several traits of interest, to consolidate them in a single genotype (Mendes et al. 2009). Once we have available genetic data for many variables of interest, it is the responsibility of breeders to identify which of them are most relevant to their breeding programs. This process must be carried out considering the specific objectives of the programs, as well as the human resources available and the capacity of the equipment to measure the plants. The characteristics presented in this study vary in terms of measurement difficulty, need for specialized equipment, processing, and cost. With variables such as plant height and diameter being cheap and easily measurable, biochemical and gas exchange assessments, involve the use of relatively expensive equipment and highly specialized labor.

Although often interrelated, the variables investigated in this study fall into distinct groups, each performing crucial functions for eucalyptus plants. A comprehensive understanding of these sets of parameters is imperative to unravel the mechanisms underlying the growth, development, productivity, and drought tolerance of these plants. This knowledge is of singular importance for breeding programs, requiring close collaboration between breeders and ecophysiologists. The synchronization of these disciplines is essential to identify the most relevant characteristics, culminating in the development of genotypes that are increasingly adapted to the specific environments in which they will be grown.

Leaf anatomical characteristics, including stomatal density, cuticle thickness, and leaf tissue structure, are fundamental to photosynthetic efficiency and water balance regulation (Silva et al. 2014, Guo et al. 2023). These characteristics influence both gas exchange parameters and water relations, contributing to the maintenance of photosynthetic rates and the control of water loss (Wu et al. 2008, Haworth et al. 2018). In addition, they affect the relationship between variations in water content and leaf water potential, playing a direct role in regulating water balance and water use efficiency (Horike et al. 2023, Petrík et al. 2023). This, in turn, influences the productivity and drought tolerance of eucalyptus plants (Oliveira et al. 2022, Pita-Barbosa et al. 2023).

Understanding the primary metabolism of the leaf, such as the levels of carbohydrates, amino acids, and proline, is essential for revealing the plant's efficiency in using photoassimilates to produce metabolites that are important for maintaining metabolism, growth, and, ultimately, for responding to water scarcity (Smith et al. 2018, Salam et al. 2023). The production and maintenance of levels of photosynthetic pigments, such as chlorophylls, and photoprotective pigments, such as carotenoids, are crucial for protecting the photosynthetic apparatus and maintaining gas exchange (Simkin et al. 2022, Sun et al. 2022). All these integrated factors optimize plant production and are responsible for plant responses under stress conditions (Kumar et al. 2018, Shakespear et al. 2024).

In addition to estimating the genetic parameters of important characteristics, criteria must be established for selecting genotypes. The selection criterion is the character or set of characters on which the selection is based, to evaluate and rank the candidates for selection according to the character targeted for improvement (Resende et al. 2014, 2015). The next step would be to assess the feasibility of obtaining such an ideotype through genetic improvement, especially considering the heritabilities and accuracies of the chosen characters. As plant responses involve many genes and different responses (Pita-Barbosa et al. 2023), we selected twelve main traits, intending to identify which of the seven species studied combine greater productivity and potentially greater drought tolerance.

The traits selected to establish an optimum combination between the various characters using the selection index can be grouped into two main groups. The first is made up of traits aimed at greater drought tolerance and better control of the plant's water content (P_{50} - greater resistance to embolism; $< g_{\mathrm{leaf\text{-}res}}$, $>C_{\mathrm{FT}}$ and C_{TLP} - greater control of water status; V_D - greater ability to distribute water within the leaves; A/g_s - greater efficiency of water use; H_V - greater ability of the stems to withstand the water demand of the leaves). The second group is made up of characteristics associated with productivity (A - higher photosynthetic rates; TDM, H, D, and S_{Vol} - higher productivity). Since Stuepp et al. (2020) demonstrated that in *E. benthamii* the plants that show the greatest initial growth are also those that show the greatest growth at 24 months of cultivation. Based on this selection index, two species ranked first together, namely *E. urophylla* and *E. dunnii*. The good performance of *E. urophylla* is no surprise, since this species is characterized by its good resistance to stress (Shen et al. 2023). Furthermore, its hybridization with *E. grandis*, generating the 'urograndis' hybrids, is considered a milestone in the success of tropical eucalyptus cultivation (Rezende et al. 2014).

The main characteristics that conferred greater tolerance to these two species over the others were P_{50} and $g_{leaf\text{-}res}$, the first of which is used as a proxy for drought tolerance in various species (Choat et al. 2012, Sperry and Love 2015, Rowland et al. 2015). Therefore, the higher its modulus values, the greater the reductions in water availability capable of compromising the hydraulic system and the inability of these plants to transport water. The $g_{leaf\text{-}res}$ is related to the amount of water that plants lose after their stomata close and is one of the main characteristics related to the lower loss of tissue water content during drought events (Duursma et al. 2019), protecting the hydraulic system of these plants and making them less susceptible during drought events (Martin-StPaul et al. 2017). Growth parameters such as total biomass, height, diameter, and stem volume were used to assess the productivity of these genotypes.

This study represents a pioneering initiative in the estimation of genetic parameters related to various characteristics, covering physiological aspects, growth, hydraulics, water relations, gas exchange, basic metabolism, and leaf anatomy. This approach allows breeders, before deciding which variables to incorporate into breeding programs, to verify the presence of variability between species, as well as the existence of heritability and accuracy. However, it is important to note that the evaluations were carried out on very young plants, with a small number of individuals (n=6), since the study is preliminary in nature and aims to identify promising variables. It is therefore recommended that future studies be carried out to assess the temporal stability of these characteristics, which could allow these variables to be used effectively in early selection. In addition, further efforts are needed with a greater number of repetitions and greater genetic variability, to identify whether these same characteristics can be used to discriminate between different genotypes within the same species.

CONCLUSION

The estimates of genetic parameters studied revealed thirty-two variables that can be used as biomarkers for phenotyping genotypes in eucalyptus breeding programs for a wide variety of purposes. These traits were selected based on the existence of variability for these traits within the species studied, as well as high heritability and accuracy. These selected traits are as follows: V_D, SD_{Aba}, SD_{Ada},

SD_{Total}, g_{wmax}, Dh_{Sperry}, K_t, Nxv, IS, TPP, A, g_s, E, WUE_i, Ψ_{100}, Ψ_{TLP}, C_{FT}, C_{TLP}, SWC, $g_{leaf\text{-}res}$, LA_{uni}, SLA, H, D, H_v, S_{Vol}, TDM, Chlo *a*, Carot, Starch, Gluc, and Fruc.

Using 12 of them and the Mulan and Mock index, we identified that of the seven species used in this study, *E. urophylla* and *E. dunnii* have the best balance between productivity and potential drought tolerance.

Acknowledgments

LAO acknowledges the financial support received from the Brazilian Federal Agency for the Support and Evaluation of Graduate Education (CAPES) and the use of the plant anatomy laboratory at Universidade Federal de Viçosa. During the final stages, this study was supported by the USDA National Institute of Food and Agriculture, Hatch Project 7003279 (AAC).

Conflicts of Interest

The authors declare that they have no conflicts of interest associated with this work.

REFERENCES

Andrade MT, Oliveira LA, Pereira TS, Cardoso AA, Batista-Silva W, Damatta FM, Zsögön A, Martins SCV (2022) Impaired auxin signaling increases vein and stomatal density but reduces hydraulic efficiency and ultimately net photosynthesis. J Exp Bot 73:4147–4156.

Baresch A, Crifò C, Boyce CK (2019) Competition for epidermal space in the evolution of leaves with high physiological rates. New Phytologist 221:628–639.

Barros Filho NF (2014) Discriminação isotópica do 13C e nutrição com cálcio e boro em clones de eucalipto submetidos ao défice hídrico. Federal University of Viçosa, Viçosa

Bartlett MK, Klein T, Jansen S, Choat B, Sack L (2016) The correlations and sequence of plant stomatal, hydraulic, and wilting responses to drought. Proc Natl Acad Sci U S A 113:13098–13103.

Bartlett MK, Scoffoni C, Sack L (2012) The determinants of leaf turgor loss point and prediction of drought tolerance of species and biomes: A global meta-analysis. Ecol Lett 15:393–405.

Beerling DJ, Kelly CK (1996) Evolutionary comparative analyses of the relationship between leaf structure and function. New Phytologist 134:35–51.

Billon LM, Blackman CJ, Cochard H, Badel E, Hitmi A, Cartailler J, Souchal R. 2020. The DroughtBox: a new tool for phenotyping residual branch conductance and its temperature dependence during drought. Plant, Cell & Environment 43: 1584-1594.

Binkley D, Campoe OC, Alvares C, Carneiro RL, Cegatta Í, Stape JL (2018) The interactions of climate, spacing and genetics on clonal *Eucalyptus* plantations across Brazil and Uruguay. For Ecol Manage 405:271–283.

Blackman CJ, Halliwell B, Hartill GE, Brodribb TJ (2023) Petiole XLA (xylem to leaf area ratio) integrates hydraulic safety and efficiency across a diverse group of eucalypt leaves. Plant Cell Environ 47:49–58.

Blackman CJ, Li X, Choat B, Rymer PD, De Kauwe MG, Duursma RA, Tissue DT, Medlyn BE (2019) Desiccation time during drought is highly predictable across species of *Eucalyptus* from contrasting climates. New Phytologist 224:632–643.

Blackman CJ, Pfautsch S, Choat B, Delzon S, Gleason SM, Duursma RA (2016) Toward an index of desiccation time to tree mortality under drought. Plant Cell Environ 39:2342–2345.

de Boer HJ, Drake PL, Wendt E, Price CA, Schulze ED, Turner NC, Nicolle D, Veneklaas EJ (2016) Apparent overinvestment in leaf venation relaxes leaf morphological constraints on photosynthesis in arid habitats. Plant Physiol 172:2286–2299.

De Boer HJ, Eppinga MB, Wassen MJ, Dekker SC (2012) A critical transition in leaf evolution facilitated the Cretaceous angiosperm revolution. Nat Commun 3

de Boer HJ, Price CA, Wagner-Cremer F, Dekker SC, Franks PJ, Veneklaas EJ (2016) Optimal allocation of leaf epidermal area for gas exchange. New Phytologist 210:1219–1228.

Bradford MM (1976) A rapid and sensitive method for the quantitation of microgram quantities of protein utilizing the principle of protein-dye binding. Anal Biochem 72:248–254.

Brodribb TJ, Feild TS, Jordan GJ (2007) Leaf maximum photosynthetic rate and venation are linked by hydraulics. Plant Physiol 144:1890–1898.

Brodribb TJ, Holbrook NM (2006) Declining hydraulic efficiency as transpiring leaves desiccate: Two types of response. Plant Cell Environ 29:2205–2215.

Brodribb TJ, Jordan GJ, Carpenter RJ (2013) Unified changes in cell size permit coordinated leaf evolution. New Phytologist 199:559–570.

Brodribb TJ, McAdam SAM, Jordan GJ, Martins SCV (2014) Conifer species adapt to low-rainfall climates by following one of two divergent pathways. Proc Natl Acad Sci U S A 111:14489–14493.

Brodribb TJ, Skelton RP, Mcadam SAM, Bienaimé D, Lucani CJ, Marmottant P (2016) Visual quantification of embolism reveals leaf vulnerability to hydraulic failure. New Phytologist 209:1403–1409.

Buckley TN (2019) How do stomata respond to water status? New Phytologist 224:21–36.

Carillo P, Gibon Y (2011) Extraction and determination of proline. https://www.researchgate.net/publication/211353600

Caringella MA, Bongers FJ, Sack L (2015) Leaf hydraulic conductance varies with vein anatomy across Arabidopsis thaliana wild-type and leaf vein mutants. Plant Cell Environ 38:2735–2746.

Carpenter RJ (1994) Cuticular morphology and aspects of the ecology and fossil history of North Queensland-rainforest Proteaceae. Botanical Journal of the Linnean Society 116:249–303.

Castro CAO, dos Santos GA, Takahashi EK, Nunes ACP, Souza GA, Resende MDV (2021) Accelerating *Eucalyptus* breeding strategies through top grafting applied to young seedlings. Ind Crops Prod 171

Chen S (2005) *Eucalyptus* source of ecological problems and countermeasures. Tropical Forestry 33:29–30.

Choat B, Jansen S, Brodribb TJ, Cochard H, Delzon S, Bhaskar R, Bucci SJ, Feild TS, Gleason SM, Hacke UG, Jacobsen AL, Lens F, Maherali H, Martínez-Vilalta J, Mayr S, Mencuccini M, Mitchell PJ, Nardini A, Pittermann J, Pratt RB, Sperry JS, Westoby M, Wright IJ, Zanne AE (2012) Global convergence in the vulnerability of forests to drought. Nature 491:752–755.

Clarke PJ, Lawes MJ, Murphy BP, Russell-Smith J, Nano CEM, Bradstock R, Enright NJ, Fontaine JB, Gosper CR, Radford I, Midgley JJ, Gunton RM (2015) A synthesis of postfire recovery traits of woody plants in Australian ecosystems. Science of the Total Environment 534:31–42.

Corrêa TR, Picoli EA de T, Souza GA de, Condé SA, Silva NM, Lopes-Mattos KLB, Resende MDV de, Zauza EAV, Oda S (2017) Phenotypic markers in early selection for tolerance to dieback in *Eucalyptus*. Ind Crops Prod 107:130–138.

Coser SM, Motoike SY, Corrêa TR, Queiroz V, Costa AC, Nascimento HR, Madeira DDC, Resende MDV (2022) Estimates of genetic parameters and selection gains for phenological and productive characteristics in macaw palm: an important plant for bioenergy. Functional Plant Breeding Journal 4:23–33.

Cowan IR, Farquhar GD (1977) Stomatal function in relation to leaf metabolism and environment. In: Symposia of the Society for Experimental Biology.

Creek D, Blackman CJ, Brodribb TJ, Choat B, Tissue DT (2018) Coordination between leaf, stem, and root hydraulics and gas exchange in three arid-zone angiosperms during severe drought and recovery. Plant Cell Environ 41:2869–2881.

Deon M, De Resende V (2016) Software Selegen-REML/BLUP: a useful tool for plant breeding ARTICLE. MDV Resende Crop Breeding and Applied Biotechnology 16:330–339. http://dx.doi.org/10.1590/1984-70332016v16n4a49

Drake PL, de Boer HJ, Schymanski SJ, Veneklaas EJ (2019) Two sides to every leaf: water and CO 2 transport in hypostomatous and amphistomatous leaves. New Phytologist 222:1179–1187.

Drake PL, Froend RH, Franks PJ (2013) Smaller, faster stomata: Scaling of stomatal size, rate of response, and stomatal conductance. J Exp Bot 64:495–505.

Duursma RA, Blackman CJ, Lopéz R, Martin-StPaul NK, Cochard H, Medlyn BE (2019) On the minimum leaf conductance: its role in models of plant water use, and ecological and environmental controls. New Phytologist 221:693–705.

Ehleringer JR, Phillips SL, Schuster WSF, Sandquist DR (1991) Differential utilization of summer rains by desert plants. Oecologia 88:430–434.

Eldridge K, Davidson J, Harwood C, Wyk GV (1994) Eucalypt domestication and breeding. Oxford University Press.

Enright NJ, Fontaine JB, Lamont BB, Miller BP, Westcott VC (2014) Resistance and resilience to changing climate and fire regime depend on plant functional traits. Journal of Ecology 102:1572–1581.

Estopa RA, Paludeto JGZ, Müller BSF, de Oliveira RA, Azevedo CF, de Resende MDV, Tambarussi EV, Grattapaglia D (2023) Genomic prediction of growth and wood quality traits in *Eucalyptus benthamii* using different genomic models and variable SNP genotyping density. New For (Dordr) 54:343–362.

Ezcurra E, Montaña C, Arizaga S, Montana C (1991) Architecture, light Interception, and distribution of Larrea species in the monte desert, Argentina. Ecology 72:23–34.

Falster DS, Westoby M (2003) Leaf size and angle vary widely across species: What consequences for light interception? New Phytologist 158:509–525.

Fan Y, Miguez-Macho G, Jobbágy EG, Jackson RB, Otero-Casal C (2017) Hydrologic regulation of plant rooting depth. Proc Natl Acad Sci U S A 114:10572–10577.

Fernie AR, Roscher A, Ratcliffe RG, Kruger NJ (2001) Fructose 2, 6-bisphosphate activates pyrophosphate: fructose-6-phosphate 1-phosphotransferase and increases triose phosphate to hexose phosphate cycling in heterotrophic cells. Planta 212:250–263.

Fick SE, Hijmans RJ (2017) WorldClim 2: new 1-km spatial resolution climate surfaces for global land areas. International Journal of Climatology 37:4302–4315.

Flexas J, Ribas-Carbó M, Diaz-Espejo A, Galmés J, Medrano H (2008) Mesophyll conductance to CO2: Current knowledge and future prospects. Plant Cell Environ 31:602–621.

Foster JR, Smith WK (1986) Influence of stomatal distribution on transpiration in low-wind environments. Plant Cell Environ 9:751–759.

Franklin HM, Chen C, Carroll AR, Saeck E, Fisher P, Burford MA (2020) Leaf litter of two riparian tree species has contrasting effects on nutrients leaching from soil during large rainfall events. Plant Soil 457:389–406.

Franklin OD, Morrissey MB. Inference of selection gradients using performance measures as fitness proxies. Methods in Ecology and Evolution. 2017 Jun;8(6):663-77.

Franks PJ, Drake PL, Beerling DJ (2009) Plasticity in maximum stomatal conductance constrained by negative correlation between stomatal size and density: An analysis using *Eucalyptus globulus*. Plant Cell Environ 32:1737–1748.

Franks PJ, Farquhar GD (2001) The effect of exogenous abscisic acid on stomatal development, stomatal mechanics, and leaf gas exchange in Tradescantia virginiana. Plant Physiol 125:935–942.

Geber MA, Griffen LR. Inheritance and natural selection on functional traits. International journal of plant sciences. 2003 May;164(S3):S21-42.

Germon A, Jourdan C, Bordron B, Robin A, Nouvellon Y, Chapuis-Lardy L, de Moraes Gonçalves JL, Pradier C, Guerrini IA, Laclau JP (2019) Consequences of clear-cutting and drought on fine root dynamics down to 17 m in coppice-managed eucalypt plantations. For Ecol Manage 445:48–59.

Gibson AC (1996) Structure-Function Relations of Warm Desert Plants. Springer Berlin Heidelberg, Berlin, Heidelberg.

Global Forest Resources Assessment 2020 (2020) FAO.

Gonçalves JLM, Alvares CA, Rocha JHT, Brandani CB, Hakamada R (2017) Eucalypt plantation management in regions with water stress. South For 79:169–183.

Griffin-Nolan RJ, Ocheltree TW, Mueller KE, Blumenthal DM, Kray JA, Knapp AK (2019) Extending the osmometer method for assessing drought tolerance in herbaceous species. Oecologia 189:353–363.

Guo W, Cherubini P, Zhang J, Li MH, Qi L (2023) Leaf stomatal traits rather than anatomical traits regulate gross primary productivity of moso bamboo (Phyllostachys edulis) stands. Front Plant Sci 14

Haverroth EJ, Oliveira LA, Andrade MT, Taggart M, McAdam SAM, Zsögön A, Thompson AJ, Martins SCV, Cardoso AA (2023) Abscisic acid acts essentially on stomata, not on the xylem, to improve drought resistance in tomato. Plant Cell Environ 46:3229–3241.

Haworth M, Marino G, Centritto M (2018) An introductory guide to gas exchange analysis of photosynthesis and its application to plant phenotyping and precision irrigation to enhance water use efficiency. Journal of Water and Climate Change 9:786–808.

Hetherington AM, Woodward & FI (2003) The role of stomata in sensing and driving environmental change. Nature 424:901–908.

Horike H, Kinoshita T, Kume A, Hanba YT (2023) Responses of leaf photosynthetic traits, water use efficiency, and water relations in five urban shrub tree species under drought stress and recovery. Trees - Structure and Function 37:53–67.

Huang R, Di N, Xi B, Yang J, Duan J, Li X, Feng J, Choat B, Tissue D (2024) Herb hydraulics: Variation and correlation for traits governing drought tolerance and efficiency of water transport. Science of the Total Environment 907

Huber B. (1928) Weitere quantitative Untersuchungen über das Wasserleitungssystem der Pflanzen.

Indústria Brasileira de Árvores. Relatório anual (2021)

Johansen DA (1940) Plant Microtechnique. McGraw-Hill, , New York.

Jordan GJ, Carpenter RJ, Brodribb TJ (2014) Using fossil leaves as evidence for open vegetation. Palaeogeogr Palaeoclimatol Palaeoecol 395:168–175.

Kahmen A, Basler D, Hoch G, Link RM, Schuldt B, Zahnd C, Arend M (2022) Root water uptake depth determines the hydraulic vulnerability of temperate European tree species during the extreme 2018 drought. Plant Biol 24:1224–1239.

King DA (1997) The functional significance of leaf angle in *Eucalyptus*. Aust J Bot 45:619–639.

Kingsolver JG, Huey RB. Introduction: the evolution of morphology, performance, and fitness. Integrative and Comparative Biology. 2003 Jul 1;43(3):361-6.

Kramer PJ, Boyer JS (1995) Water relations of plants and soil, First. Academic Press, San Diego, USA.

Kumar S, Sachdeva S, Bhat K V., Vats S (2018) Plant responses to drought stress: Physiological, biochemical and molecular basis. In: Biotic and Abiotic Stress Tolerance in Plants. Springer Singapore, pp 1–25.

Kushwah A, Dharminder Bhatia •, Singh G, Singh I, Bindra S, Suruchi Vij •, Singh S (2021) Phenotypic evaluation of genetic variability and selection of yield contributing traits in chickpea recombinant inbred line population under high temperature stress. Physiology and Molecular Biology of Plants 27:747–767. https://doi.org/10.1007/s12298-

Lewis AM, Boose ER (1995) Estimating Volume Flow Rates Through Xylem Conduits. Am J Bot 82:1112–1116.

Li X, Blackman CJ, Choat B, Duursma RA, Rymer PD, Medlyn BE, Tissue DT (2018) Tree hydraulic traits are coordinated and strongly linked to climate-of-origin across a rainfall gradient. Plant Cell Environ 41:646–660.

Lisec J, Schauer N, Kopka J, Willmitzer L, Fernie AR (2006) Gas chromatography mass spectrometry-based metabolite profiling in plants. Nat Protoc 1:387–396.

Lucani CJ, Brodribb TJ, Jordan G, Mitchell PJ (2019) Intraspecific variation in drought susceptibility in *Eucalyptus globulus* is linked to differences in leaf vulnerability. Functional Plant Biology 46:286–293.

Machado R, Loram-Lourenço L, Farnese FS, Alves RD, de Sousa LF, Silva FG, Filho SC, Torres-Ruiz JM, Cochard H, Menezes-Silva PE. Where do leaf water leaks come from? Trade-offs underlying the variability in minimum conductance across tropical savanna species with contrasting growth strategies. New Phytologist. 2021 Feb;229(3):1415-30.

Majidi MM, Mirlohi A, Amini F (2009) Genetic variation, heritability and correlations of agro-morphological traits in tall fescue (Festuca arundinacea Schreb.). Euphytica 167:323–331.

Mantova M, Herbette S, Cochard H, Torres-Ruiz JM (2022) Hydraulic failure and tree mortality: from correlation to causation. Trends Plant Sci 27:335–345.

Marcatti GE, Resende RT, Resende MD V., Ribeiro CAAS, dos Santos AR, da Cruz JP, Leite HG (2017) GIS-based approach applied to optimizing recommendations of *Eucalyptus* genotypes. For Ecol Manage 392:144–153.

Márquez DA, Stuart-Williams H, Farquhar GD, Busch FA (2022) Cuticular conductance of adaxial and abaxial leaf surfaces and its relation to minimum leaf surface conductance. New Phytologist 233:156–168.

Martin-StPaul N, Delzon S, Cochard H (2017a) Plant resistance to drought depends on timely stomatal closure. Ecol Lett 20:1437–1447.

Martin-StPaul N, Delzon S, Cochard H (2017b) Plant resistance to drought depends on timely stomatal closure. Ecol Lett 20:1437–1447.

Masson-Delmotte V, Zhai P, Pörtner H-O, Roberts D, Skea J, Calvo E, Priyadarshi B, Shukla R, Ferrat M, Haughey E, Luz S, Neogi S, Pathak M, Petzold J, Pereira JP, Vyas P, Huntley E, Kissick K, Belkacemi M, Malley J (2019) Climate Change and Land An IPCC Special Report on climate change, desertification, land degradation, sustainable land management, food security, and greenhouse gas fluxes in terrestrial ecosystems Head of TSU (Operations) IT/Web Manager Senior Administrator. www.ipcc.ch

Matusick G, Ruthrof KX, Fontaine JB, Hardy GESJ (2016) *Eucalyptus* forest shows low structural resistance and resilience to climate change-type drought. Journal of Vegetation Science 27:493–503.

Maydel Von HJ Appraisal of practices to manage woody plants in semiarid environment. In: Bruns S, Furberg J, Luukanen O, Woods P (eds) Dryland Forestry Research . International Foundation for Science, Stockholm, Sweden, pp 47–64.

McAdam SAM, Eléouët MP, Best M, Brodribb TJ, Carins Murphy M, Cook SD, Dalmais M, Dimitriou T, Gélinas-Marion A, Gill WM, Hegarty M, Hofer JMI, Maconochie M, McAdam EL, McGuiness P, Nichols DS, Ross JJ, Sussmilch FC, Urquhart S (2017) Linking auxin with photosynthetic rate via leaf venation. Plant Physiol 175:351–360.

McCulloh KA, Domec JC, Johnson DM, Smith DD, Meinzer FC (2019) A dynamic yet vulnerable pipeline: Integration and coordination of hydraulic traits across whole plants. Plant Cell Environ 42:2789–2807.

Mendes FF, Ramalho MAP, Abreu ÂFB (2009) Índice de seleção para escolha de populações segregantes de feijoeiro-comum Selection index for choosing segregating populations in common bean.

Messier C, Bauhus J, Sousa-Silva R, Auge H, Baeten L, Barsoum N, Bruelheide H, Caldwell B, Cavender-Bares J, Dhiedt E, Eisenhauer N, Ganade G, Gravel D, Guillemot J, Hall JS, Hector A, Hérault B, Jactel H, Koricheva J, Kreft H, Mereu S, Muys B, Nock CA, Paquette A, Parker JD, Perring MP, Ponette Q, Potvin C, Reich PB, Scherer-Lorenzen M, Schnabel F, Verheyen K, Weih M, Wollni M, Zemp DC (2022) For the sake of resilience and multifunctionality, let's diversify planted forests! Conserv Lett 15

Metcalfe C R., Chalf L., Chattaway M M., Hare C L., Richardson R F., Slatter E M. (1951) Anatomy of the dicotyledons. leaves, stem, and wood in relation to taxonomy, with notes on economic uses.

Moraes CB, Freitas TGM, Pieroni GB, Resende MDV, Zimback L, Mori ES (2014) Genetic parameters of *Eucalyptus* clones for early selection in frost occurrence region. Sci For 42:219–227.

Mott KA, Gibson AC, O'Leary JW (1982) The adaptive significance of amphistomatic leaves. Plant Cell Environ 5:455–460.

Muchow R. C., Sinclair T. R. (1989) Epidermal conductance, stomatal density and stomatal size among genotypes of Sorghum. Plant Cell Environ 12:425–431.

Muir CD (2018) Light and growth form interact to shape stomatal ratio among British angiosperms. New Phytologist 218:242–252.

Mulamba NN, Mock JJ (1978) Improvement of yield potential of the ETO blanco maize (Zea mays L.) population by breeding for plant traits [Mexico]. Egypt J Genet Cytol 1:40–51.

Myburg AA, Grattapaglia D, Tuskan GA, Hellsten U, Hayes RD, Grimwood J, Jenkins J, Lindquist E, Tice H, Bauer D, Goodstein DM, Dubchak I, Poliakov A, Mizrachi E, Kullan ARK, Hussey SG, Pinard D, Van Der Merwe K, Singh P, Van Jaarsveld I, Silva-Junior OB, Togawa RC, Pappas MR, Faria DA, Sansaloni CP, Petroli CD, Yang X, Ranjan P, Tschaplinski TJ, Ye CY, Li T, Sterck L, Vanneste K, Murat F, Soler M, Clemente HS, Saidi N, Cassan-Wang H, Dunand C, Hefer CA, Bornberg-Bauer E, Kersting AR, Vining K, Amarasinghe V, Ranik M, Naithani S, Elser J, Boyd AE, Liston A, Spatafora JW, Dharmwardhana P, Raja R, Sullivan C, Romanel E, Alves-Ferreira M, Külheim C, Foley W, Carocha V, Paiva J, Kudrna

D, Brommonschenkel SH, Pasquali G, Byrne M, Rigault P, Tibbits J, Spokevicius A, Jones RC, Steane DA, Vaillancourt RE, Potts BM, Joubert F, Barry K, Pappas GJ, Strauss SH, Jaiswal P, Grima-Pettenati J, Salse J, Van De Peer Y, Rokhsar DS, Schmutz J (2014) The genome of *Eucalyptus grandis*. Nature 510:356–362.

O'brien TP, Feder N, Mccully ME (1964) Polyehromatic staining of plant cell walls by Toluidine Blue O. Protoplasma 63:368–373.

Ocheltree TW, Mueller KM, Chesus K, LeCain DR, Kray JA, Blumenthal DM (2020) Identification of suites of traits that explains drought resistance and phenological patterns of plants in a semi-arid grassland community. Oecologia 192:55–66.

Oliveira LA, Cardoso AA, Andrade MT, Pereira TS, Araújo WL, Santos GA, Damatta FM, Martins SCV (2022) Exploring leaf hydraulic traits to predict drought tolerance of *Eucalyptus* clones. Tree Physiol 42:1750–1761.

Parkhurst DF (1978) The adaptive significance of stomatal occurrence on one or both surfaces of leaves. Journal of Ecology 66:367–383.

Parkhurst DF, Mott KA (1990) Intercellular diffusion limits to CO2 uptake in leaves. Plant Physiol 94:1024–1032.

Pereira TS, Oliveira LA, Andrade MT, Haverroth EJ, Cardoso AA, Martins SCV (2024) Linking water-use strategies with drought resistance across herbaceous crops. Physiol Plant 176:e14114.

Petek-Petrik A, Petrík P, Lamarque LJ, Cochard H, Burlett R, Delzon S (2023) Drought survival in conifer species is related to the time required to cross the stomatal safety margin. J Exp Bot 74:6847–6859.

Petrík P, Petek-Petrik A, Mukarram M, Schuldt B, Lamarque LJ (2023) Leaf physiological and morphological constraints of water-use efficiency in C3plants. AoB Plants 15

Pfautsch S, Dodson W, Madden S, Adams MA (2015) Assessing the impact of large-scale water table modifications on riparian trees: A case study from Australia. Ecohydrology 8:642–651.

Pita-Barbosa A, Oliveira LA, de Barros NF, Hodecker BER, Oliveira FS, Araújo WL, Martins SCV (2023) Developing a roadmap to define a potential ideotype for drought tolerance in *Eucalyptus*. Forest Science 69:101–114.

Pivovaroff AL, Pasquini SC, De Guzman ME, Alstad KP, Stemke JS, Santiago LS (2016) Multiple strategies for drought survival among woody plant species. Funct Ecol 30:517–526.

Ramantswana M, Guerra SPS, Ersson BT (2020) Advances in the mechanization of regenerating plantation forests: a review. Current Forestry Reports 6:143–158.

Rejmánek M, Richardson DM (2011) The eucalypts. In: Rejmánek M, Richardson DM (eds) Encyclopedia of biological invasions. University of California Press, Berkeley and Los Angeles, pp 203–209.

Resende MDV (2007) SELEGEN-REML/BLUP Sistema Estatístico e Seleção Genética Computadorizada via Modelos Lineares Mistos.

Resende MDV (2009) Genética biométrica e estatística no melhoramento de plantas perenes, First. Embrapa.

Resende MDV (2015) Genética quantitativa e de populações, 1st edn. Editora UFV, Viçosa.

Resende MDV, Alves RS (2020) Linear, generalized, hierarchical, bayesian and random regression mixed models in genetics/genomics in plant breeding. Functional Plant Breeding Journal 2:1–31.

Resende MDV, Alves RS (2022) Statistical significance, selection accuracy, and experimental precision in plant breeding Statistical significance, selection accuracy, and experimental precision in plant breeding. Crop Breeding and Applied Biotechnology 22:42712238. http://dx.doi.org/10.1590/1984-70332022v22n3a31

Resende MDV, Duarte JB (2007) Precisão e controle de qualidade em experimentos de avaliação de cultivares. www.agro.ufg.br/pat

Resende MAV, Freitas JA, Lanza MA, Resende MDV, Azevedo CF (2014) Divergência genética e índice de seleção via BLUP em acessos de algodoeiro para características tecnológicas da fibra. Pesqui Agropecu Trop:334–340.

Rezende GDSP, Resende MDV, Assis TF (2014) *Eucalyptus* breeding for clonal forestry. In: Fenning T (ed) Challenges and opportunities for the world's forests in the 21st century. Forestry Sciences, Dordrecht, pp 393–424.

Richardson F, Brodribb TJ, Jordan GJ (2017) Amphistomatic leaf surfaces independently regulate gas exchange in response to variations in evaporative demand. Tree Physiol 37:869–878.

Rowland L, Da Costa ACL, Galbraith DR, Oliveira RS, Binks OJ, Oliveira AAR, Pullen AM, Doughty CE, Metcalfe DB, Vasconcelos SS, Ferreira L V., Malhi Y, Grace J, Mencuccini M, Meir P (2015) Death from drought in tropical forests is triggered by hydraulics not carbon starvation. Nature 528:119–122.

Ryel RJ, Beyschlag W, Caldwell MM, Caldwellt MM (1993) Foliage orientation and carbon gain in two tussock grasses as assessed with a new whole-plant gas-exchanage model foliage orientation and carbon gain in two tussock grasses as assessed with a new whole-plant gas-exchange model. Funct Ecol 7:115–124.

Sack L, Melcher PJ, Zwieniecki MA, Holbrook NM (2002) The hydraulic conductance of the angiosperm leaf lamina: A comparison of three measurement methods. J Exp Bot 53:2177–2184.

Sack L, Cowan PD, Jaikumar N, Holbrook NM. 2003. The 'hydrology' of leaves: co-ordination of structure and function in temperate woody species. Plant, Cell & Environment 26: 1343–1356.

Salam U, Ullah S, Tang ZH, Elateeq AA, Khan Y, Khan J, Khan A, Ali S (2023) Plant Metabolomics: An Overview of the Role of Primary and Secondary Metabolites against Different Environmental Stress Factors. Life 13

Salisbury EJ (1927) On the causes and ecological significance of stomatal frequency, with special reference to the woodland flora. Philosophical Transactions of the Roval Society of London 216:1–65.

Schenk HJ, Jackson RB (2005) Mapping the global distribution of deep roots in relation to climate and soil characteristics. Geoderma 126:129–140.

Scoffoni C, Chatelet DS, Pasquet-Kok J, Rawls M, Donoghue MJ, Edwards EJ, Sack L (2016) Hydraulic basis for the evolution of photosynthetic productivity. Nat Plants 2

Scolforo HF, Scolforo JRS, Stape JL, McTague JP, Burkhart H, McCarter J, de Castro Neto F, Loos RA, Sartorio RC (2017) Incorporating rainfall data to better plan eucalyptus clones deployment in eastern Brazil. For Ecol Manage 391:145–153.

Seng Hua L, Wei Chen L, Antov P, Kristak L, Md Tahir P (2022) Engineering wood products from *Eucalyptus spp*. Advances in Materials Science and Engineering 2022

Shakespear S, Sivaji M, Kumar V, Arumugam Pillai M, Wani SH, Penna S, Yasin JK (2024) Navigating Through Harsh Conditions: Coordinated Networks of Plant Adaptation to Abiotic Stress. J Plant Growth Regul

Shen C, Li L, Ouyang L, Su M, Guo K (2023) *E. urophylla* × *E. grandis* high-quality genome and comparative genomics provide insights on evolution and diversification of eucalyptus. BMC Genomics 24

Slavic B. 1974. Methods of studying plant water relations. Berlin, Germany: Springer.

Silva VE, Nogueira TAR, Abreu-Junior CH, He Z, Buzetti S, Laclau JP, Teixeira Filho MCM, Grilli E, Murgia I, Capra GF (2020) Influences of edaphoclimatic conditions on deep rooting and soil water availability in Brazilian *Eucalyptus* plantations. For Ecol Manage 455:117673.

Silva H, Sagardia S, Ortiz M, Franck N, Opazo M, Quiroz M, Baginsky C, Tapia C (2014) Relationships between leaf anatomy, morphology, and water use efficiency in Aloe vera (L) Burm f. As a function of water availability. Revista Chilena de Historia Natural 87

Simkin AJ, Kapoor L, Doss CGP, Hofmann TA, Lawson T, Ramamoorthy S (2022) The role of photosynthesis related pigments in light harvesting, photoprotection and enhancement of photosynthetic yield in planta. Photosynth Res 152:23–42.

Smith MR, Rao IM, Merchant A (2018) Source-sink relationships in crop plants and their influence on yield development and nutritional quality. Front Plant Sci 871

Sperry JS, Donnelly JR, Tyree MT (1988) A method for measuring hydraulic conductivity and embolism in xylem. Plant Cell Environ 11:35–40.

Sperry J S., Ikeda T (1997) Xylem cavitation in roots and stems of Douglas-fir and white fir. Tree Physiol 17:275–280.

Sperry JS, Love DM (2015) What plant hydraulics can tell us about responses to climate-change droughts. New Phytologist 207:14–27.

Stanturf JA, Vance ED, Fox TR, Kirst M (2013) *Eucalyptus* beyond Its Native Range: Environmental Issues in Exotic Bioenergy Plantations. International Journal of Forestry Research 2013:1–5.

de Strittmatter C (1973) Nueva tecnica de diafanizacion. Boletin de la sociedad Argentina de Botanica 15:126–129.

Stuepp CA, Kratz D, Gabira MM, Wendling I (2020) Survival and initial growth in the field of eucalyptus seedlings produced in different substrates. Pesqui Agropecu Bras 55:1–12.

Sun T, Rao S, Zhou X, Li L (2022) Plant carotenoids: recent advances and future perspectives. Molecular Horticulture 2

Trenberth KE, Dai A, Van Der Schrier G, Jones PD, Barichivich J, Briffa KR, Sheffield J (2014) Global warming and changes in drought. Nat Clim Chang 4:17–22.

Trueba S, Pan R, Scoffoni C, John GP, Davis SD, Sack L (2019) Thresholds for leaf damage due to dehydration: declines of hydraulic function, stomatal conductance and cellular integrity precede those for photochemistry. New Phytologist 223:134–149.

Tyree MT, Hammel HT (1972) The measurement of the turgor pressure and the water relations of plants by the pressure-bomb technique. J Exp Bot 23:267–282.

Tyree M T., Ewers F W. (1991) The hydraulic architecture of trees and other woody plants. New Phytologist 119:345–360.

Valladares F, Pugnaire FI (1999) Tradeoffs between irradiance capture and avoidance in semi-arid environments assessed with a crown architecture model. Ann Bot 83:459–469.

De Villemereuil P, Gaggiotti OE, Mouterde M, Till-Bottraud I (2016) Common garden experiments in the genomic era: New perspectives and opportunities. Heredity (Edinb) 116:249–254.

Wellburn AR (1994) The spectral determination of chlorophylls a and b, as well as total carotenoids, using various solvents with spectrophotometers of different resolution. J Plant Physiol 144:307–313.

Werner C, Ryel RJ, Correia O, Beyschlag W (2001) Effects of photoinhibition on whole-plant carbon gain assessed with a photosynthesis model. Plant Cell Environ 24:27–40.

Wood JG (1934) The physiology of xerophytism in Australian plants: the stomatal frequencies, transpiration and osmotic pressures of sclerophyll and tomentose-succulent leaved plants. Journal of Ecology 22:69–87.

Wu FZ, Bao WK, Li FL, Wu N (2008) Effects of water stress and nitrogen supply on leaf gas exchange and fluorescence parameters of Sophora davidii seedlings.

Xiong D, Flexas J (2020) From one side to two sides: the effects of stomatal distribution on photosynthesis. New Phytologist 228:1754–1766.

Yemm EW, Cocking EC, Ricketts RE (1955) The determination of amino-acids with ninhydrin. Analyst 80:209–214.

Zencich SJ, Froend RH, Turner J V., Gailitis V (2002) Influence of groundwater depth on the seasonal sources of water accessed by Banksia tree species on a shallow, sandy coastal aquifer. Oecologia 131:8–19.

Zhang YX, Wang XJ (2021) Geographical spatial distribution and productivity dynamic change of eucalyptus plantations in China. Sci Rep 11

Zhou X, Zhu H, Wen Y, Goodale UM, Li X, You Y, Ye D, Liang H (2018) Effects of understory management on trade-offs and synergies between biomass carbon stock, plant diversity and timber production in eucalyptus plantations. For Ecol Manage 410:164–173.

Zomer RJ, Trabucco A, Bossio DA, Verchot L V. (2008) Climate change mitigation: A spatial analysis of global land suitability for clean development mechanism afforestation and reforestation. Agric Ecosyst Environ 126:67–80.

TABLES

Table 1: Variance components (REML Individual) for the anatomical characters in leaves of seven eucalyptus species. V_D (vein density; mm mm^{-2}); SD_{Aba}, SD_{Ada}, SD_{Total} (abaxial, adaxial, and total stomatal density; n° mm^{-2}); g_{wmax} (maximum stomatal conductance to water vapor; mol m^{-2} s^{-1}); Dh_{Sperry} (Sperry hydraulic diameter; µm); K_t (theoretical hydraulic conductance; mmol m^{-1} s^{-1} MPa^{-1}); N_{XV} (number of xylem vessels; n°).

	V_D	SD_{Aba}	SD_{Ada}	SD_{Total}	g_{wmax}	Dh_{Sperry}	K_t	N_{XV}
Vg	1.95	3894.21	23577.27	8724.75	0.25	9.88	9.21	4712.66
Ve	1.12	6734.96	1829.25	10686.52	0.23	7.05	5.89	7257.66
Vp	3.07	10629.17	25406.52	19411.27	0.49	16.93	15.11	11970.33
CVg%	**11.59**	**14.46**	**124.69**	**16.84**	**13.93**	**15.92**	**15.63**	**15.02**
h^2	**0.91**	**0.78**	**0.99**	**0.83**	**0.86**	**0.89**	**0.90**	**0.80**
Acc	**0.96**	**0.88**	**0.99**	**0.91**	**0.93**	**0.95**	**0.95**	**0.89**
Overall average	12.06	431.69	123.14	554.78	3.59	19.75	8.93	457.14
LRT	21.65**	7.44**	68.56**	10.84**	14.13**	18.08**	19.84**	8.48**

Vg = genetic variance; Ve = environmental variance; Vp = phenotypic variance; h^2: average heritability of genotypes; Acc: accuracy; CVg% = coefficient of genotypic variation; Overall average: average of the values measured for each characteristic. Tabulated chi-squared: 3.84 and 6.63 for the 5% and 1% significance levels. Asterisks indicate a significant difference between genotypes according to the likelihood ratio test (LRT): ** $P < 0.01$, * $P < 0.05$. Values of heritability, accuracy, and coefficient of genotypic variation in bold are considered high following (Resende and Duarte 2007, Kushwah et al. 2021, Resende and Alves 2020, 2022).

Table 2: Components of variance (Individual REML) for the anatomical characters in the leaves of seven eucalyptus species. IS (intercellular space; %); TUE (thickness of the upper epidermis; µm), TPP (thickness of palisade parenchyma; µm), and LBT (leaf blade thickness; µm).

	IS	TUE	TPP	LBT
Vg	62.31	1.84	99.21	270.97
Ve	14.45	3.71	118.25	463.32
Vp	76.76	5.56	217.47	734.29
CVg%	**38.38**	8.65	**11.94**	5.26
h^2	**0.96**	**0.75**	**0.83**	**0.78**
Acc	**0.98**	**0.87**	**0.91**	**0.88**
Overall average	20.57	15.69	83.40	236.98
LRT	40.38**	6.22*	11.15**	7.54**

Vg = genetic variance; Ve = environmental variance; Vp = phenotypic variance; h^2: average heritability of genotypes; Ac: accuracy; CVg% = coefficient of genotypic variation; Overall average: average of the values measured for each characteristic. Tabulated chi-squared: 3.84 and 6.63 for the 5% and 1% significance levels. Asterisks indicate a significant difference between genotypes according to the likelihood ratio test (LRT): ** P <0.01, * P <0.05. Values of heritability, accuracy, and coefficient of genotypic variation in italics are considered high following (Resende and Duarte 2007, Kushwah et al. 2021, Resende and Alves 2020, 2022).

Table 3: Variance components (Individual REML) for gas exchange parameters in leaves of seven eucalyptus species. *A* (net photosynthetic rate; µmol CO_2 m^{-2} s^{-1}); g_s (stomatal conductance; mol H_2O m^{-2} s^{-1}); WUE_i (intrinsic water use efficiency); *E* (transpiration rate; mol H_2O m^{-2} s^{-1}).

	A	***E***	g_s	WUE_i
Vg	5.36	0.94	0.011	103.90
Ve	7.53	2.21	0.012	231.26
Vp	12.89	3.15	0.023	335.17
CVgi%	**11.08**	**20.90**	**27.24**	**16.41**
h^2	**0.81**	**0.72**	**0.85**	**0.73**
Acc	**0.90**	**0.85**	**0.92**	**0.85**
Overall average	20.90	4.63	0.38	62.13
LRT	9.39**	5.11*	12.14**	5.51*

Vg = genetic variance; Ve = environmental variance; Vp = phenotypic variance; h^2: average heritability of genotypes; Acc: accuracy; CVg% = coefficient of genotypic variation; Overall average: average of the values measured for each characteristic. Tabulated chi-squared: 3.84 and 6.63 for the 5% and 1% significance levels. Asterisks indicate a significant difference between genotypes according to the likelihood ratio test (LRT): ** P <0.01, * P <0.05. Values of heritability, accuracy, and coefficient of genotypic variation in italics are considered high following (Resende and Duarte 2007, Kushwah et al. 2021, Resende and Alves 2020, 2022).

Table 4: Variance components (Individual REML) for water relations parameters in leaves of seven eucalyptus species. P_{50} (water potential responsible for 50% of the cumulative embolism area; -MPa); $\square_{100}$ (osmotic potential at full turgor; MPa); $\square_{TLP}$ (water potential at the point of turgor loss; MPa); RWC_{TLP} (relative water content at the point of turgor loss; %); □□ (elasticity bulk; MPa); C_{FT} and C_{TLP} (leaf capacitance pre-turgor loss and post-turgor loss; mol m^{-2} MPa^{-1}); SWC (saturated water content; g H_2O g^{-1} DM); $g_{leaf-res}$ (leaf residual conductance; mmol m^{-2} s^{-1}).

	P_{50}	$\square_{100}$	$\square_{TLP}$	RWC_{TLP}	□□	C_{FT}	C_{TLP}	SWC	$g_{leaf-res}$
Vg	0.048	0.044	0.057	3.21	1.50	0.0041	0.17	0.050	1.24
Ve	0.39	0.029	0.033	3.041	3.39	0.0039	0.11	0.012	0.45
Vp	0.44	0.073	0.090	6.25	4.89	0.0079	0.28	0.062	1.69
CVgi%	6.21	**13.93**	**12.15**	2.04	8.38	**13.78**	**30.06**	**13.64**	**45.13**
h^2	0.42	**0.90**	**0.91**	**0.86**	**0.73**	**0.86**	**0.91**	**0.96**	**0.94**
Acc	0.65	**0.95**	**0.96**	**0.93**	**0.85**	**0.93**	**0.95**	**0.98**	**0.97**
Overall average	3.52	1.50	1.96	87.78	14.60	0.46	1.38	1.64	2.46
LRT	16.72**	19.42**	21.70**	13.96**	5.39*	13.99**	20.14**	40**	30.26**

Vg = genetic variance; Ve = environmental variance; Vp = phenotypic variance; h^2: average heritability of genotypes; Acc: accuracy; CVg% = coefficient of genotypic variation; Overall average: average of the values measured for each characteristic. Tabulated chi-squared: 3.84 and 6.63 for the 5% and 1% significance levels. Asterisks indicate a significant difference between genotypes according to the likelihood ratio test (LRT): ** $P < 0.01$, * $P < 0.05$. Values of heritability, accuracy, and coefficient of genotypic variation in italics are considered high following (Resende and Duarte 2007, Kushwah et al. 2021, Resende and Alves 2020, 2022).

Table 5: Variance components (Individual REML) for allometric and growth parameters of seven eucalyptus species. LAun (unit leaf area; cm^2); SLA (specific leaf area; cm^2 g^{-1}); H (plant height; m); D (stem diameter; mm); Hv (Huber value; x10^4); S$_{Vol}$ (stem volume; cm^3); TDM (total dry mass; g).

	LA$_{un}$	**SLA**	**H**	**D**	**Hv**	**S$_{Vol}$**	**TDM**
Vg	101.19	241.35	0.12	6.58	0.01	4581.27	7843.25
Ve	53.03	132.56	0.03	5.13	0.03	6814.27	8103.75
Vp	154.22	373.92	0.15	11.71	0.04	11395.54	15947.00
CVg%	**28.73**	**18.23**	**15.31**	**10.00**	**12.75**	**12.75**	**13.66**
h^2	**0.92**	**0.92**	**0.96**	**0.89**	**0.74**	**0.80**	**0.85**
Acc	**0.96**	**0.96**	**0.98**	**0.94**	**0.86**	**0.90**	**0.92**
Overall average	35.01	114.30	2.25	26.12	0.91	401.32	648.50
LRT	23.31**	22.46**	37.61**	16.75**	6.08*	8.81**	12.86**

Vg = genetic variance; Ve = environmental variance; Vp = phenotypic variance; h^2: average heritability of genotypes; Acc: accuracy; CVg% = coefficient of genotypic variation; Overall average: average of the values measured for each characteristic. Tabulated chi-squared: 3.84 and 6.63 for the 5% and 1% significance levels. Asterisks indicate a significant difference between genotypes according to the likelihood ratio test (LRT): ** P <0.01, * P <0.05. Values of heritability, accuracy, and coefficient of genotypic variation in italics are considered high following (Resende and Duarte 2007, Kushwah et al. 2021, Resende and Alves 2020, 2022).

Table 6: Components of variance (Individual REML) for the characters content of compounds of basic metabolism in leaves of seven eucalyptus species. Chlor *a* (chlorophyll a content; mg g^{-1} DM); Carot (carotenoid content; mg g^{-1} DM); Starch (starch content; mmol g^{-1} DM); Gluc (glucose content; mmol g^{-1} DM); Suc (sucrose content; mmol g^{-1} DM); Fruct (fructose content; mmol g^{-1} DM).

	Chlor *a*	**Carot**	**Starch**	**Gluc**	**Suc**	**Fruct**
Vg	0.29	0.036	0.042	0.00010	0.0005	0.0005
Ve	0.28	0.033	0.034	0.00002	0.0006	0.0006
Vp	0.56	0.070	0.076	0.00012	0.00012	0.0012
CVg%	**31.55**	**15.51**	**32.44**	**15.45**	2.49	**25.50**
h^2	**0.86**	**0.87**	**0.88**	**0.79**	**0.96**	**0.84**
Acc	**0.93**	**0.93**	**0.94**	**0.89**	**0.99**	**0.92**
Overall average	1.70	0.59	0.99	0.04	0.023	0.051
LRT	13.71*	14.34*	16.07*	8.01*	50.44*	0.0005*

Vg = genetic variance; Ve = environmental variance; Vp = phenotypic variance; h^2: average heritability of genotypes; Acc: accuracy; CVg% = coefficient of genotypic variation; Overall average: average of the values measured for each characteristic. Tabulated chi-squared: 3.84 and 6.63 for the 5% and 1% significance levels. Asterisks indicate a significant difference between genotypes according to the likelihood ratio test (LRT): ** P <0.01, * P <0.05. Values of heritability, accuracy, and coefficient of genotypic variation in italics are considered high following (Resende and Duarte 2007, Kushwah et al. 2021, Resende and Alves 2020, 2022).

Table 7: Rank of the variables related to the composition of a more productive and drought-tolerant eucalyptus ideotype. P_{50} (water potential responsible for 50% of the cumulative embolism area; -MPa); $g_{leaf\text{-}res}$ (leaf residual conductance; mmol m^{-2} s^{-1}); C_{FT} and C_{TLP} (leaf capacitance pre-loss of turgor and post-loss of turgor; mol m^{-2} MPa^{-1}); V_D (vein density; mm mm^{-2}); H_V (Huber value; x10^4); A (net photosynthetic rate; µmol CO_2 m^{-2} s^{-1}); WUE_i (intrinsic water use efficiency); TDM (total dry mass; g); H (height; m); D (diameter; mm); S_{Vol} (stem volume; cm^3). Lower average values for the combination indicate a more favorable mix of established characters and higher values indicate an unfavorable combination.

	P_{50}	$g_{leaf\text{-}res}$	**C_{FT}**	**C_{TLP}**	**V_D**	**H_V**	**A**	**WUEi**	**TDM**	**H**	**D**	**S_{Vol}**	**Average**
E. urophylla	1	4	4	4	6	4	6	1	3	6	2	3	3.67
E. dunnii	3	1	6	6	7	6	7	2	1	1	3	1	3.67
E. pilularis	6	3	5	7	3	1	3	5	4	5	1	2	3.75
E. camaldulensis	4	5	2	2	4	3	2	6	5	2	6	5	3.83
E. pellita	2	7	1	1	1	5	4	4	6	3	7	6	3.92
E. tereticornis	7	6	3	3	2	2	1	7	7	4	5	4	4.25
E. grandis	5	2	7	5	5	7	5	3	2	7	4	7	4.92
h^2	0.42	0.94	0.86	0.91	0.91	0.74	0.81	0.73	0.85	0.96	0.80	0.89	0.82
Acc	0.65	0.97	0.93	0.95	0.96	0.86	0.90	0.85	0.92	0.98	0.90	0.94	0.90
CVg	6.21	45.13	13.78	30.06	11.59	12.75	11.08	16.41	13.66	15.31	16.87	9.82	16.89

SUPPLEMENTARY MATERIAL

Table S1: Variance components (Individual REML) for the anatomical characters in leaves of seven eucalyptus species. P_{12} and P_{88} (water potential responsible for 12 and 88 % of the cumulative embolism area; - MPa); SSM_{50} and SSM_{88} (stomatal safety margin; - MPa); K_{leaf} (leaf hydraulic conductance; mmol m^2 s^{-1} MPa^{-1}); K_{plant} (whole plant hydraulic conductance; mmol m^2 s^{-1} MPa^{-1}); ETR (electron transport rate; µmol eletrons m^{-2} s^{-1}).

	P_{12}	P_{88}	SSM_{88}	SSM_{50}	K_{leaf}	K_{plant}	ETR
Vg	0.076	0.113	0.058	0.024	0.28	0.01	2.27
Ve	0.26	0.73	0.77	0.41	2.34	4.97	725.07
Vp	0.33	0.85	0.83	0.44	2.62	4.98	727.33
CVg%	8.71	6.21	8.21	*11.19*	9.85	4.24	*12.74*
h^2	*0.64*	0.48	0.31	0.26	0.42	0.01	0.02
Acc	*0.80*	*0.69*	0.56	0.51	0.65	0.10	0.14
Overall average	3.16	4.09	2.15	1.58	6.47	2.24	195.59
LRT	3.21	1.23	0.37	0.25	0.85	0.00	0.00

Vg = genetic variance; Ve = environmental variance; Vp = phenotypic variance; h^2: average heritability of genotypes; Acc: accuracy; CVg% = coefficient of genotypic variation; Overall average: average of the values measured for each characteristic. Tabulated chi-squared: 3.84 and 6.63 for the 5% and 1% significance levels. Asterisks indicate a significant difference between genotypes according to the likelihood ratio test (LRT): ** P <0.01, * P <0.05. Values of heritability, accuracy, and coefficient of genotypic variation in italics are considered high following (Resende and Duarte 2007, Kushwah et al. 2021, Resende and Alves 2020, 2022).

Table S2: Variance components (Individual REML) for anatomical and biochemical characters in leaves of seven eucalyptus species. Chlor b (chlorophyll b content; mg g^{-1} DM); Prot (protein content; mg g^{-1} DM); Amin (amino acid content; µmol g^{-1} DM); Prol (proline content; µmol g^{-1} DM); T_{LA} (total leaf area; m^2); S_{Den} (specific density of the stem; g cm^{-3}); TLP (thickness of lacunose parenchyma; µm) and TLE (thickness of lacunose parenchyma and lower epidermis; µm); $(t/b)^3$ (cell wall thickness to lumen breadth ratio; $x10^{-3}$).

	Chlor *b*	**Prot**	**Amin**	**Prol**	**T_{LA}**	**S_{Den}**	**TLP**	**TLE**	**$(t/b)^3$**
Vg	0.01	2012.74	0.00	0.00	0.64	0.000	48.64	0.19	0.42
Ve	0.03	4948.34	1.63	0.00	1.93	0.034	206.56	1.62	1.92
Vp	0.03	6961.08	1.63	0.00	2.57	0.034	255.20	1.81	2.34
CVg%	*15.51*	*32.44*	*15.45*	2.49	*31.49*	1.54	5.26	3.34	*15.63*
h^2	*0.64*	*0.71*	0.01	*0.51*	*0.66*	0.010	*0.59*	0.41	*0.57*
Acc	*0.80*	*0.84*	0.11	*0.71*	*0.82*	0.10	*0.77*	0.64	*0.75*
Overall average	0.57	290.37	2.26	0.03	2.54	0.49	132.71	13.08	4.16
LRT	3.28	4.88	0.00	1.42	3.73	0.00	2.33	0.80	2.11

Vg = genetic variance; Ve = environmental variance; Vp = phenotypic variance; h^2: average heritability of genotypes; Acc: accuracy; CVg% = coefficient of genotypic variation; Overall average: average of the values measured for each characteristic. Tabulated chi-squared: 3.84 and 6.63 for the 5% and 1% significance levels. Asterisks indicate a significant difference between genotypes according to the likelihood ratio test (LRT): ** $P < 0.01$, * $P < 0.05$. Values of heritability, accuracy, and coefficient of genotypic variation in italics are considered high following (Resende and Duarte 2007, Kushwah et al. 2021, Resende and Alves 2020, 2022).

GENERAL CONCLUSION

We have investigated the stomatal behavior and genetic parameters of *Eucalyptus* species, aiming to better understand their responses to drought stress. Through the analysis of stomatal density and conductance, we found that amphistomatic species exhibit higher stomatal density and conductance compared to hypostomatic species. However, despite these seemingly advantageous traits, amphistomatic species demonstrate a vulnerability to drought due to factors such as higher water loss, and decreased rehydration capacity, partiality compensated by the highest capacitances before and after turgor loss point. Future research efforts are needed to validate these results through drying experiments and in situ assessments of soil water potentials during natural droughts. In addition, further exploration of drought resistance mechanisms at the root and stem level is warranted.

Our study also identified a set of thirty-two genetic biomarkers that could be used for phenotyping genotypes in *Eucalyptus* breeding programs. These biomarkers cover a wide range of traits related to stomatal conductance, leaf morphology, physiological characteristics, and biochemical composition. By focusing on a subset of these variables, together with the Mulan and Mock index, we determined that *E. urophylla* and *E. dunnii* have the most favorable balance between productivity and potential drought tolerance among the species studied. By integrating physiological and genetic perspectives, it is possible to gain a more complete understanding of drought susceptibility and resilience in *Eucalyptus* species, as well as identify possible biomarkers for the early selection of genotypes of interest. This will reduce the time needed to develop new genotypes and increase the efficiency of breeding programs.